Magnetic properties of [NiFe/Au/Co/Au] multilayers

magnetostatic coupling and giant magnetoresistance

Zakopane 2009

Maciej Urbaniak, Feliks Stobiecki, Bogdan Szymański
Institute of Molecular Physics, Polish Academy of Sciences

Magnetic properties of [NiFe/Au/Co/Au] multilayers

magnetostatic coupling and giant magnetoresistance

Cooperation between:

Institute of Molecular Physics, Polish Academy of Sciences, Poznań, Poland

Prof. A. Ehresmann
Department of Physics , University of Kassel, Kassel, Germany

Prof. M. Kopcewicz
Institute of Electronic Materials Technology, Warszawa, Poland

Prof. A. Maziewski
Laboratory of Magnetism, Faculty of Physics, University of Białystok, Poland

Magnetic properties of [NiFe/Au/Co/Au] multilayers

- Introduction
- Magnetic properties
- Giant magnetoresistance
- Magnetostatic coupling
- Magnetic patterning
- Conclusions

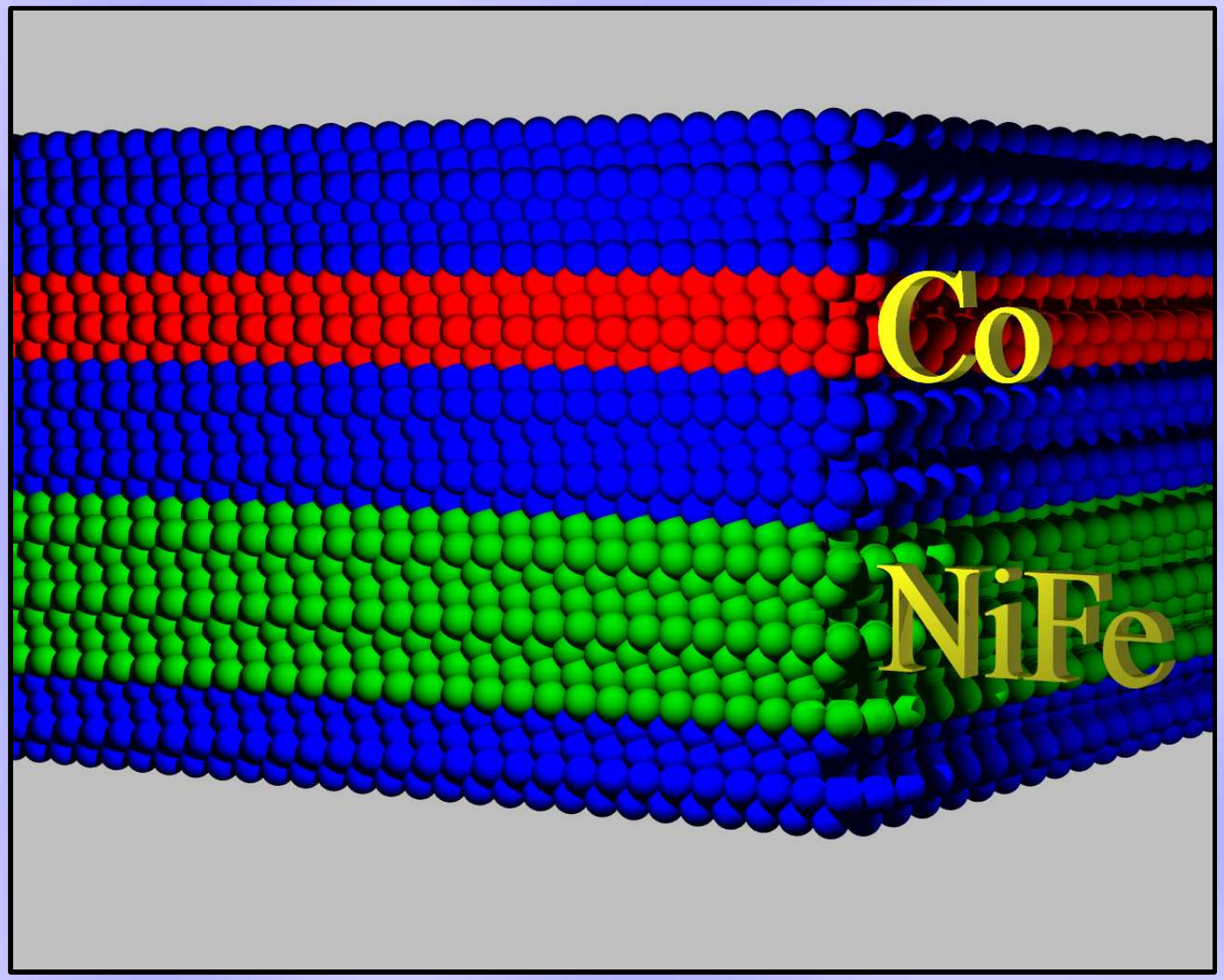

Substrate:
naturally oxidized
Si(100)

$t_{Co(CoFe)}$=0.2-1.5 nm

t_{NiFe}=0.5-4 nm

t_{Au}=1.5-3 nm

Magnetron sputtering

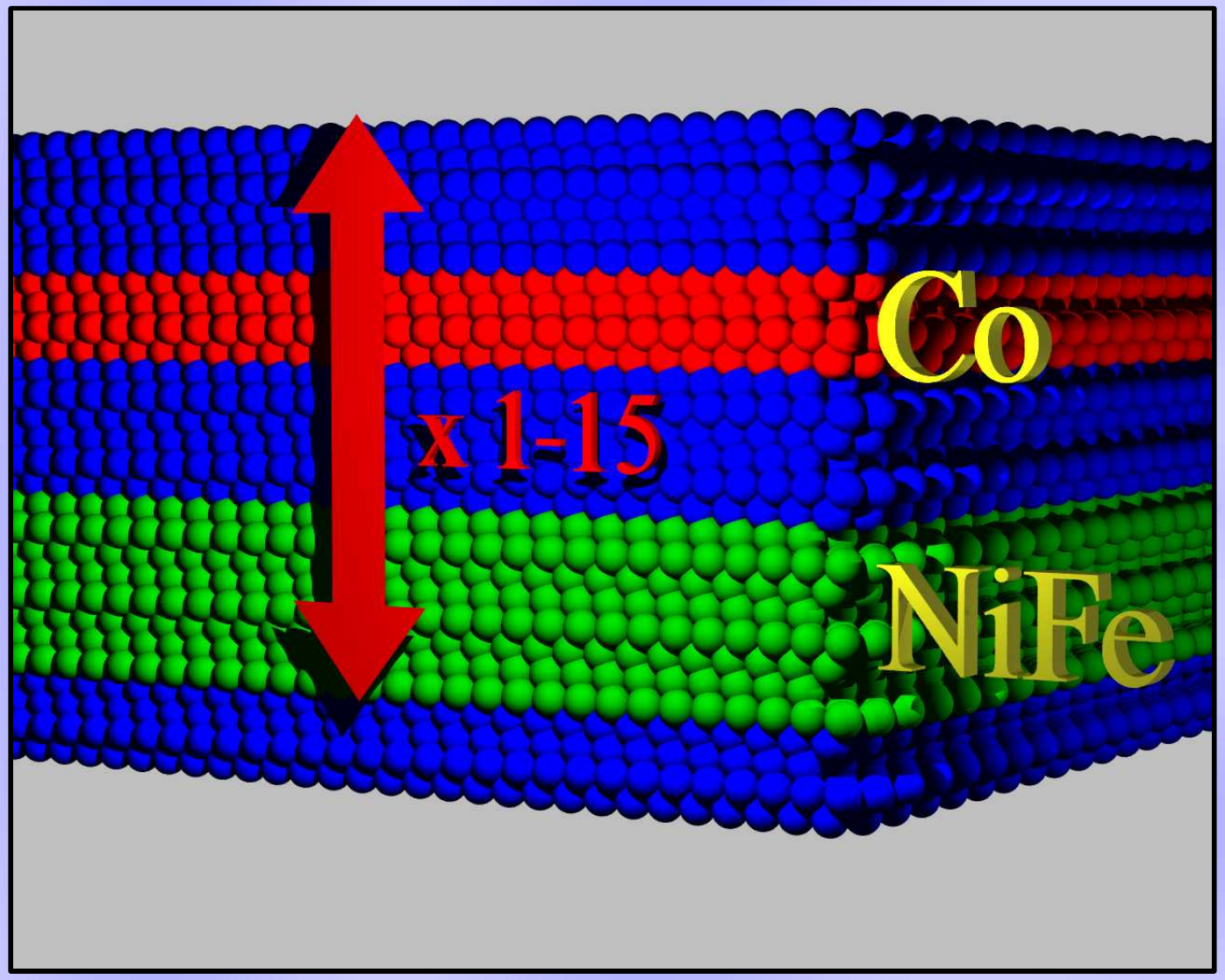

Substrate:
naturally oxidized
Si(100)

$t_{Co(CoFe)}$=0.2-1.5 nm

t_{NiFe}=0.5-4 nm

t_{Au}=1.5-3 nm

Magnetron sputtering

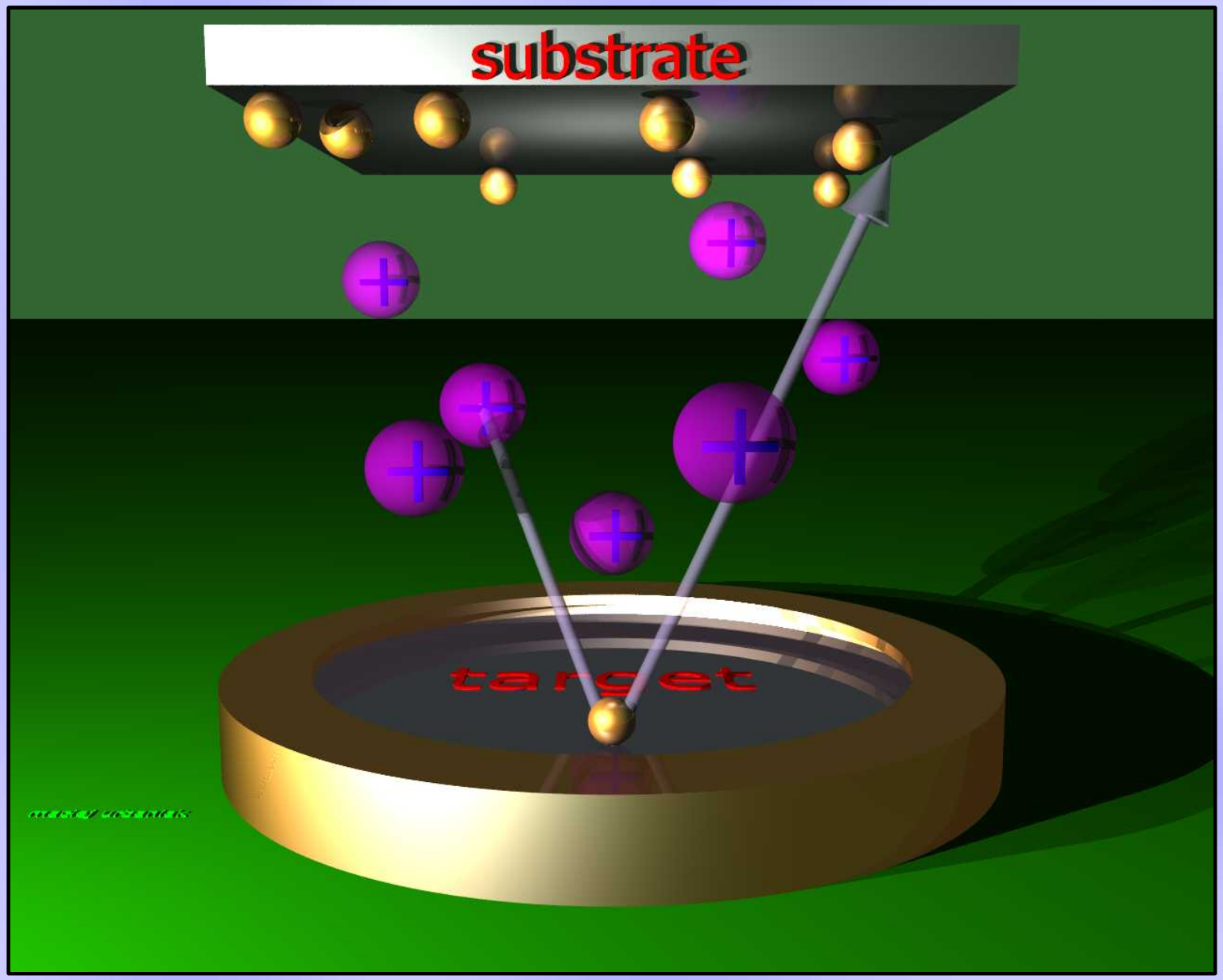

Target:

NiFe, Au, Co

Substrate:

Si(100), glass, adhesive tape

Magnetron sputtering

Target- negative potential

Introduction

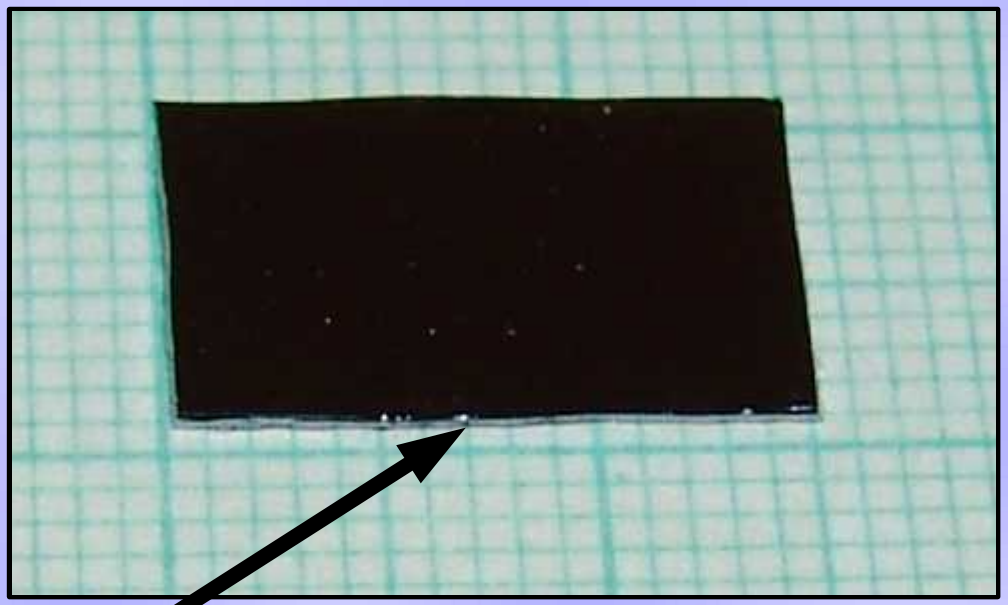

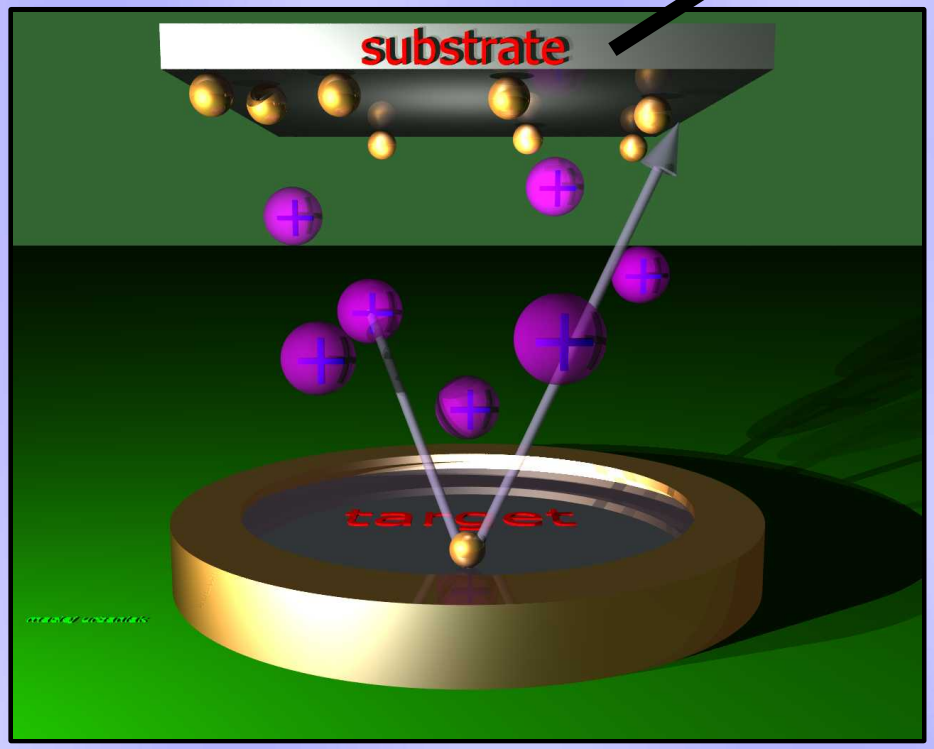

Target:

NiFe, Au, Co

Substrate:

Si(100), glass, adhesive tape

Magnetron sputtering

Target- negative potential

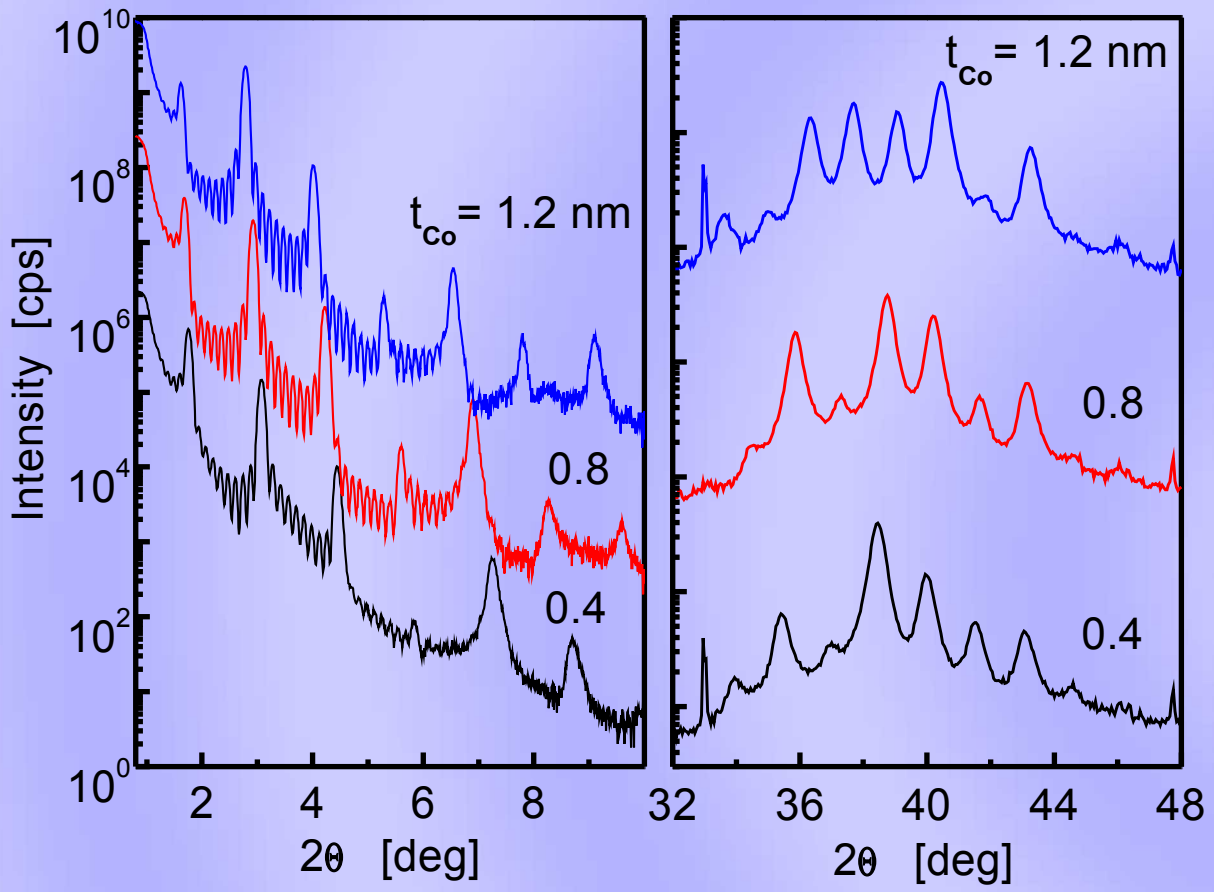

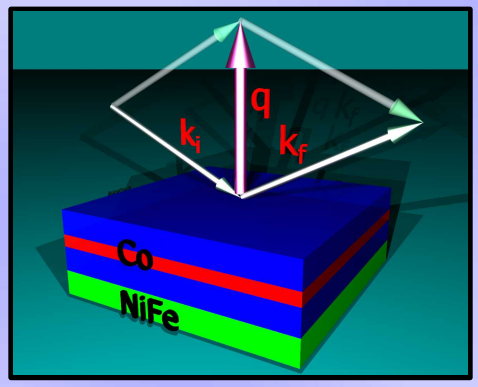

good periodicity

defined fcc(111) texture

$[Ni_{80}Fe_{20}(2\ nm)/Au(1.9\ nm)/Co(t_{Co})/Au(1.9\ nm)]_{10}$

Cu Kα 0.154nm

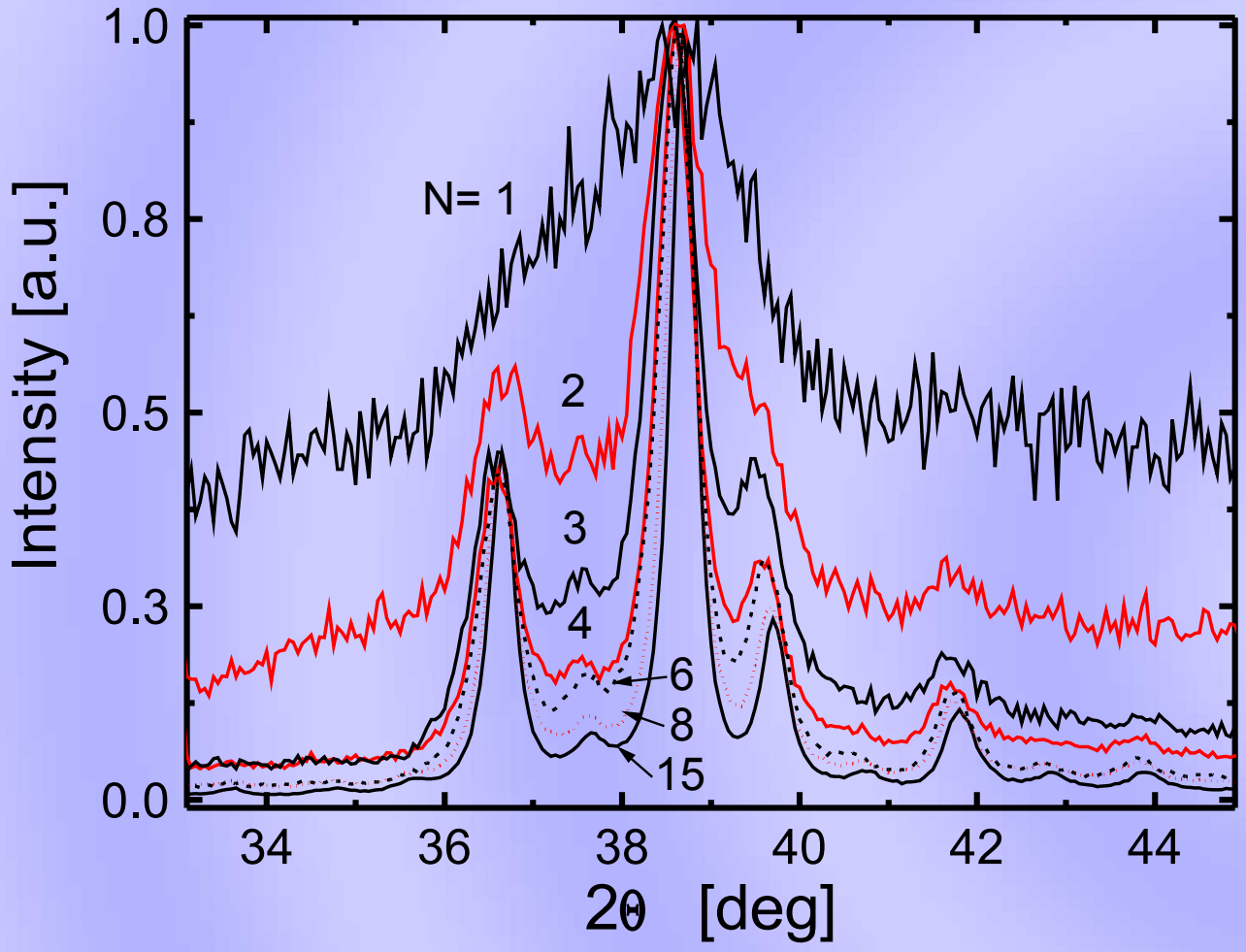

"the profile for MLs with N = 3 shows all features typical of profiles for large N."

$[Ni_{80}Fe_{20}(2\ nm)/Au(3\ nm)/Co(0.8)/Au(3\ nm)]_N$

Cu Kα 0.154nm

B. Szymański et al., Acta. Phys. Polon. **113**, 205 (2008)

Magnetic properties

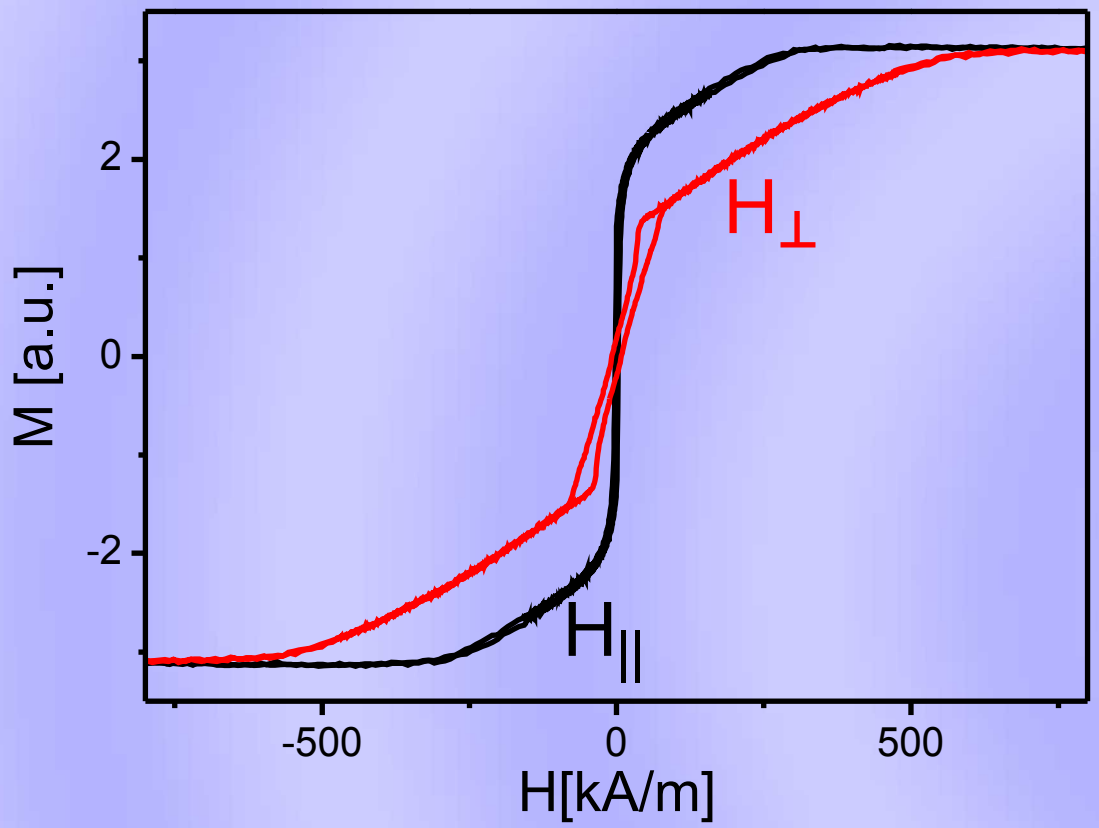

NiFe – magnetic easy axis in-plane

Co – magnetic easy axis perpendicular to plane of the sample

- Small field range of hysteresis with field applied perpendicularly is characteristic of systems with **stripe domains**.
- In both field configurations NiFe and Co layers reverse quasi independently.

$[Ni_{80}Fe_{20}(2\ nm)/Au(1.9\ nm)/Co(0.8\ nm)/Au(1.9\ nm)]_{10}$

Magnetic properties

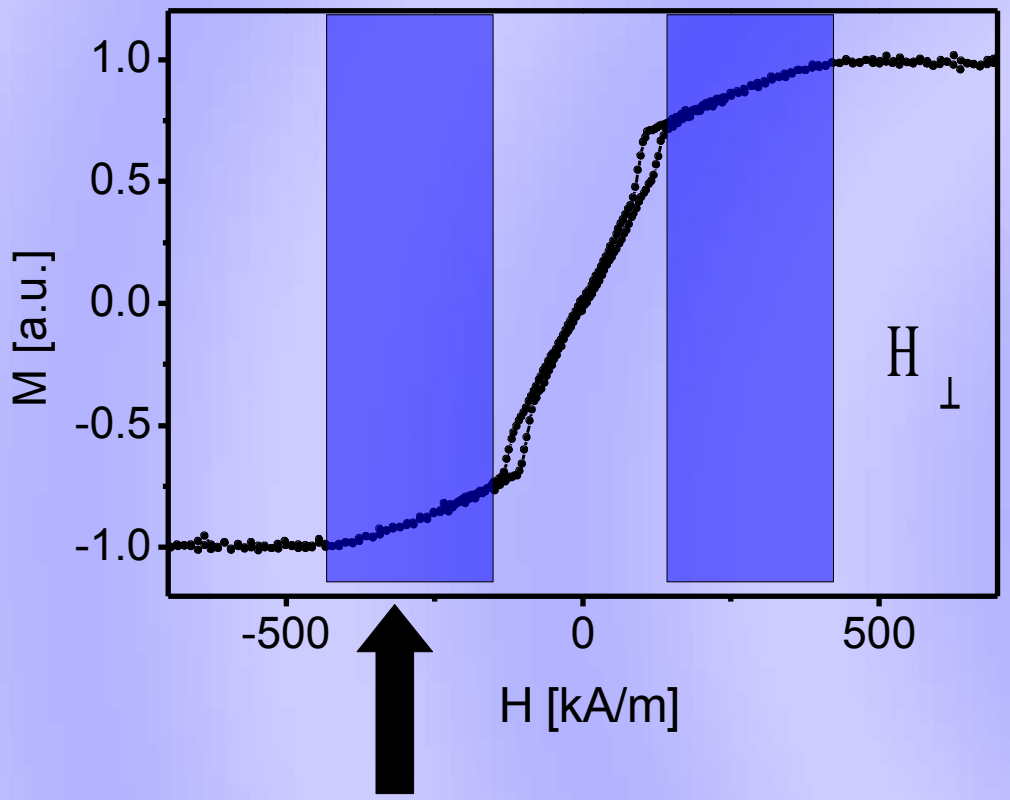

Reversal of NiFe only

$$K_u = \frac{1}{2}\mu_0 (M_S^{NiFe})^2$$

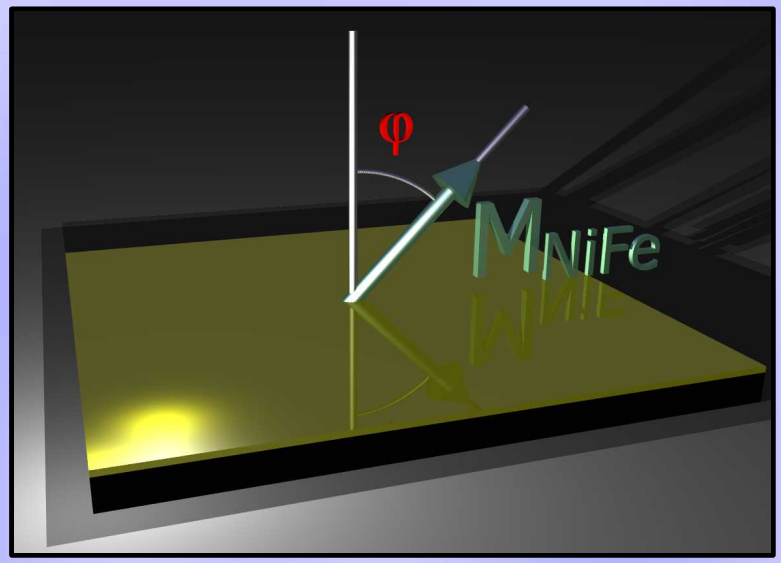

Shape anisotropy:

$$\cos(\varphi) = \frac{H}{M_S}$$

Magnetic properties

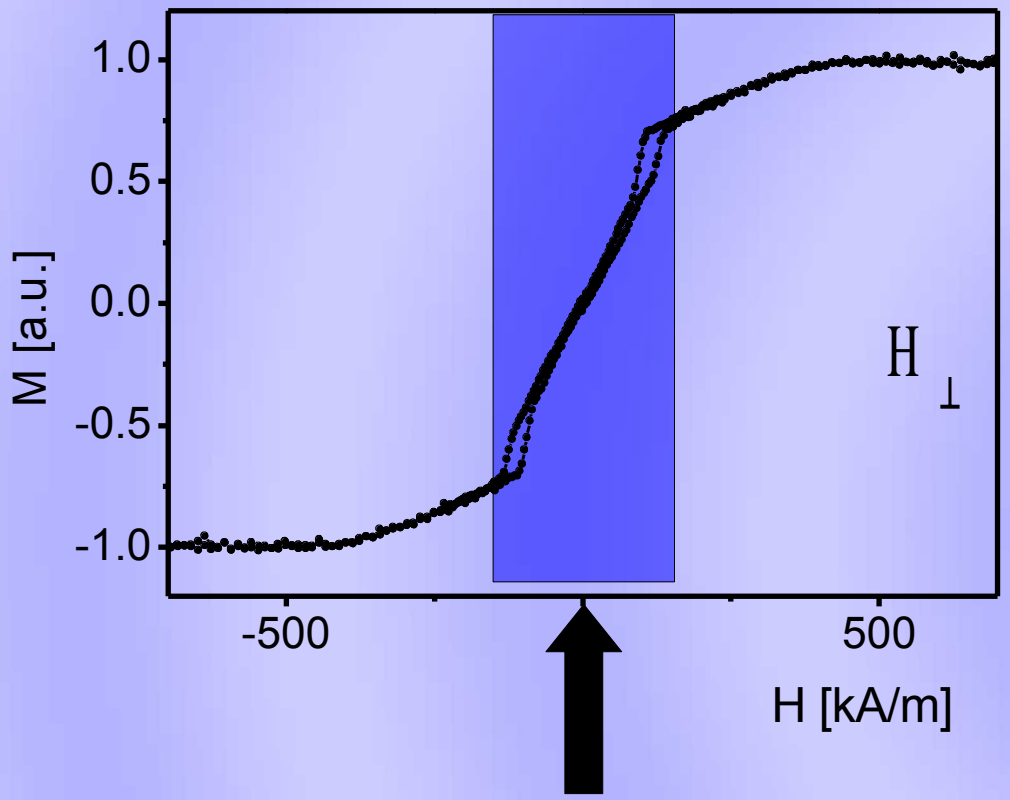

Simultaneous reversal
of
NiFe and Co

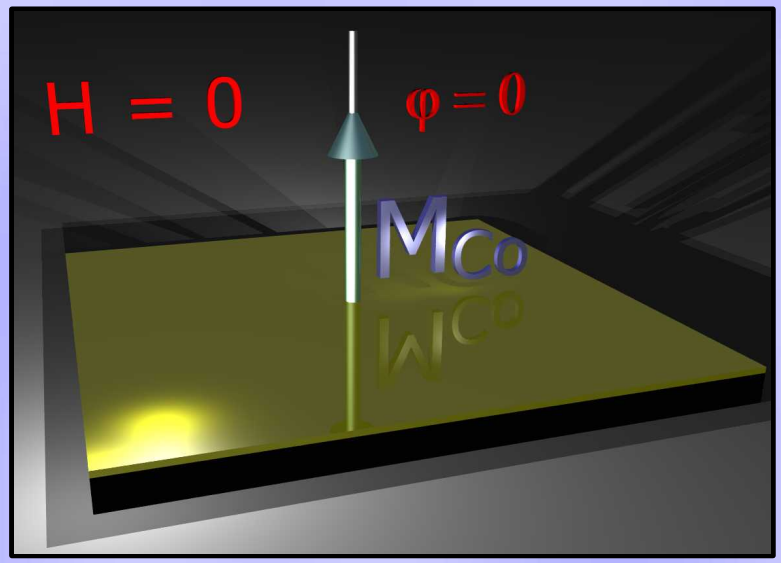

An easy axis of the Co layers is perpendicular to surface of multilayer.

Magnetic properties

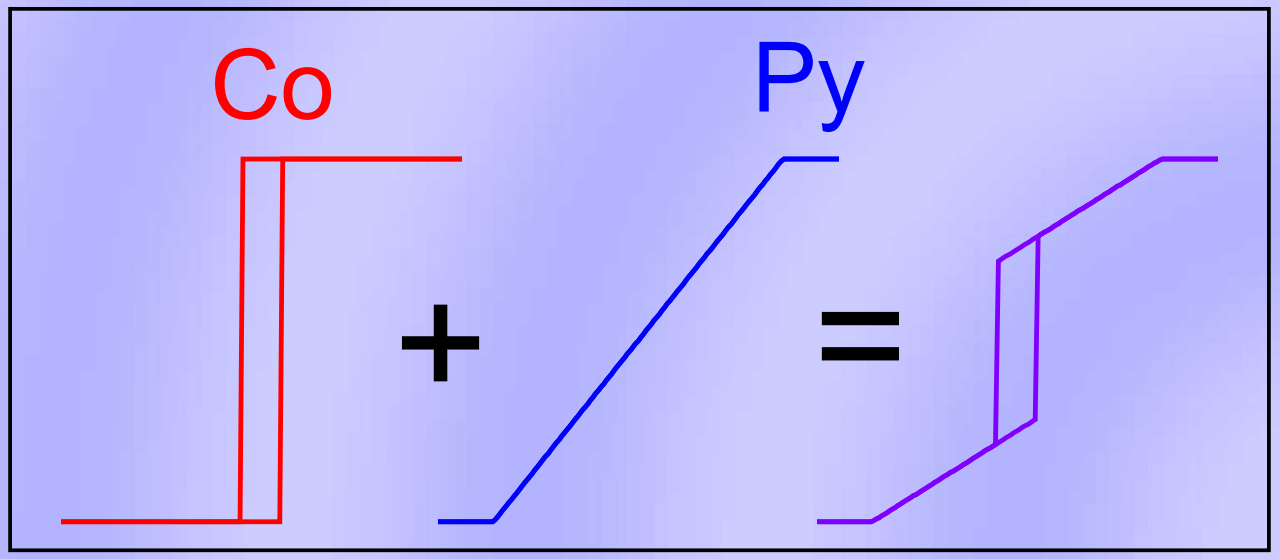

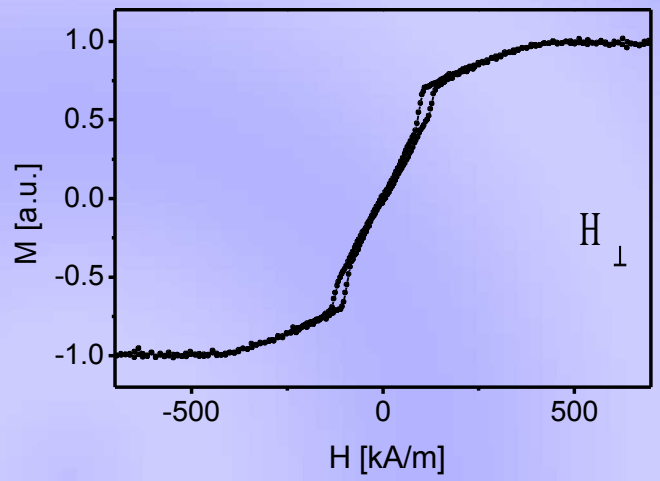

In the first approximation Co and NiFe layers can be thougt of as uncoupled.

M(*H*) dependence of the NiFe/Au/Co structure is then an arithmetic sum of the *M*(*H*) dependencies of Co and NiFe layers.

Magnetic properties

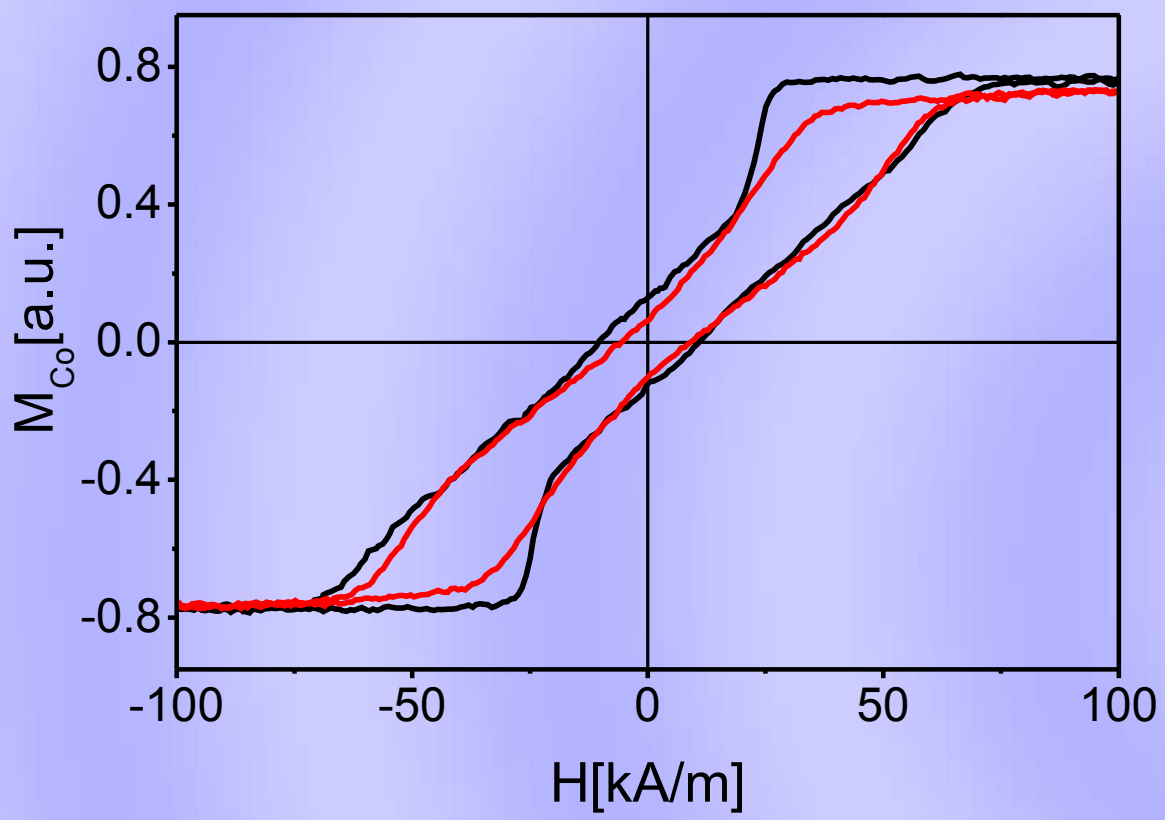

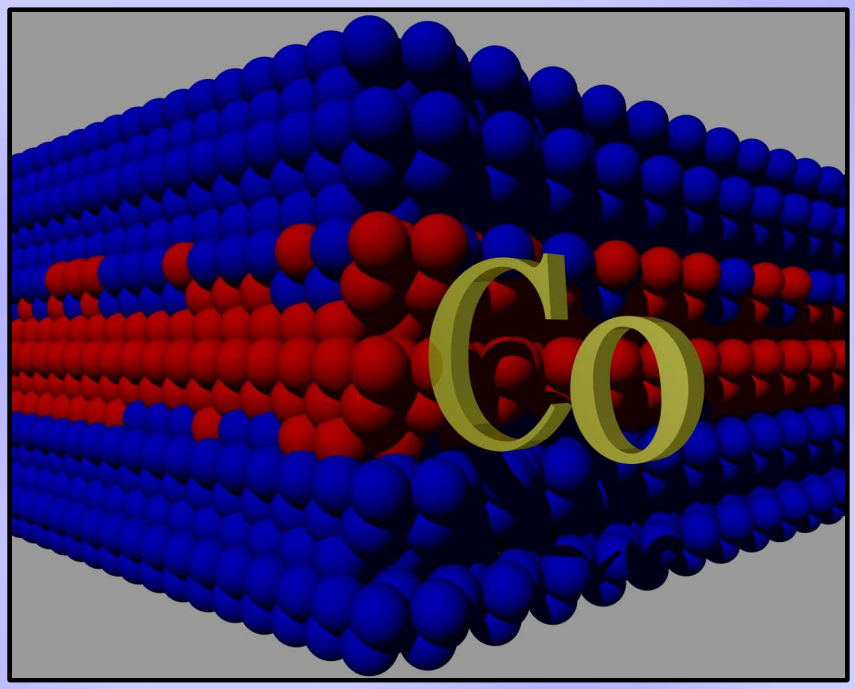

H

$[Ni_{80}Fe_{20}(2\ nm)/Au(1.9\ nm)/\mathbf{Co(0.6\ nm)}/Au(1.9\ nm)]_{10}$

$[Co(0.6\ nm)/Au(4.4\ nm)]_{15}$

NiFe sublayers do not considerably influence the reversal of Co sublayers.

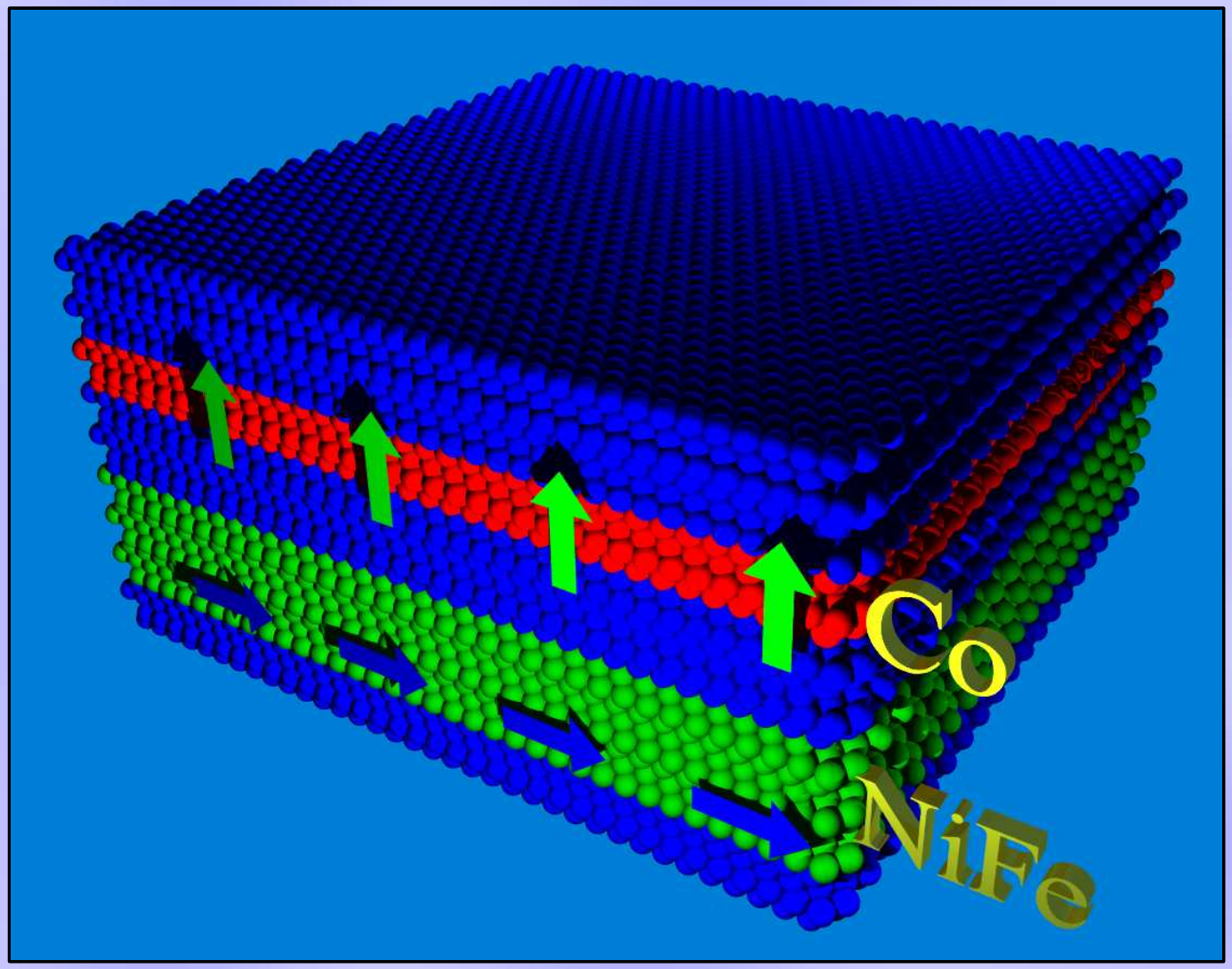

K_{eff} strongly depends on t_{Co}

Co sublayers: perpendicular effective magnetic anisotropy for **t_{Co}=0.5÷1.2nm**

$$K_{eff} = \frac{2K_{1s}}{t_{Co}} + K_{1v} - \frac{1}{2}\mu_0 (M_S^{Co})^2$$

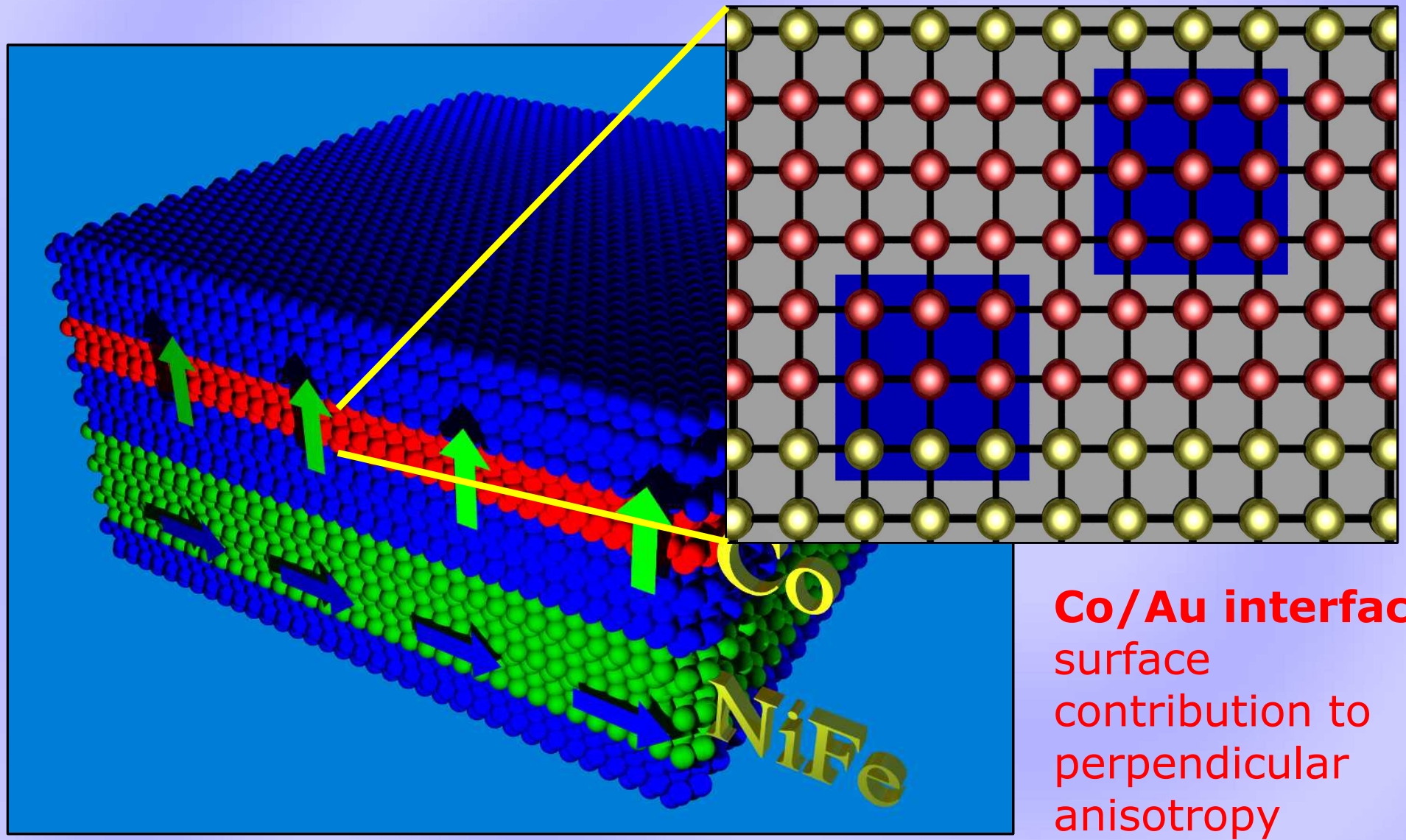

Co/Au interface- surface contribution to perpendicular anisotropy

$$K_{eff} = \frac{2K_{1s}}{t_{Co}} + K_{1v} - \frac{1}{2}\mu_0 (M_S^{Co})^2$$

Magnetic properties

Stripe domains

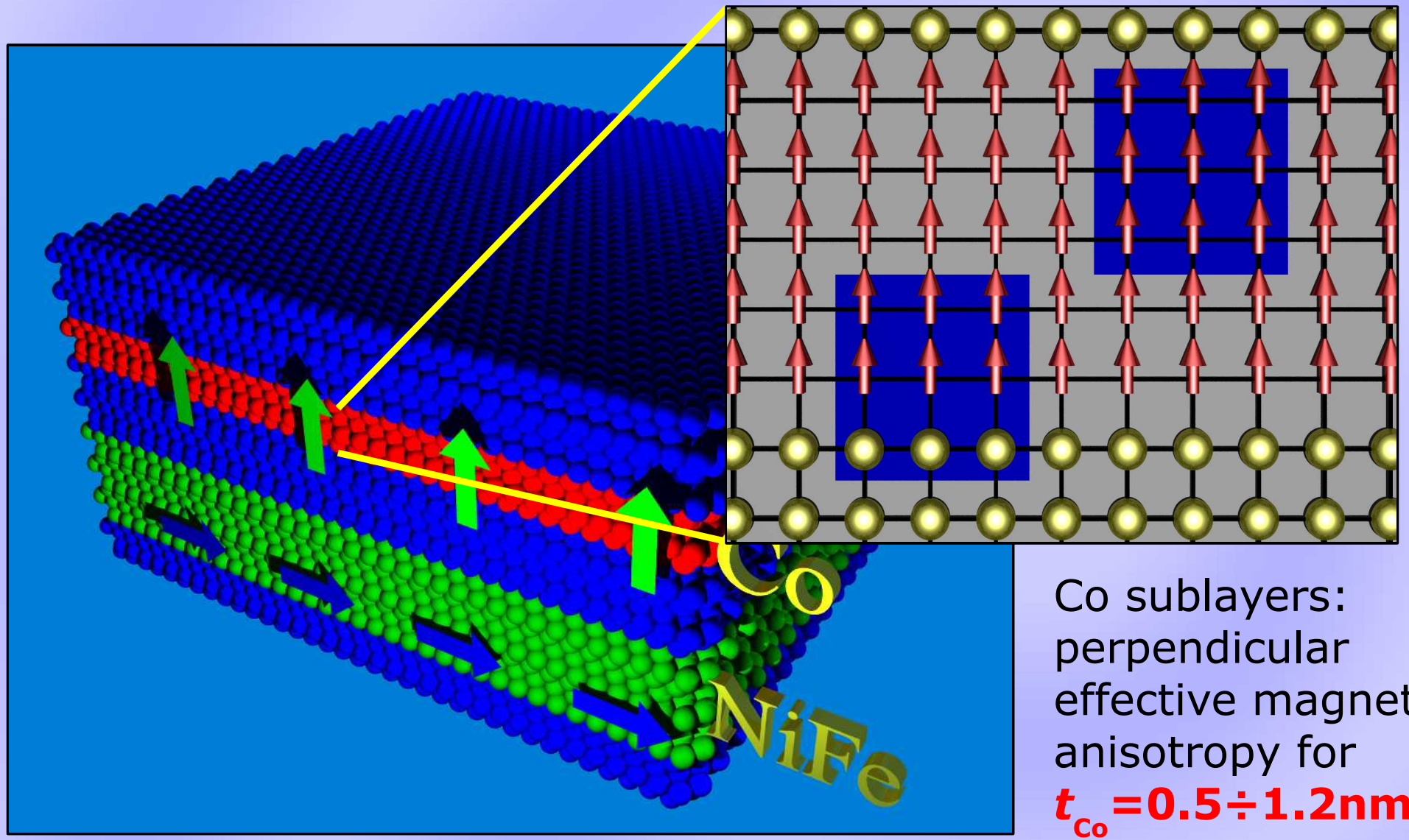

Co sublayers: perpendicular effective magnetic anisotropy for t_{Co}=0.5÷1.2nm

$$K_{eff} = \frac{2K_{1s}}{t_{Co}} + K_{1v} - \frac{1}{2}\mu_0 (M_S^{Co})^2$$

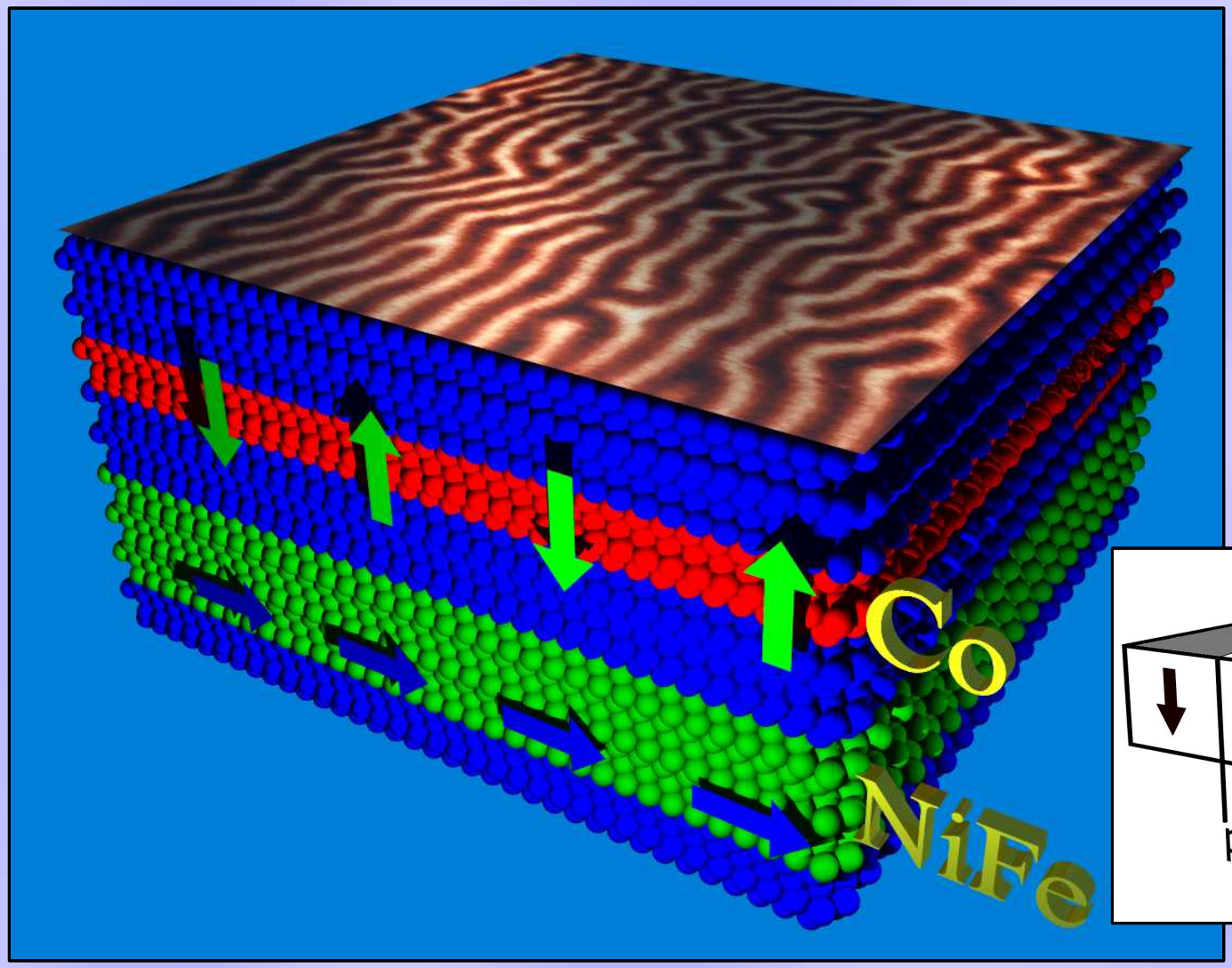

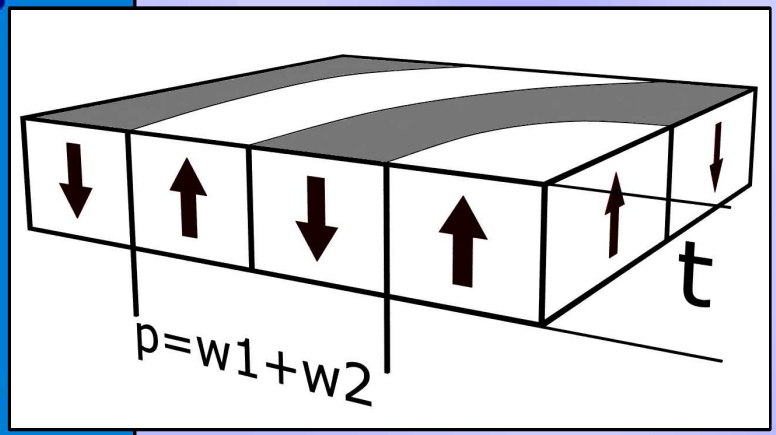

Magnetic **F**orce **M**icroscopy confirms the presence of the stripe domain structure characteristic for systems with perpendicular anisotropy.

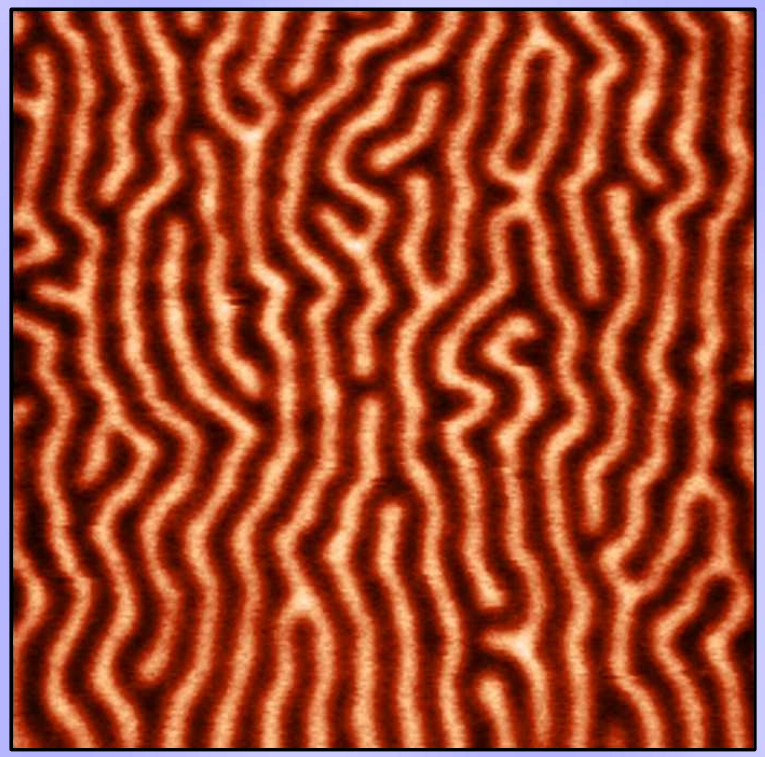

AC demagnetization
5x5μm²

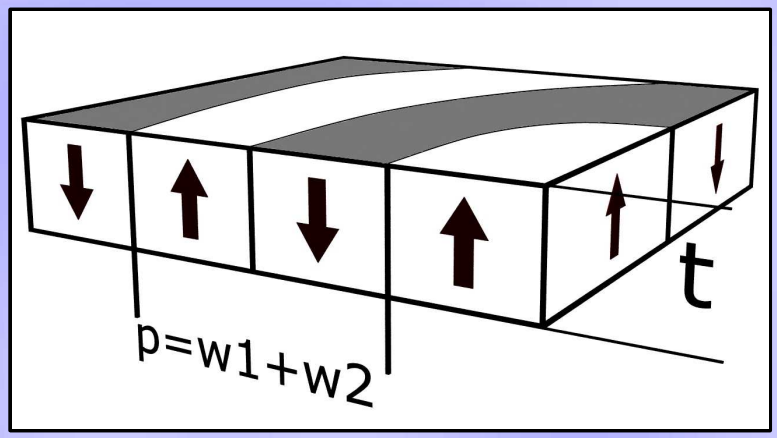

spatial period 400-1000 nm

Spatial period of the stripe domain structure depends strongly on the thicknesses of Co and Au sublayers.

$[Ni_{80}Fe_{20}*(2\ nm)/Au(2.4\ nm)/Co(1.2\ nm)/Au(2.4\ nm)]_{10}$

* with ^{57}Fe

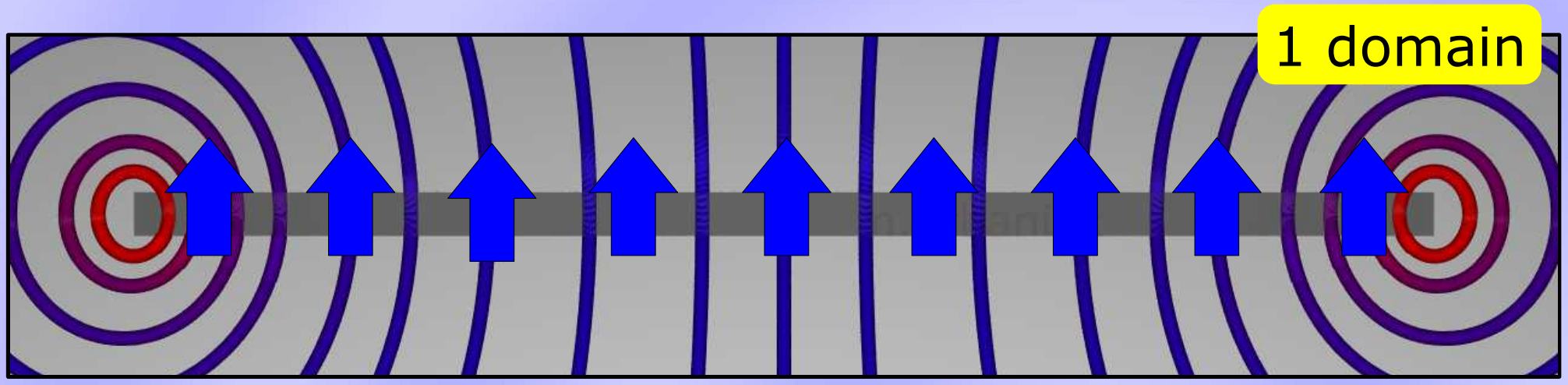

Division into **the magnetic stripe domains** increases the magnetic induction within the layer and leads to the decrease of magnetostatic energy:

$$E_{magn} = -\vec{B} \cdot \vec{M}$$

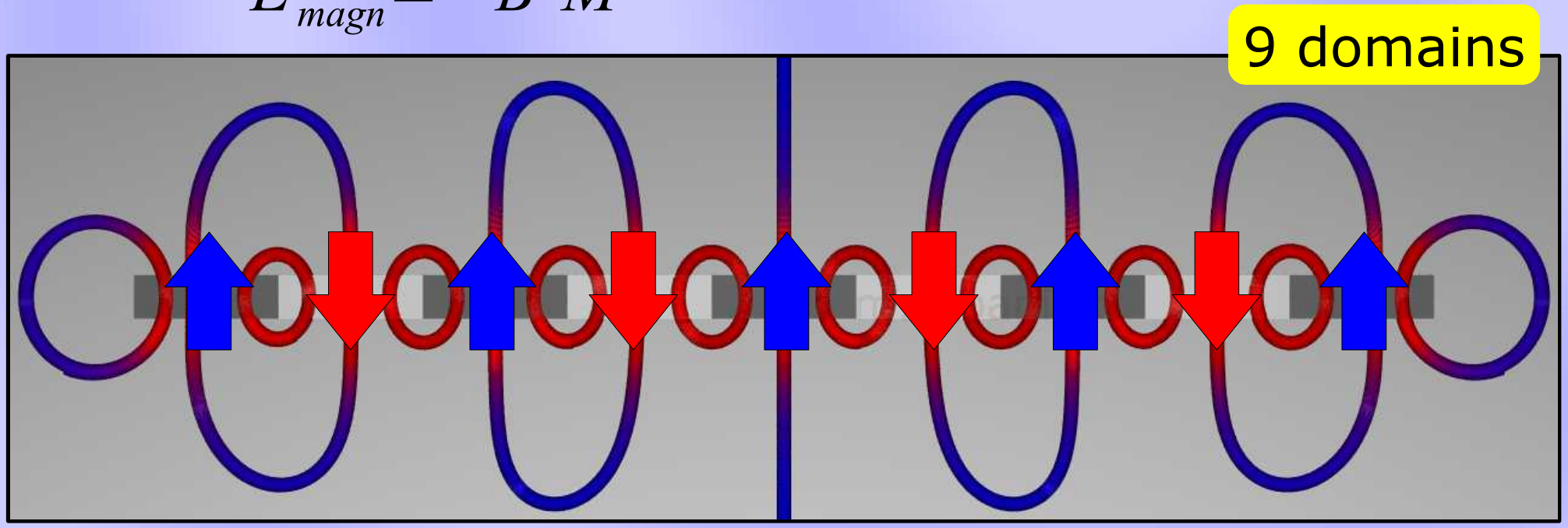

Giant magnetoresistance

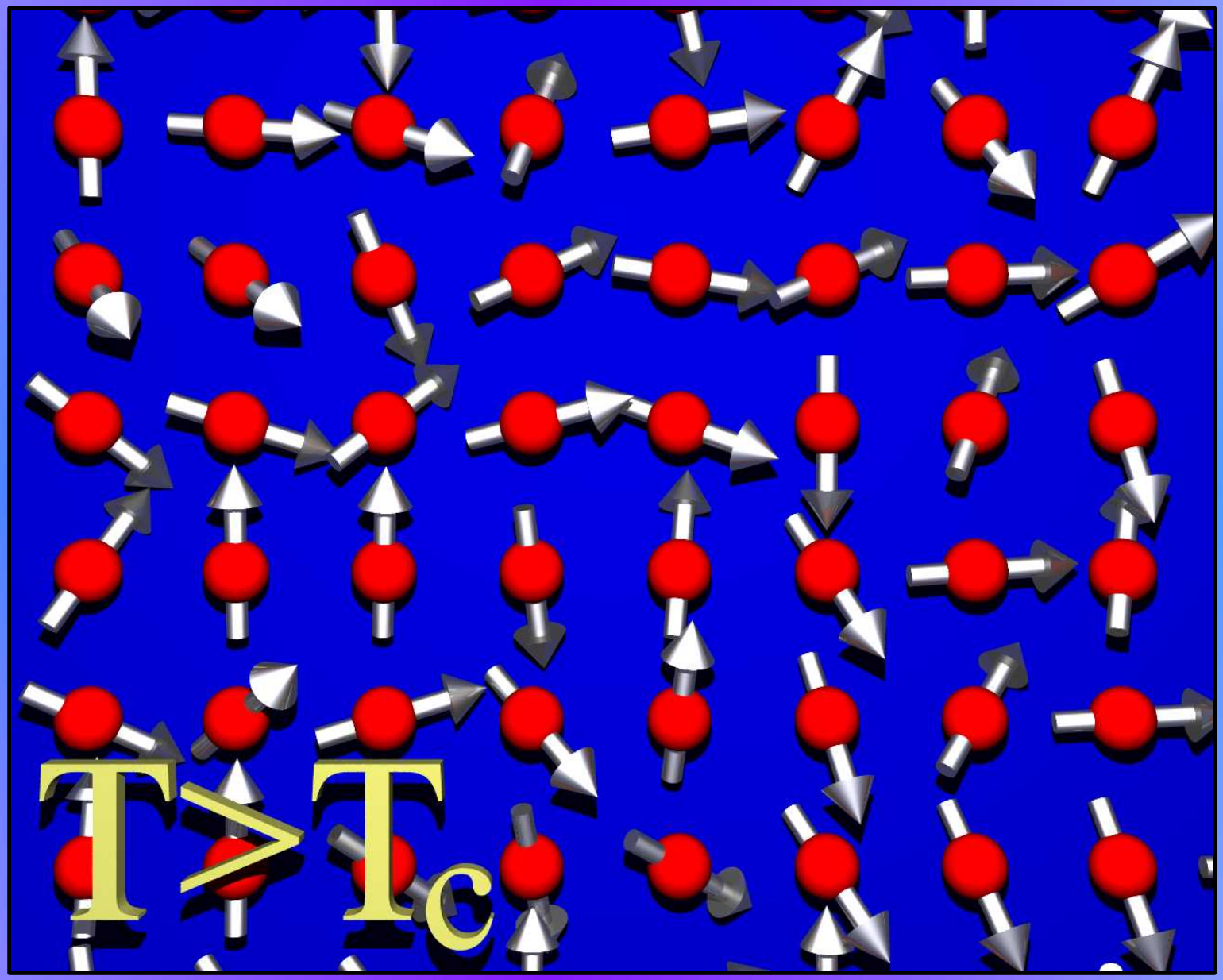

T_{Curie}:

Fe 1044 K

Co 1388 K

Ni 627 K

NiFe 660 K

Giant magnetoresistance

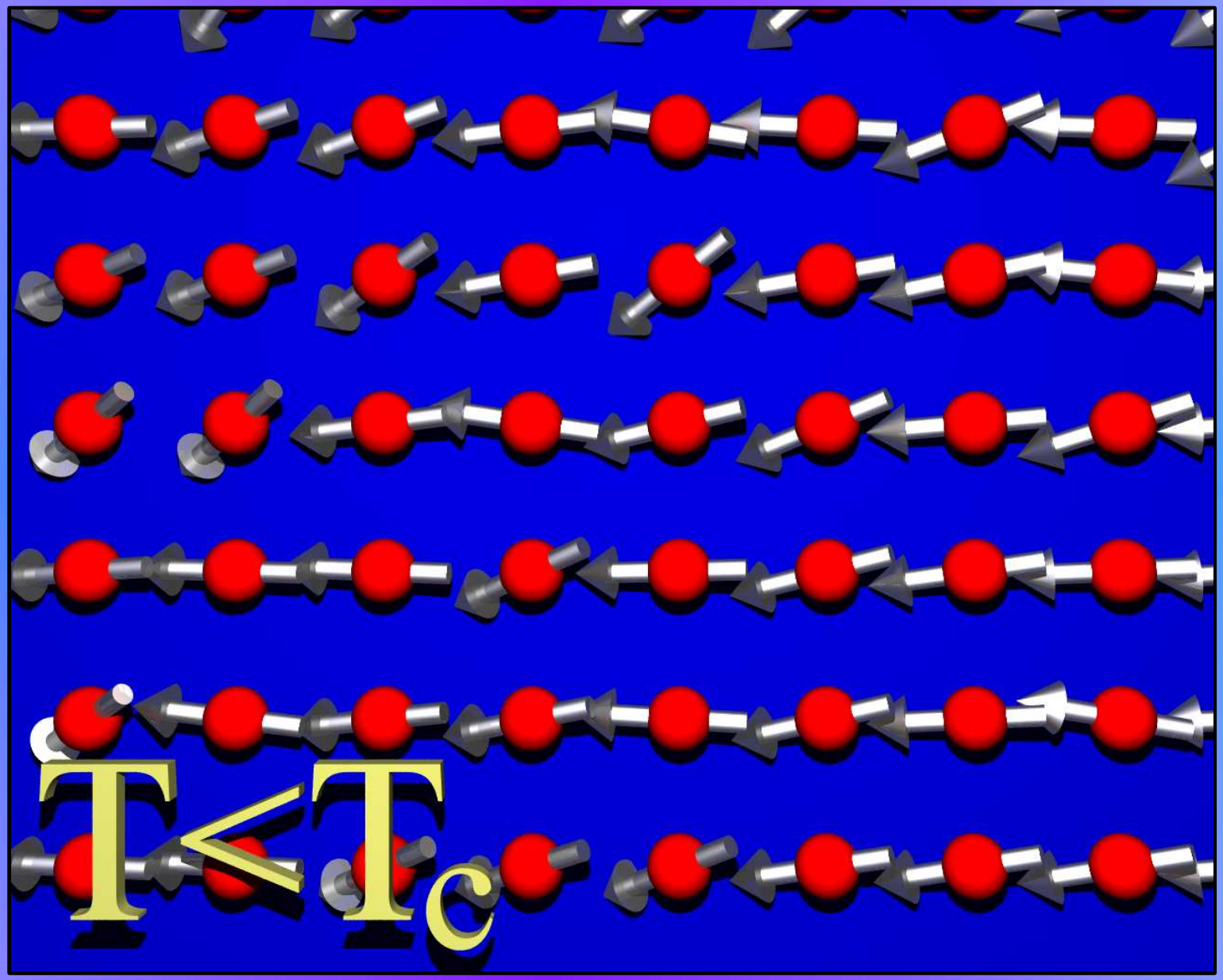

T_{Curie}:

Fe 1044 K

Co 1388 K

Ni 627 K

NiFe 660 K

Giant magnetoresistance

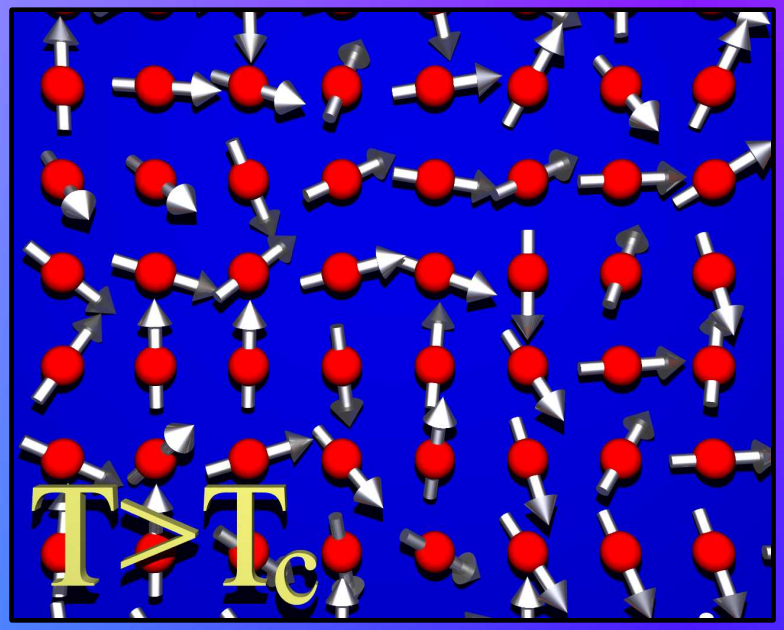

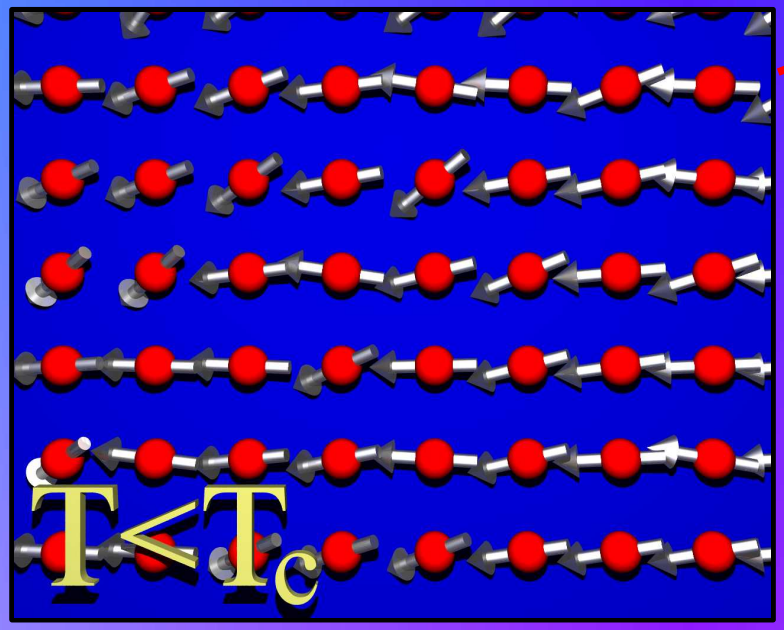

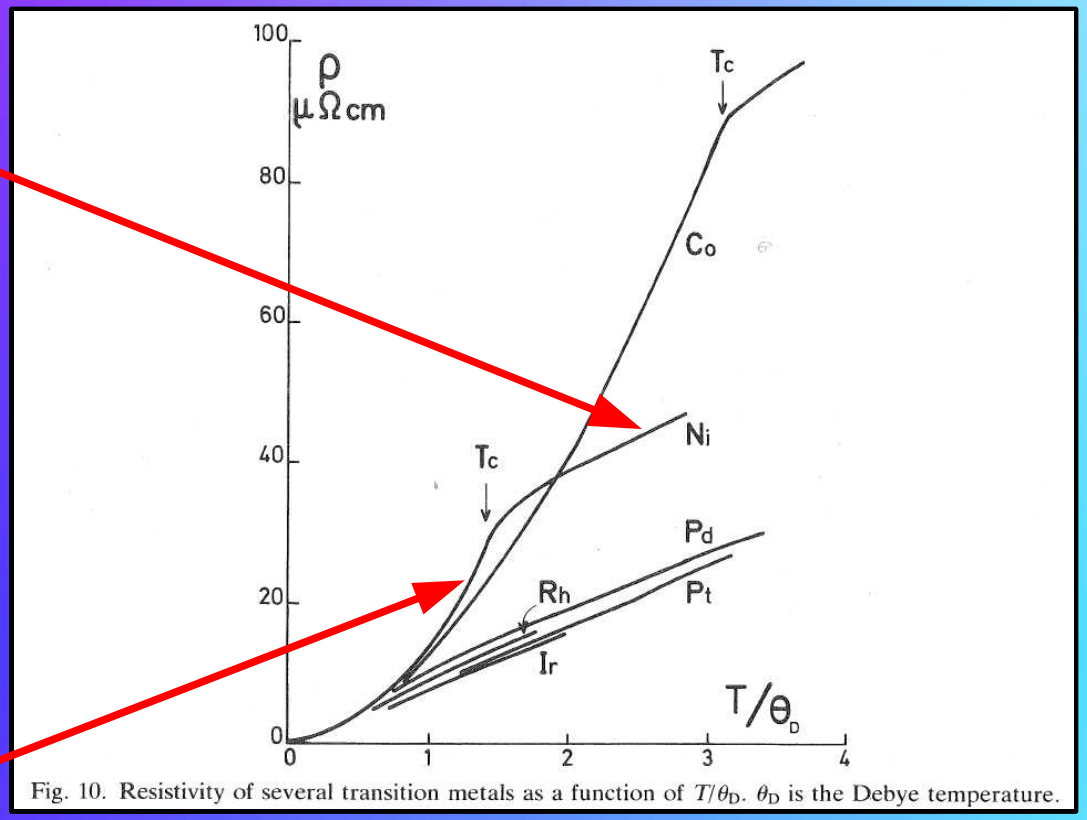

Fig. 10. Resistivity of several transition metals as a function of T/θ_D. θ_D is the Debye temperature.

Below Curie temperature the resistance of ferromagnetic materials decreases below that of non-ferromagnetic metals.

I.A.Campbell, A.Fert, in “Ferromagnetic Materials” 1982

Giant magnetoresistance

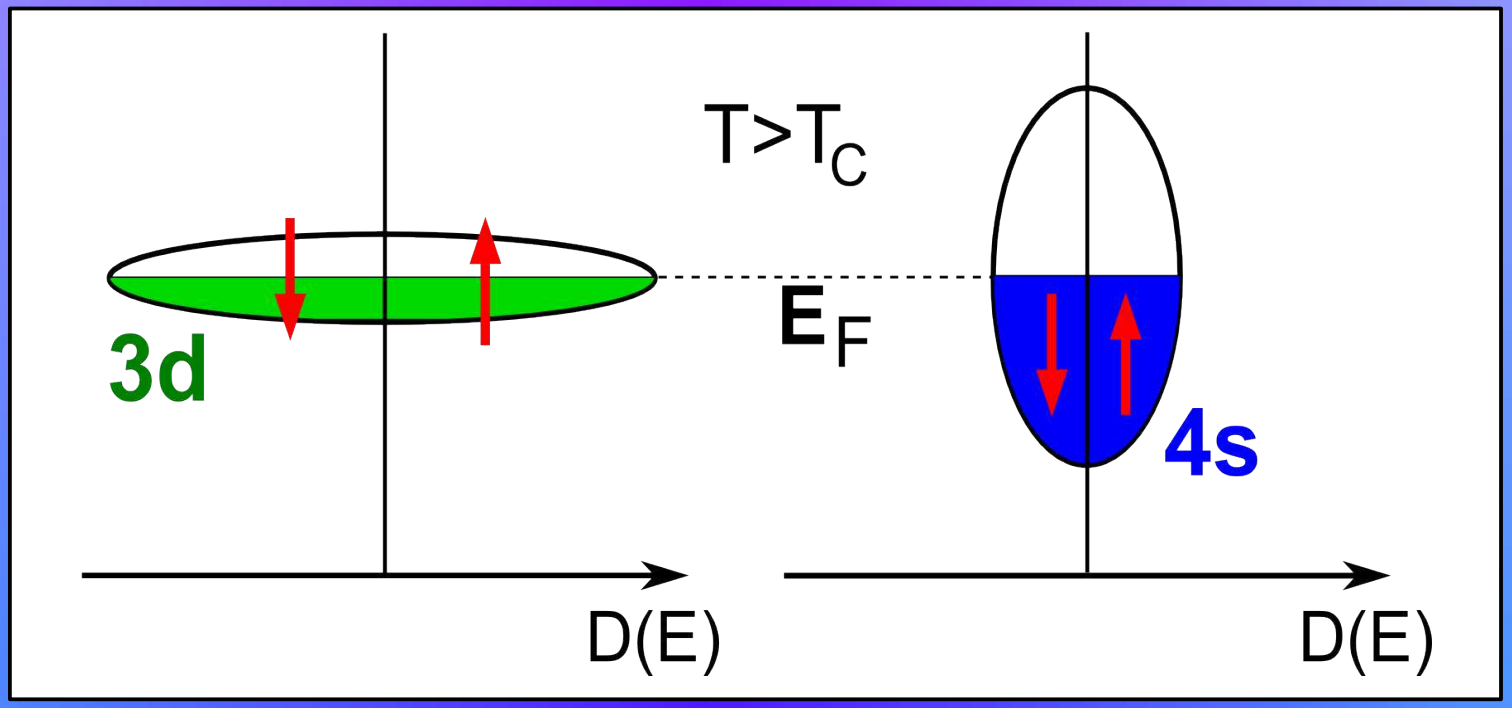

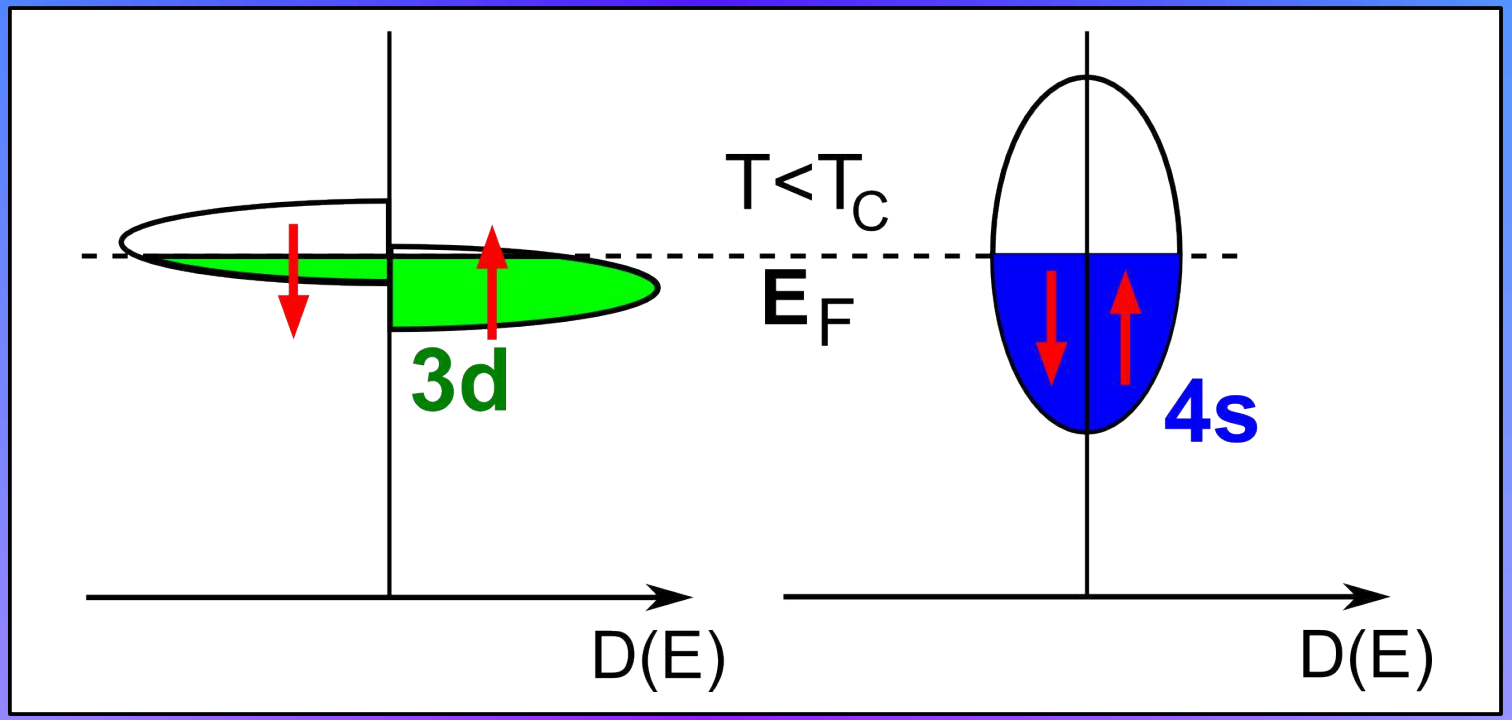

Scattering:

$s\uparrow \rightarrow d\uparrow$

$s\downarrow \rightarrow d\downarrow$

$\rho \sim D(E_F)$

$s\uparrow \rightarrow d\uparrow$

$s\downarrow \rightarrow d\downarrow$

Giant magnetoresistance

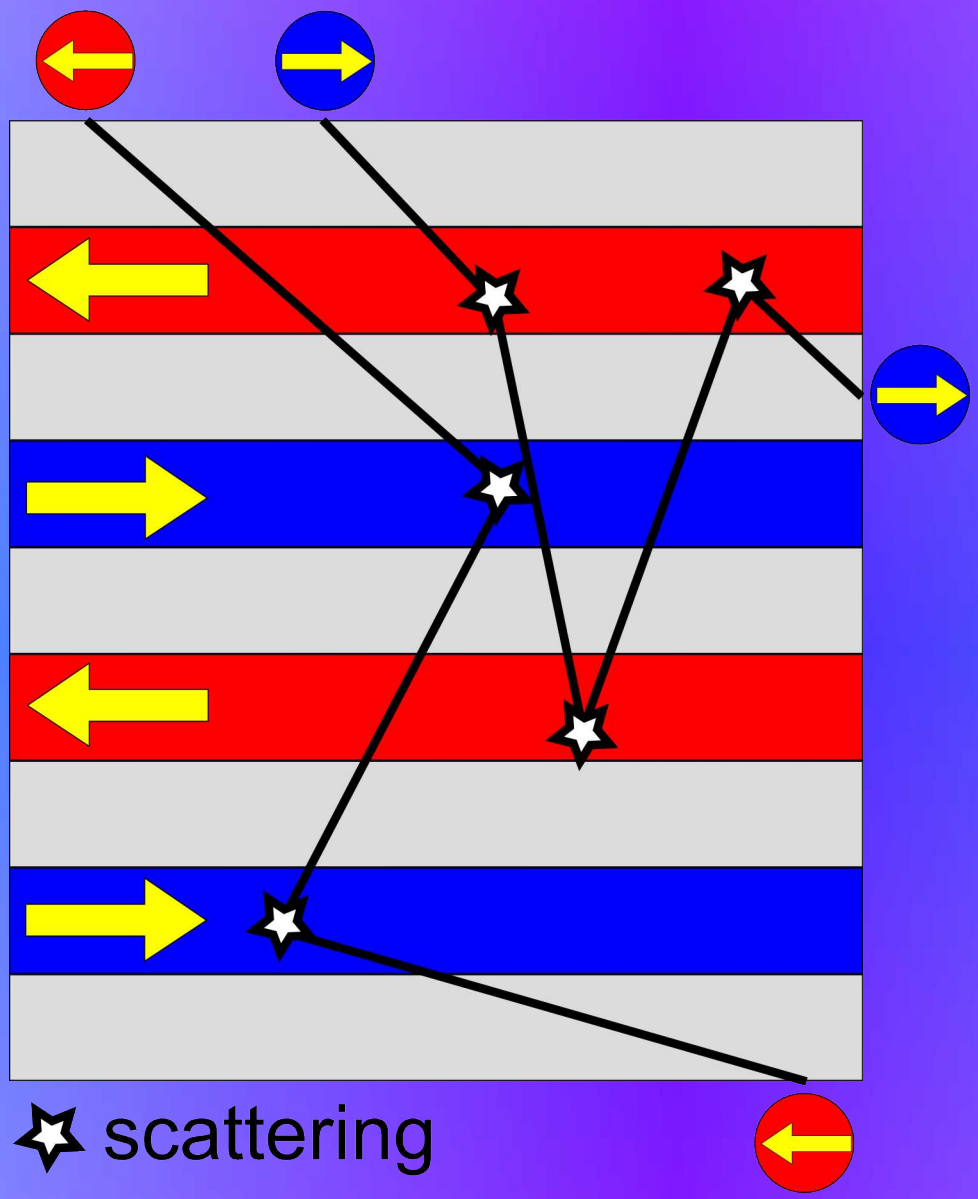

scattering

Antiparallel – high resistance

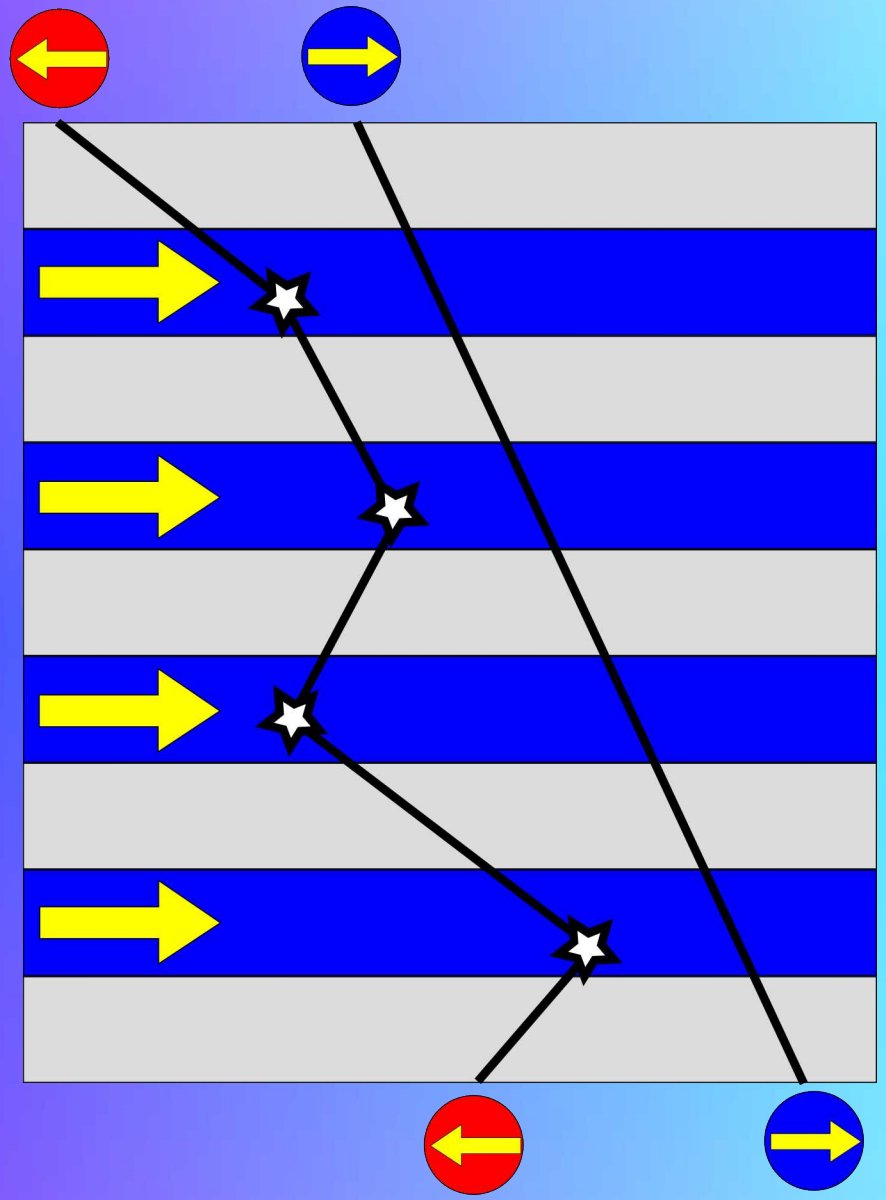

Parallel – low resistance

R.E. Camley, J. Barnaś, PRL **63**, 664 (1989)

Giant magnetoresistance

Nobel 2007 (Fert, Grünberg)

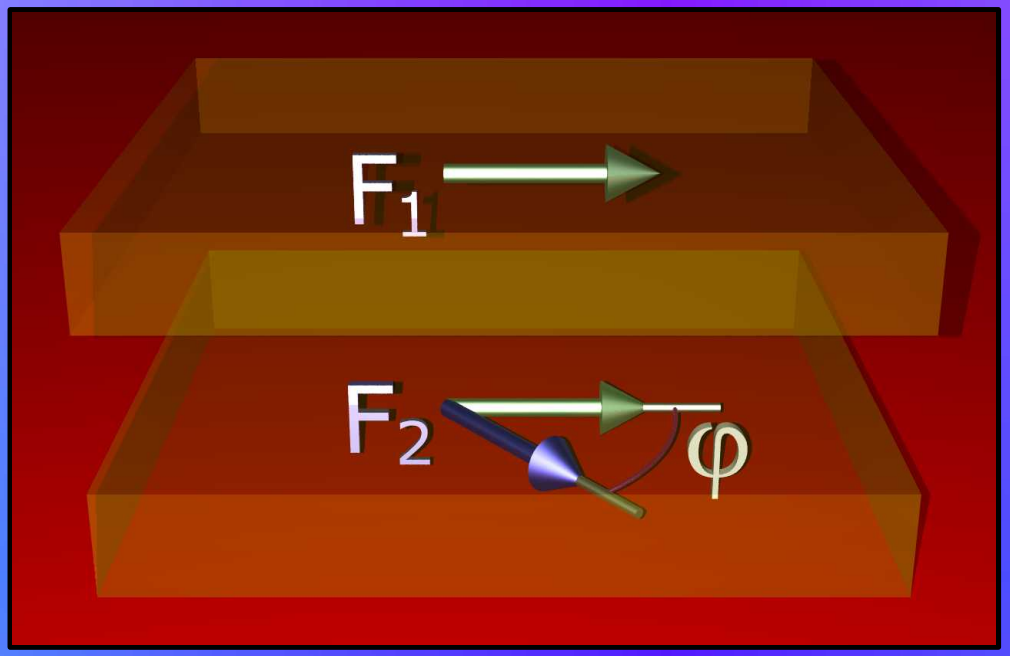

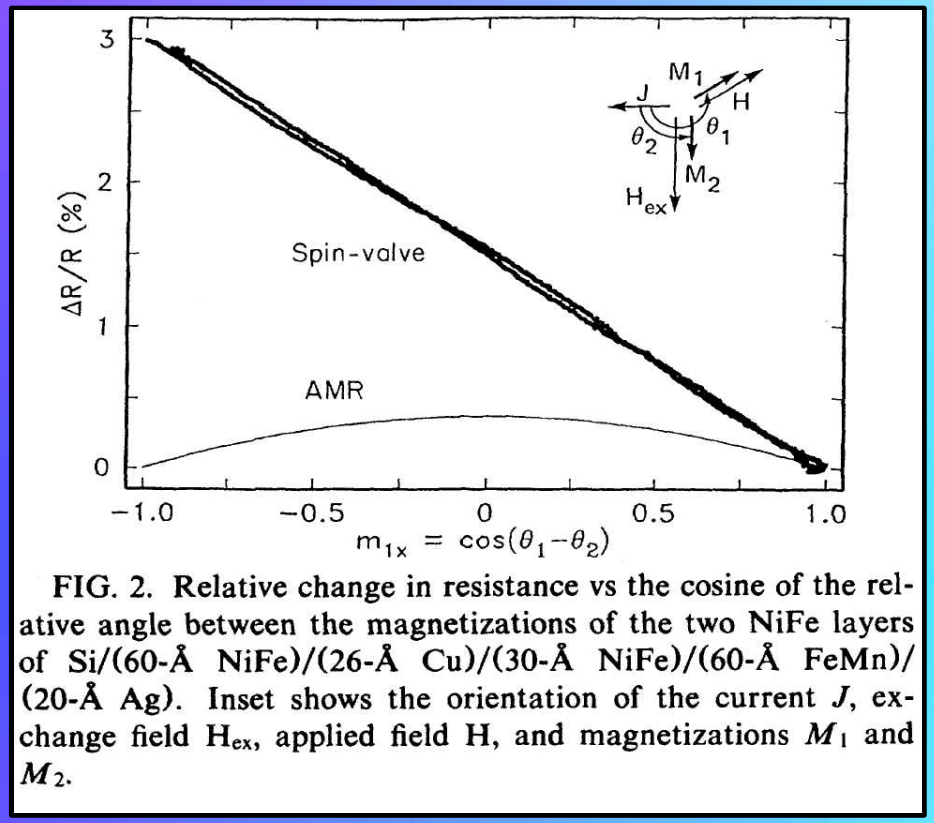

FIG. 2. Relative change in resistance vs the cosine of the relative angle between the magnetizations of the two NiFe layers of Si/(60-Å NiFe)/(26-Å Cu)/(30-Å NiFe)/(60-Å FeMn)/(20-Å Ag). Inset shows the orientation of the current J, exchange field H_{ex}, applied field H, and magnetizations M_1 and M_2.

$$\Delta R \propto \cos(\varphi)$$

B. Dieny et al., Phys. Rev. B, **43** (1991) 1297

Giant magnetoresistance

Nobel 2007 (Fert, Grünberg)

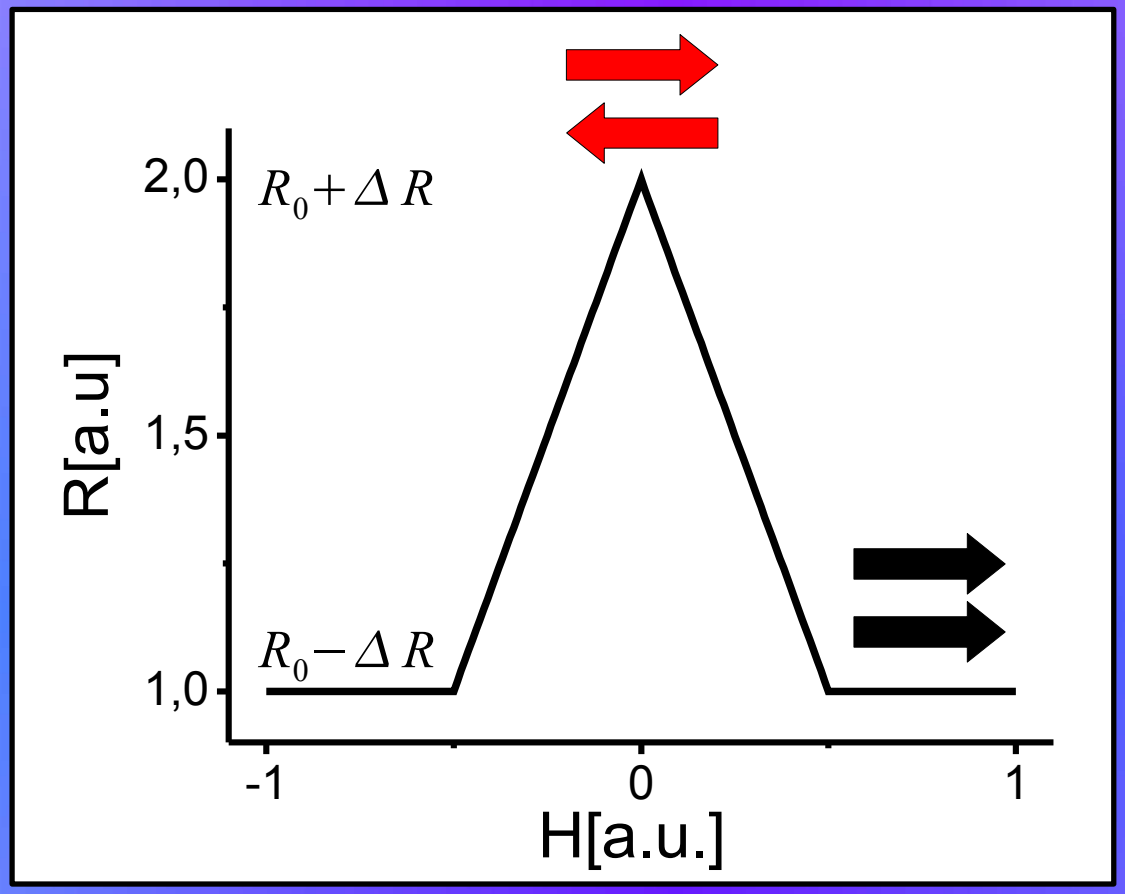

$2\Delta R/(R_0 - \Delta R) = 1 \div 100\ \%$

Co/Au,
NiFe/Au,
NiFe/Cu,
Fe/Au,.....

$$R = R_0 - \Delta R \cos(\varphi)$$

Giant magnetoresistance

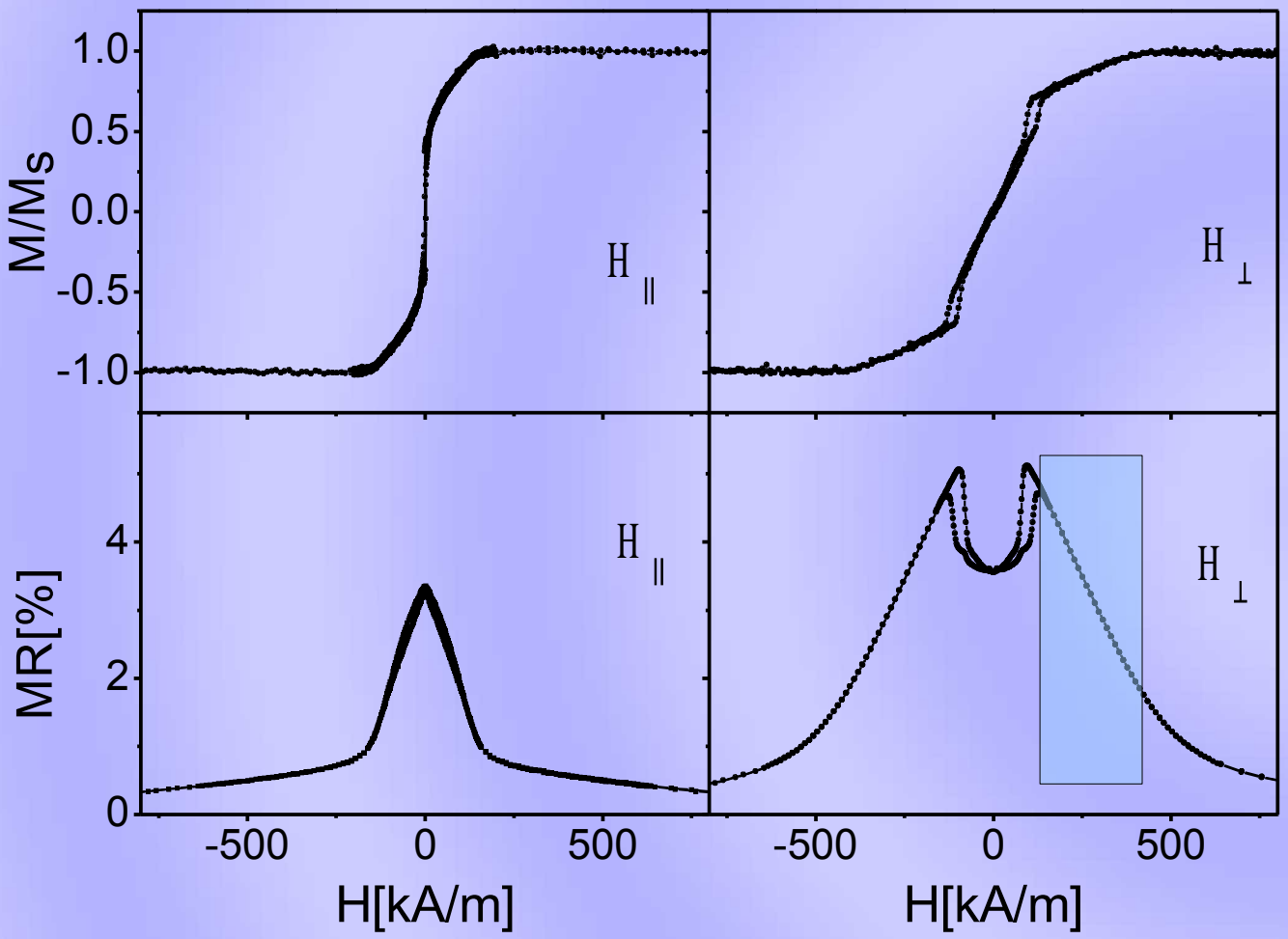

Broad linearity range in $R(H)$ dependence:

-magnetic layer magnetized along hard axis

-no hysteresis in linear range

$[Ni_{80}Fe_{20}(2\ nm)/Au(1.9\ nm)/Co(1\ nm)/Au(1.9\ nm)]_{10}$

Giant magnetoresistance

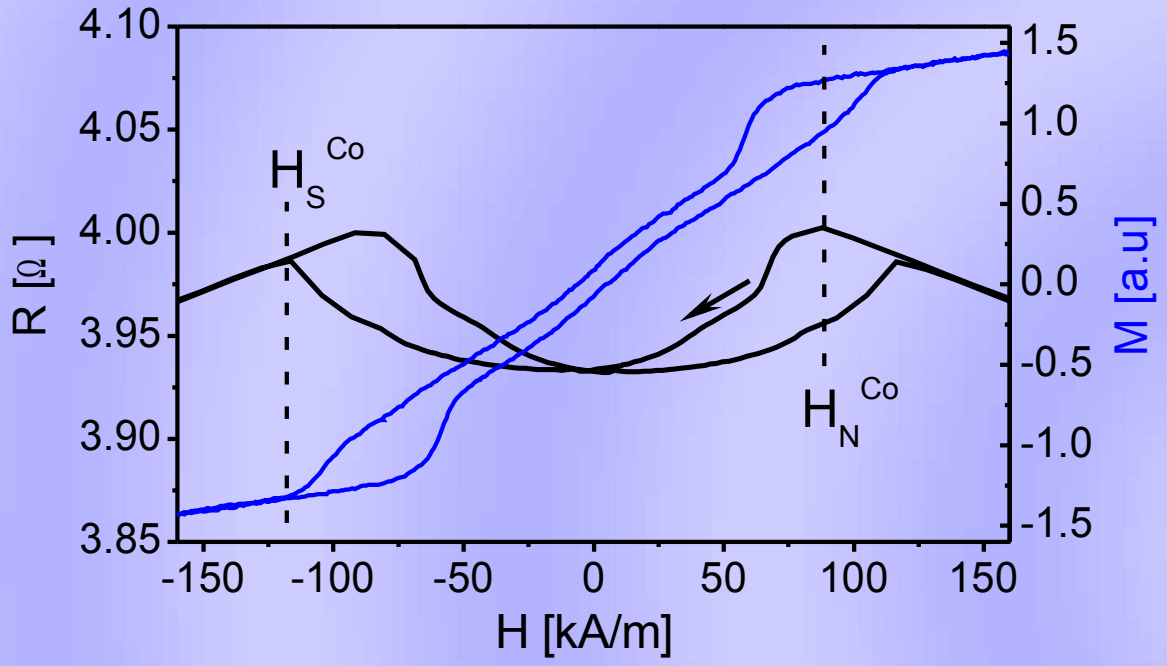

There is a local minimum of resistance in the $R(H)$ dependence.

The nucleation field (creation of the domain structure) and the annihilation field (saturation of Co layers) are visible both in $R(H)$ and $M(H)$ dependencies.

Giant magnetoresistance

Explaining the R(H) dependence

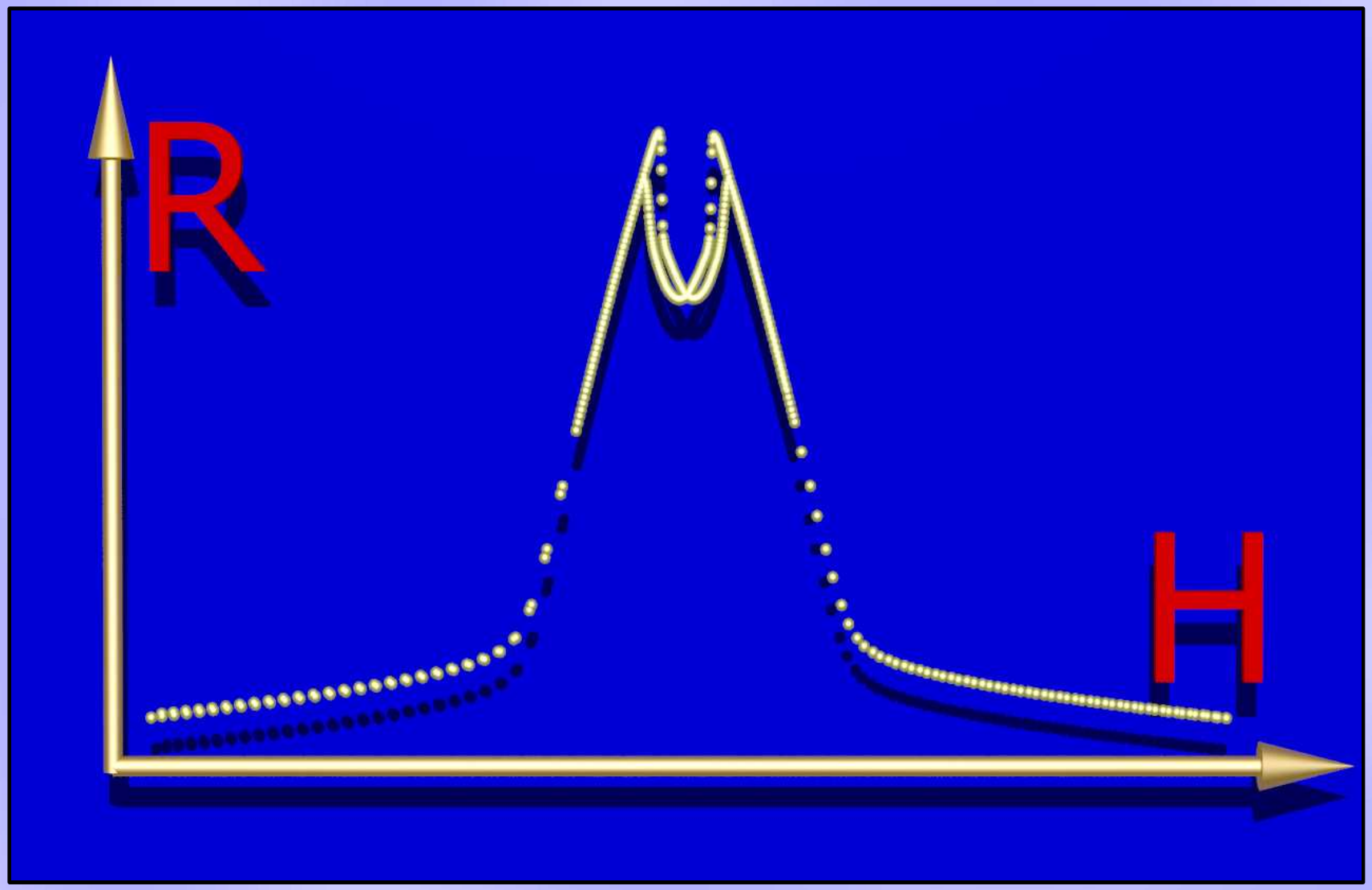

Giant magnetoresistance

Explaining the R(H) dependence

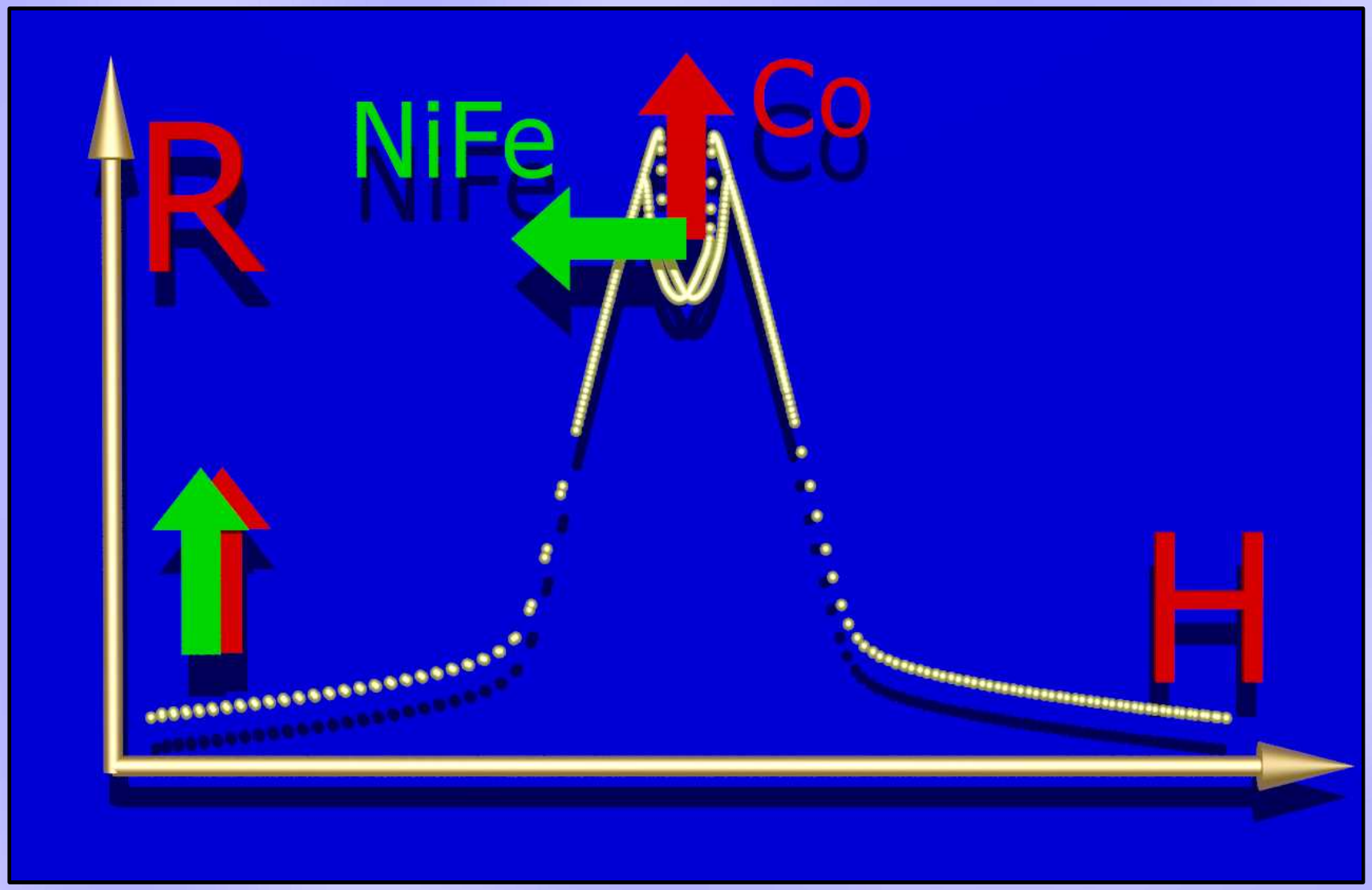

Giant magnetoresistance

Explaining the R(H) dependence

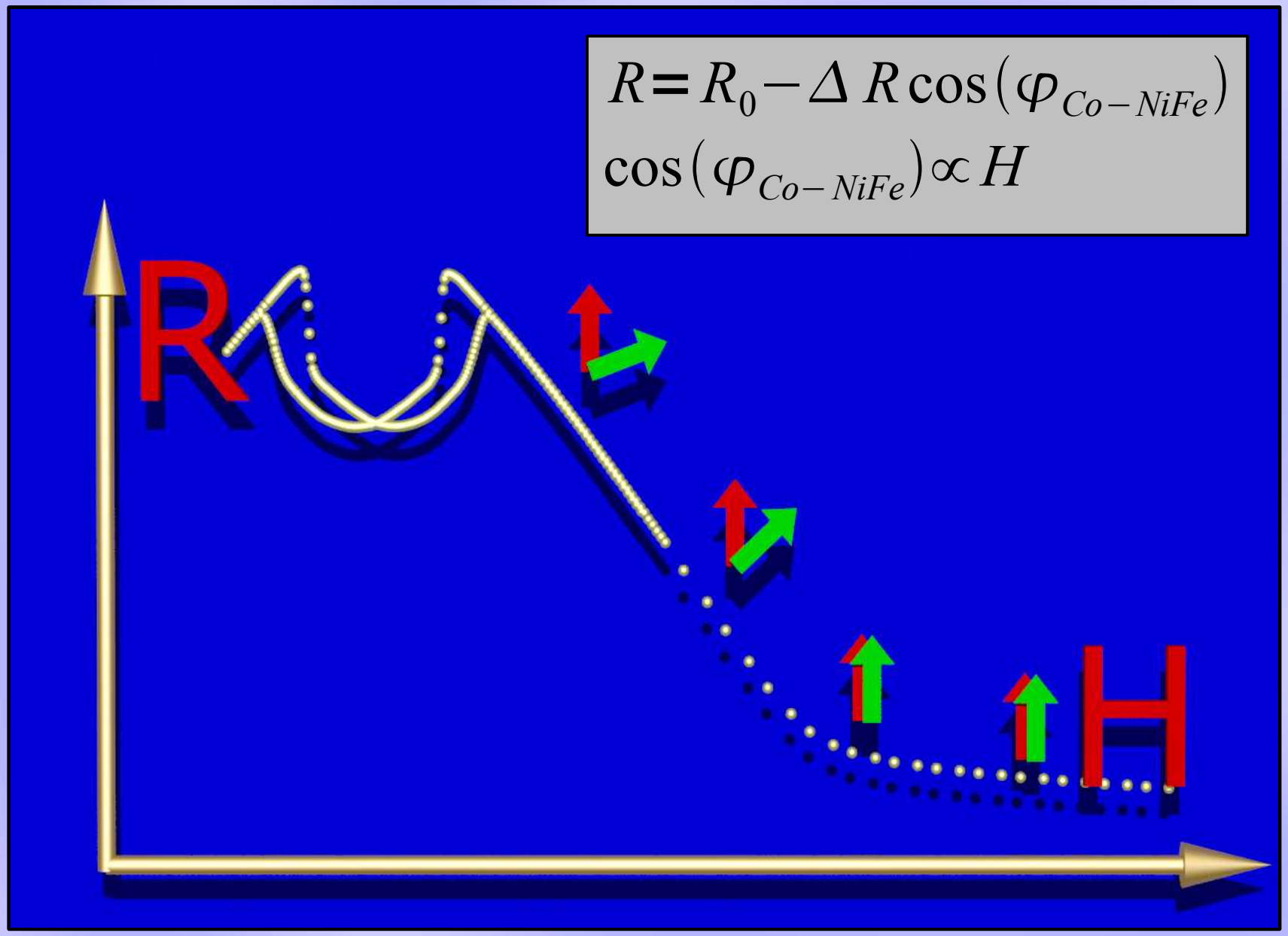

Giant magnetoresistance

Explaining the R(H) dependence

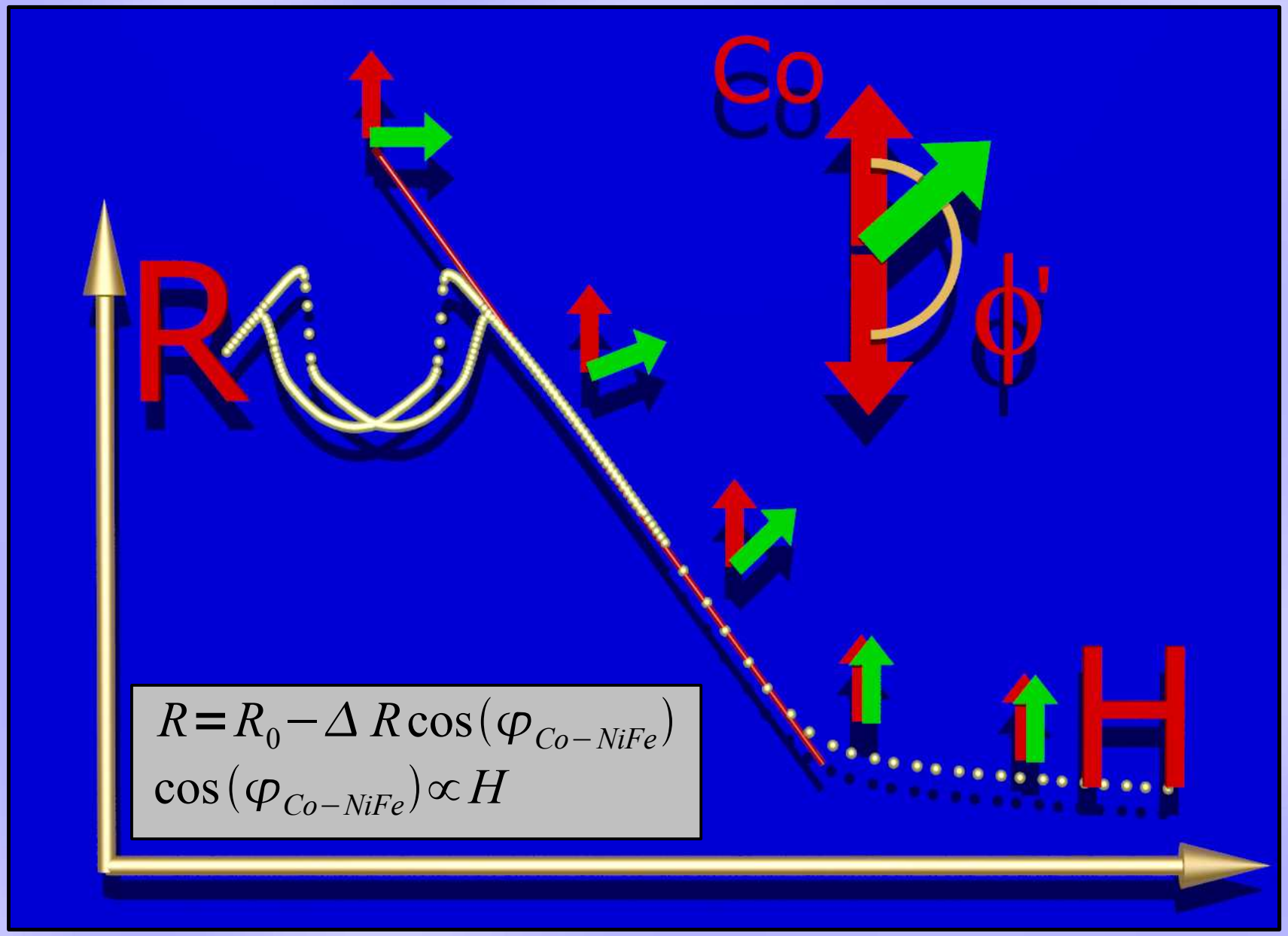

Giant magnetoresistance

Anisotropic magnetoresistance

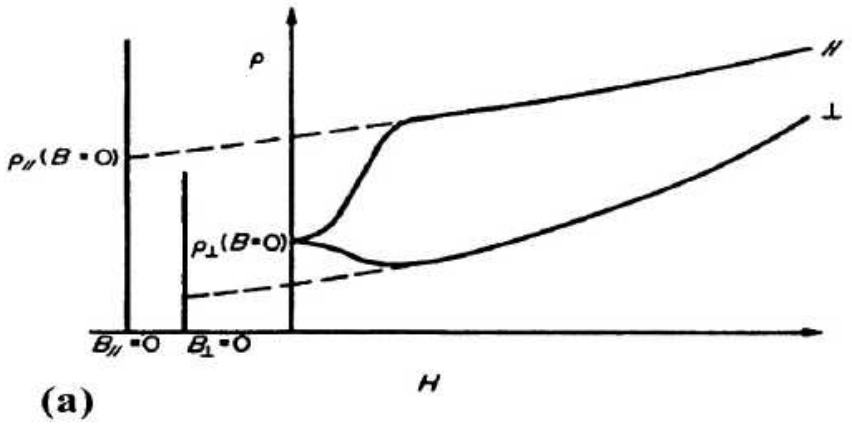

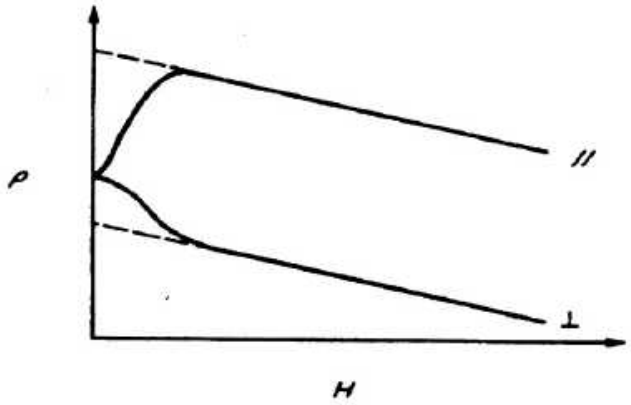

Abbildung 2.3: Schematische Darstellung der Magnetfeldabhängigkeit des spezifischen Widerstands in einem ferromagnetischen Metall. Im Niederfeldbereich dominiert der AMR, wogegen oberhalb des Sättigungsmagnetfeldes der positive Magnetwiderstand (a) oder der negative Magnetwiderstand durch Reduzierung der Spinunordnung (b) dominiert. Die gestrichelten Linien deuten an, wie man durch Rückextrapolation den positiven oder negativen Magnetwiderstandsbeitrag bei kleinen Feldern eliminieren kann, um den reinen AMR-Effekt zu erhalten.

AMR in NiFe alloys reaches 5%.

resistance of the system depends on **the angle** between the measuring current and the local magnetic moment

Grundlagen der Magnetoelektronik, Rudolf Gross, Achim Marx, Garching, Oktober 2000
http://www.wmi.badw-muenchen.de/teaching/Lecturenotes/

Giant magnetoresistance

Anisotropic magnetoresistance

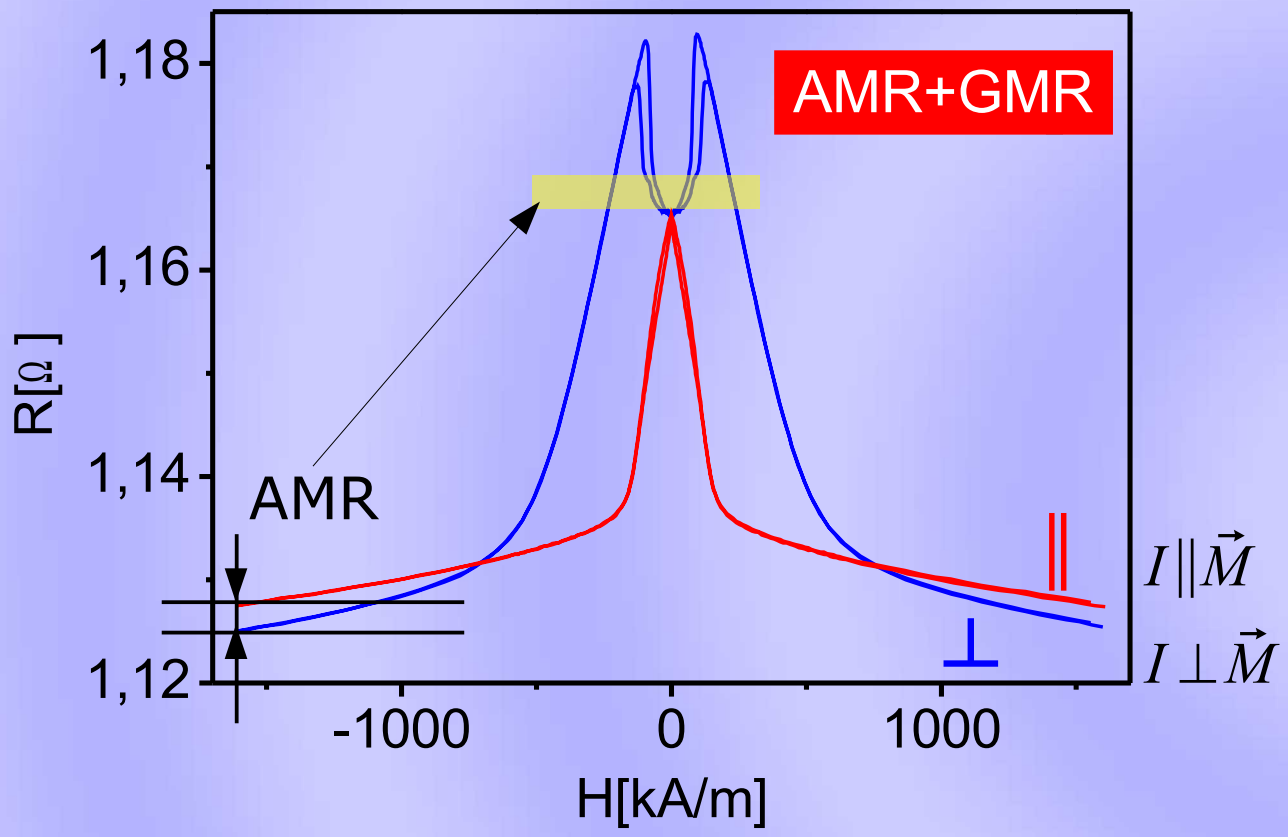

Anisotropic magnetoresistance to small to account for the observed local minima of resistance.

$[Ni_{80}Fe_{20}(2\ nm)/Au(1.9\ nm)/Co(1nm)/Au(1.9\ nm)]_{10}$

Giant magnetoresistance

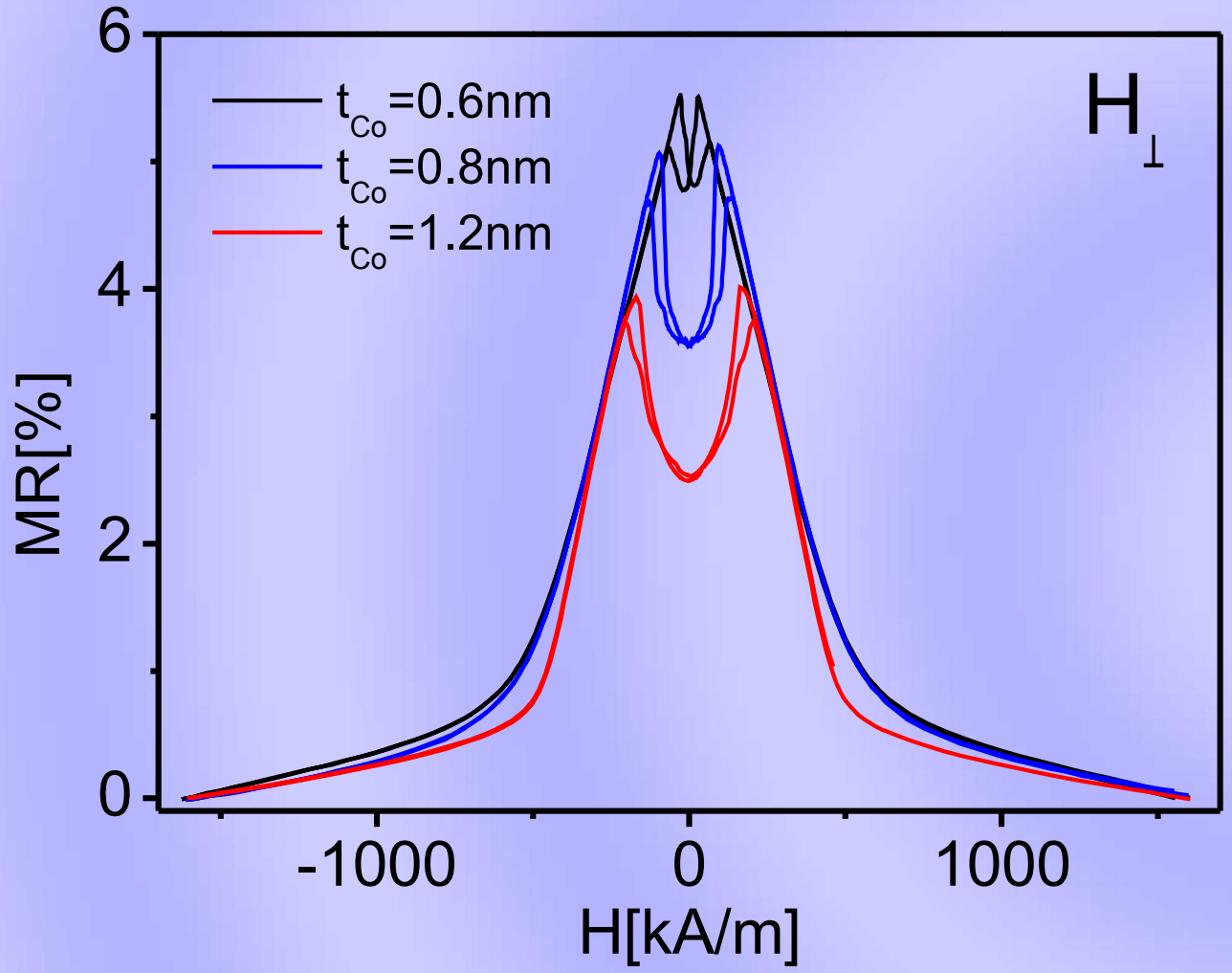

A relative "depth" of resistance minimum is a strong function of Co layers thickness.

?

Magnetostatic coupling

$[Ni_{80}Fe_{20}(2\ nm)/Au(1.9\ nm)/Co(\boldsymbol{t_{Co}})/Au(1.9\ nm)]_{10}$

Interlayer coupling in magnetic multilayers

- coupling through magnetic bridging

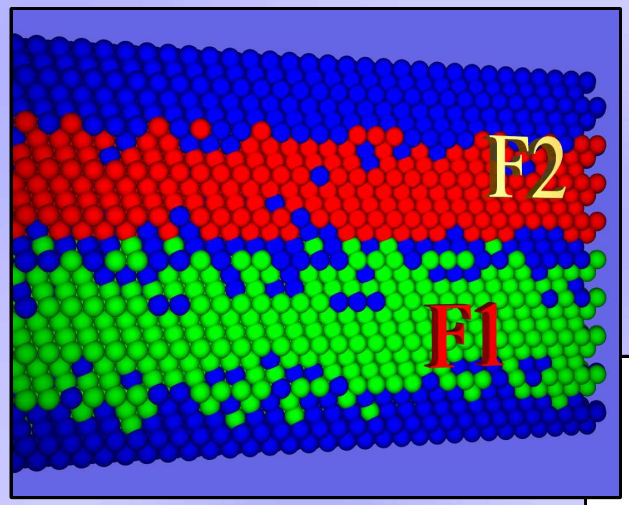

- magnetostatic coupling

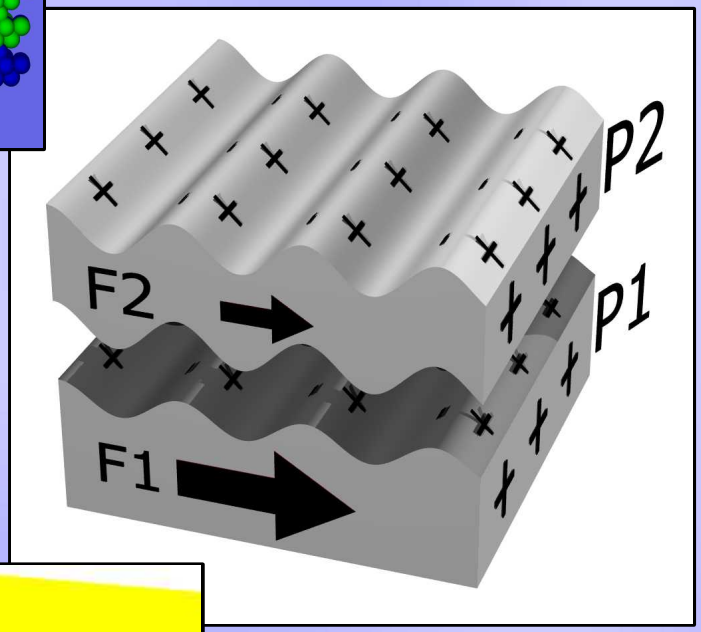

- Ruderman–Kittel–Kasuya–Yosida like coupling

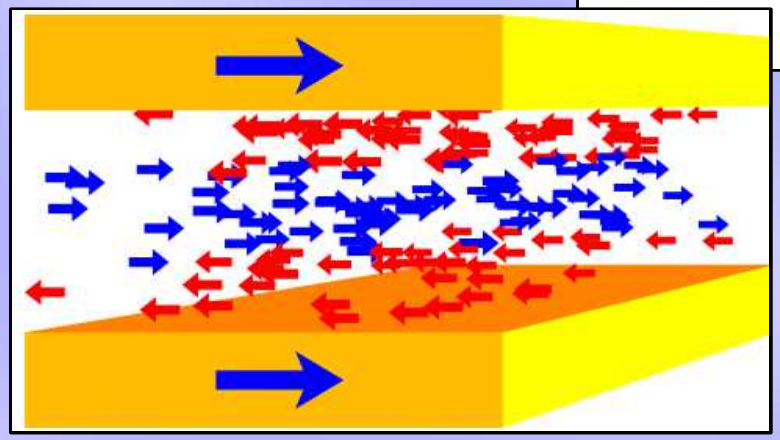

Magnetostatic coupling

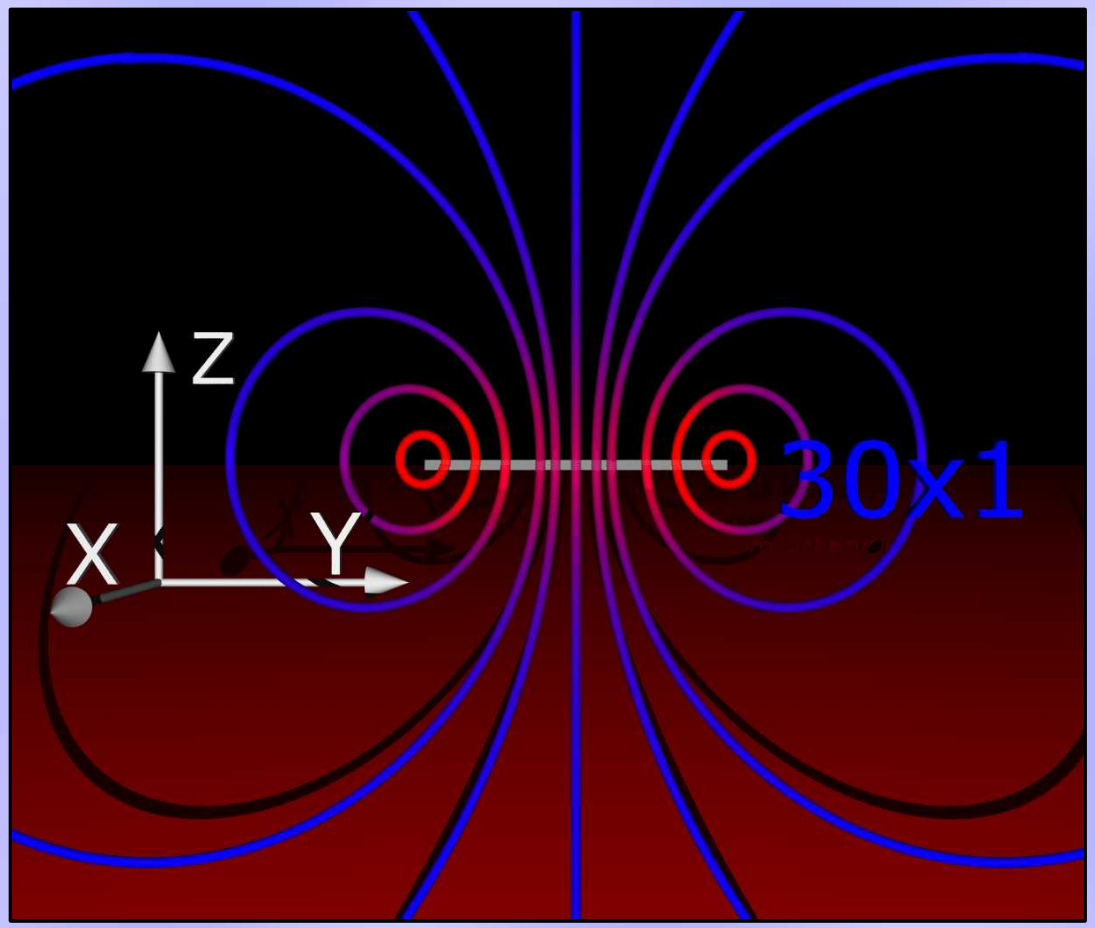

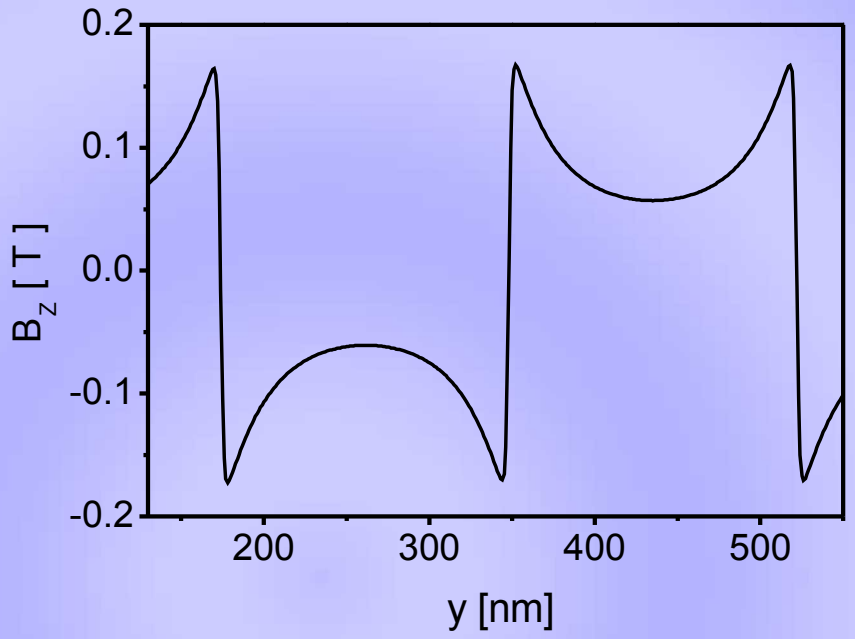

Model:

Domains width: 174 nm

t_{Co}=0.6 nm **10 Co layers**

Magnetic fields that originate from the stripe domain structure in $[NiFe/Au/Co/Au]_N$ multilayers are of the order of 0.1 T.

Magnetostatic coupling

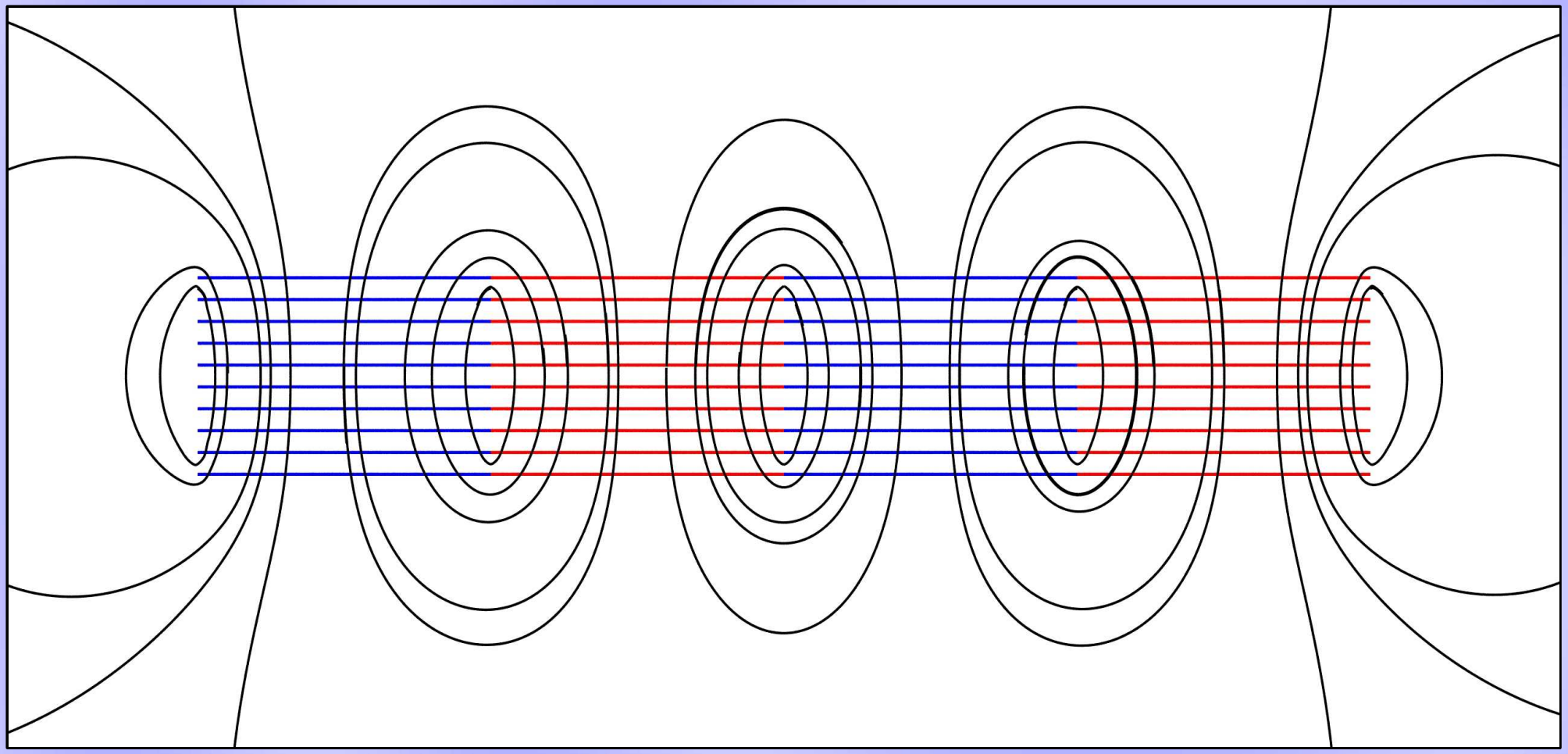

Magnetic field of the stack of the infinite “stripe domains” (from Biot-Savart law). Domain width=100, thickness=1, multilayer period=7.

Magnetostatic coupling

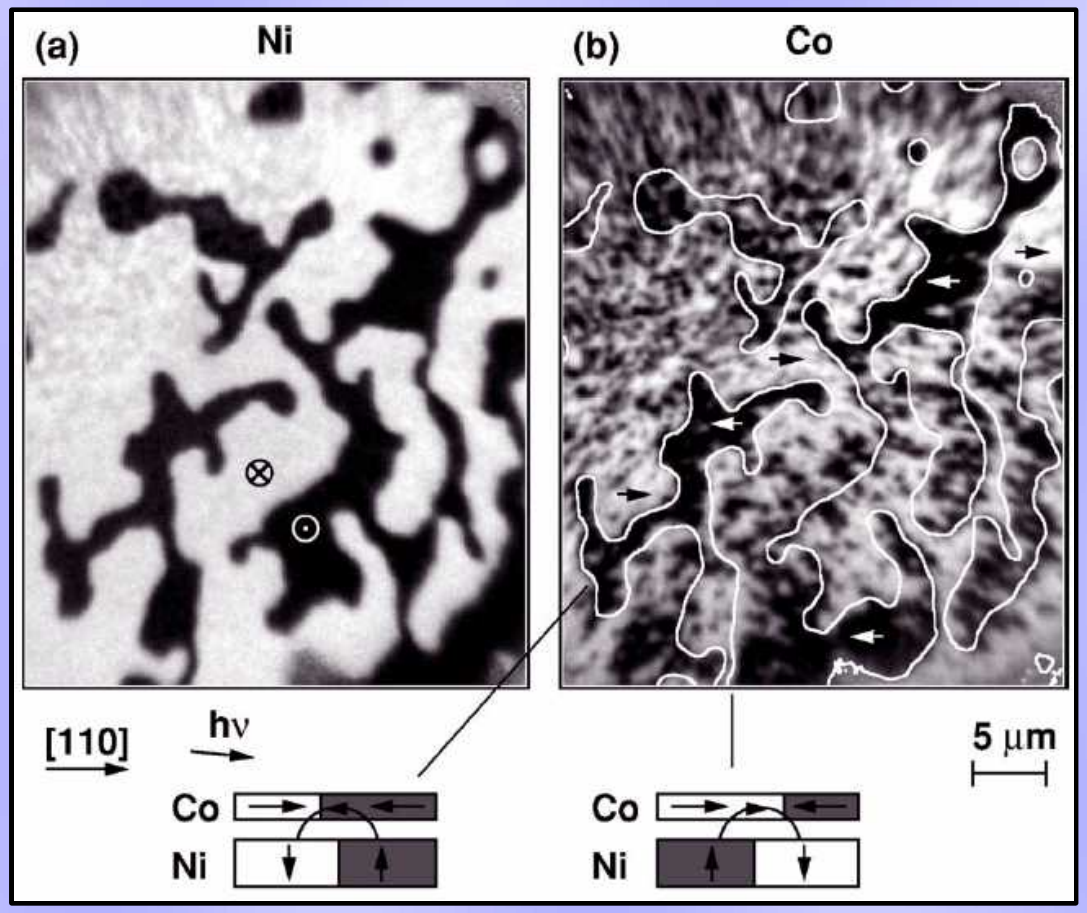

photoemission electron microscopy (PEEM) +
X ray magnetic circular dichroism (XMCD)

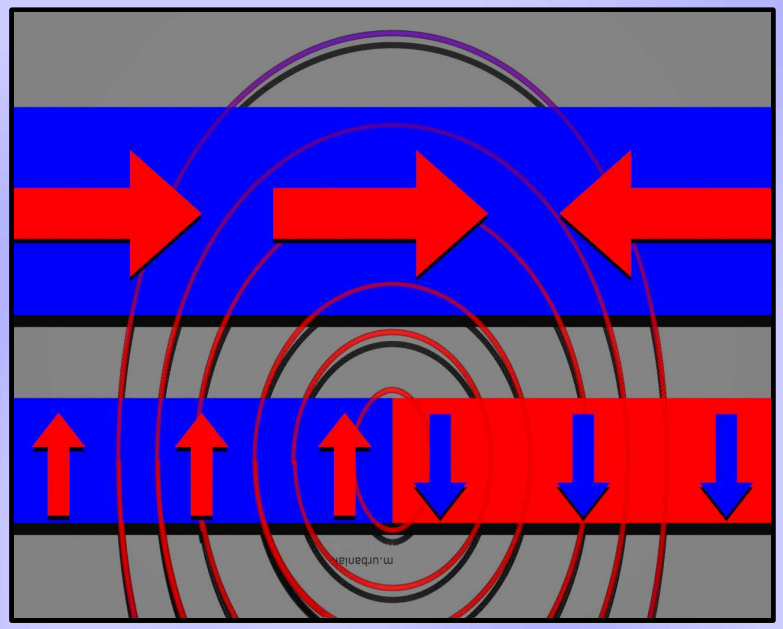

-Cu(001)/Ni/Cu/Co
-Cu – wedge (1ML/10m)
-electron beam evaporation
-**Ni – perpendicular anisotropy**
-field of Ni DW in Co: 250Oe

W. Kuch, L. I. Chelaru, K. Fukumoko, F. Porrati, F. Offi, M. Kotsugi, J. Kirchner,
Phys. Rev. B **67,** 214403 (2003)

Magnetostatic coupling

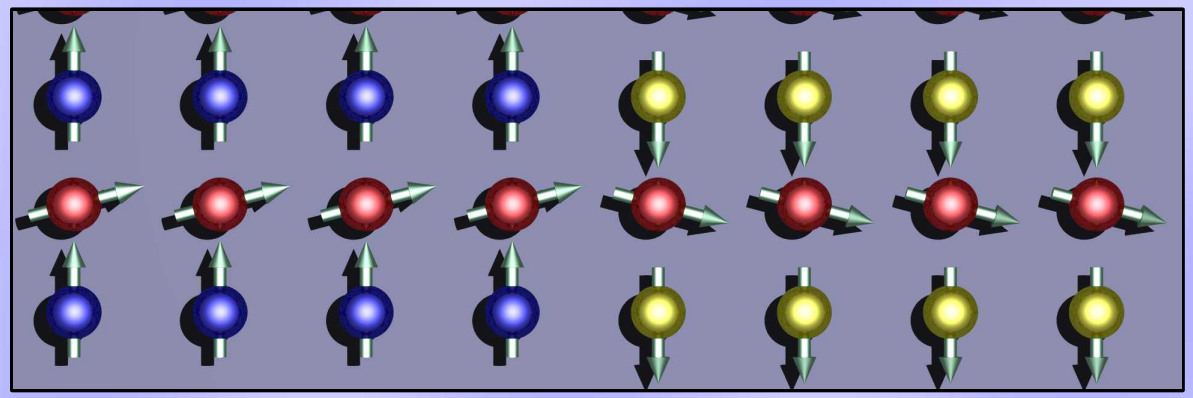

Co
NiFe
Co

$H = H_{domains}$

$$\cos(\varphi_{\uparrow}) = \frac{H_{appl} + H_d}{M_S^{Co}}$$

$$\cos(\varphi_{\downarrow}) = \frac{H_{appl} - H_d}{M_S^{Co}}$$

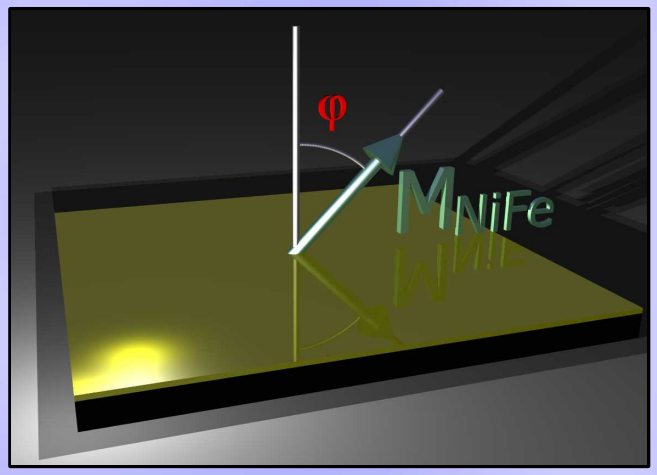

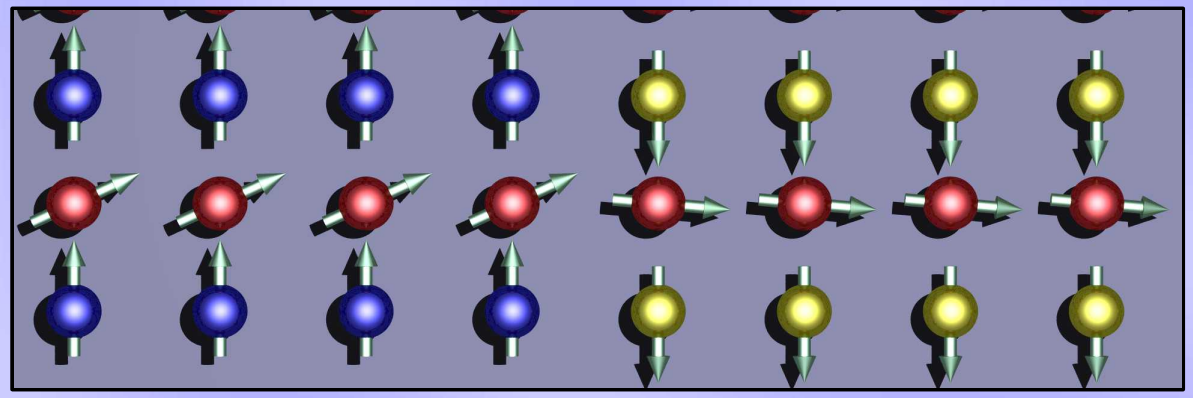

$H = H_{domains} + H_{appl}$

H_{appl}

Magnetostatic coupling

Micromagnetic simulation

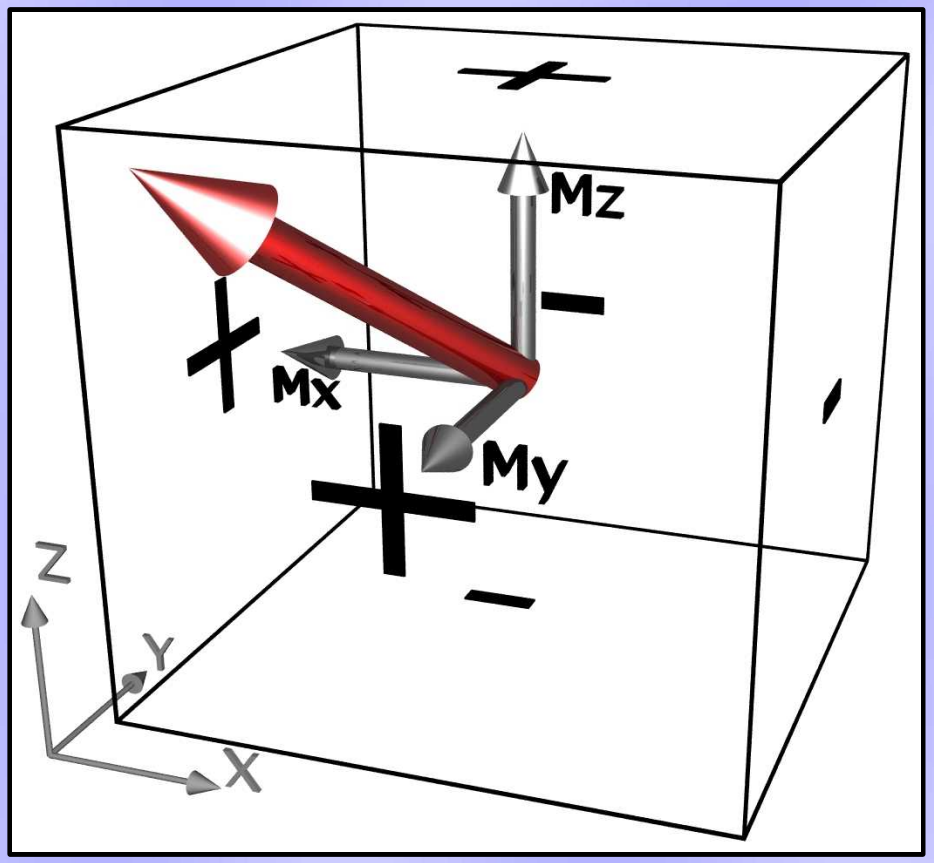

$$r=[(x_n-x_q)^2+(z_n-z_q)^2+(z_n-z_q)^2]^{1/2}$$

$$\phi_m^{(i)}=\frac{1}{4\pi}\frac{(\vec{\mu}\,\vec{r})}{r^3}$$

$$\vec{H}=-\vec{\nabla}\,\phi$$

$$\phi_m=\frac{1}{4\pi}\int d\tau\,(\vec{M}\,\nabla_q r^{-1})$$

$$(\vec{M}\,\nabla_q r^{-1})=\nabla_q(r^{-1}\vec{M})-\frac{1}{r}\nabla_q\vec{M}$$

$$\phi_m=\frac{1}{4\pi}\left(-\int d\tau\,\frac{\nabla_q\vec{M}}{r}+\oint dS\,\frac{\vec{n}\,\vec{M}}{r}\right)$$

С. В. Вонсовский, МАГНЕТИЗМ
«Наука», 1971

"Magnetic charges" present within the volume of the magnetized body
And on its outer boundaries are the sources of magnetic field.

Magnetostatic coupling

Micromagnetic simulation

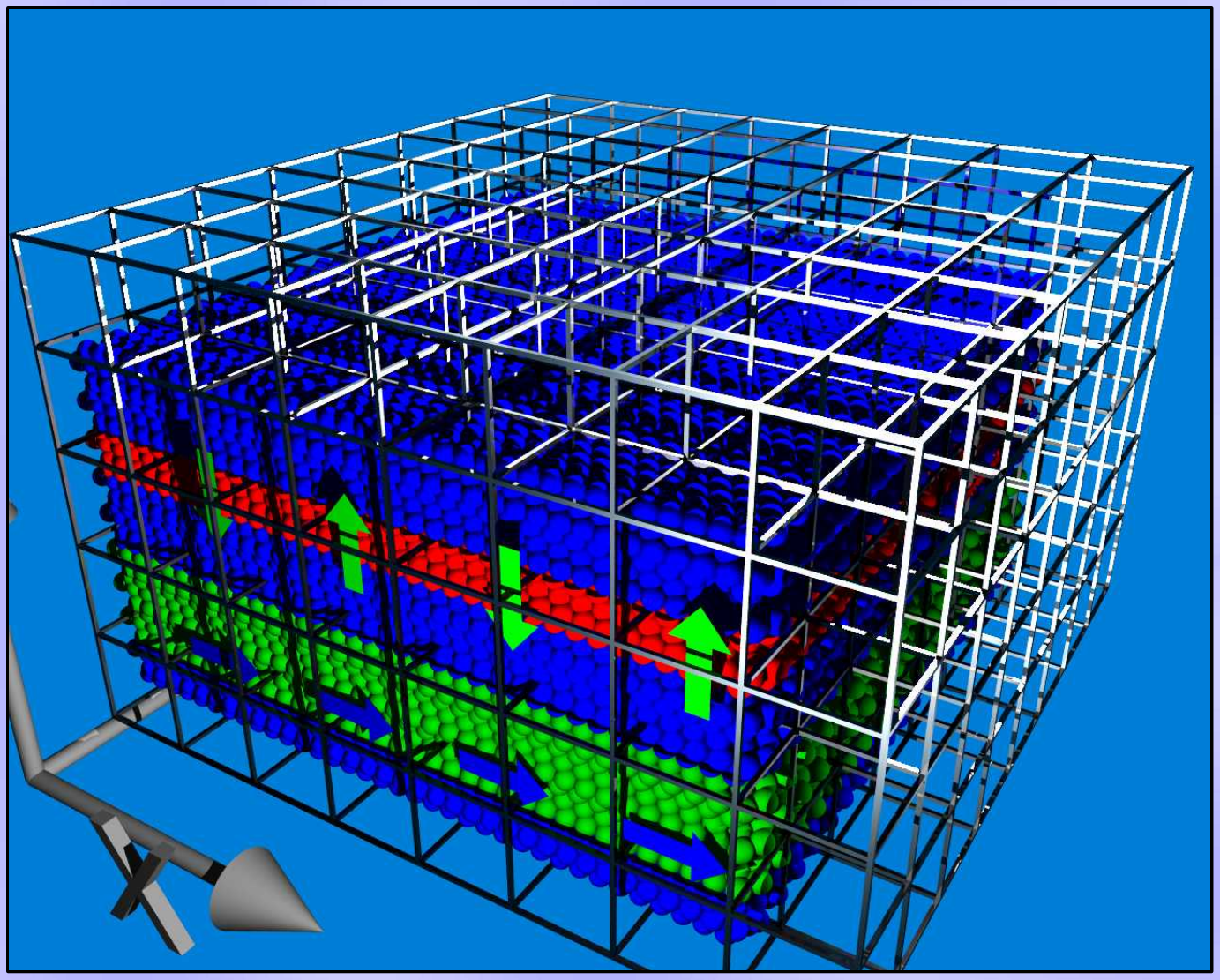

A single cell contains MANY atoms.

Continuous approximation - the magnetization is a continuous function of the position.

Magnetostatic coupling

Micromagnetic simulation

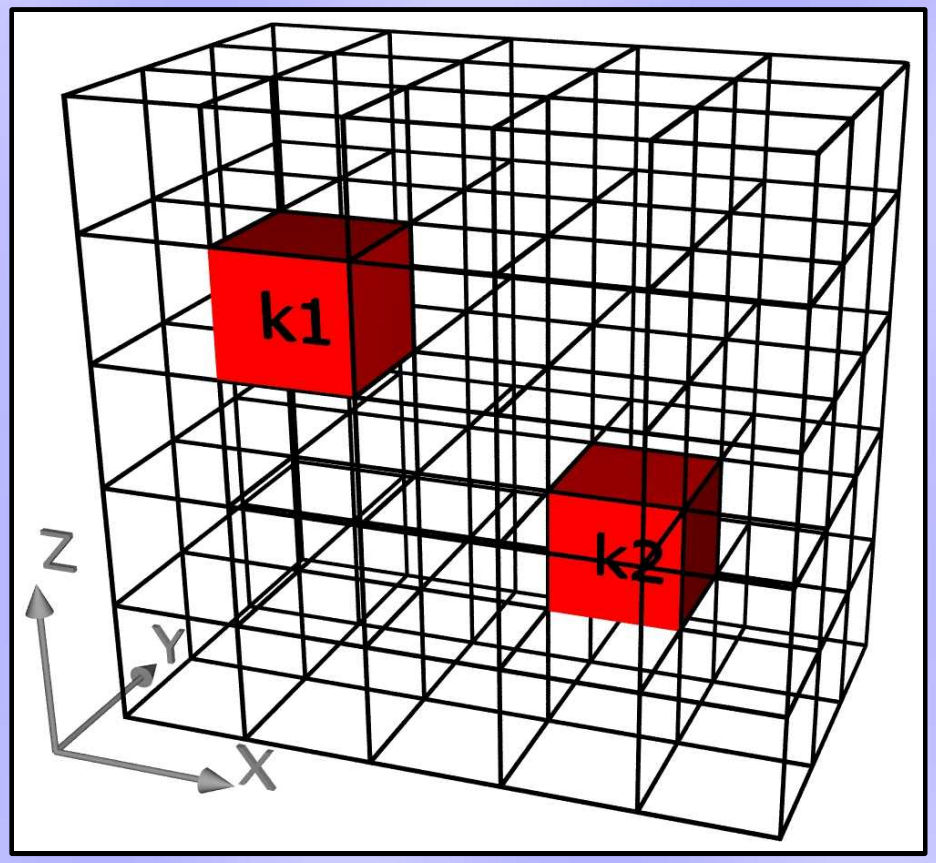

LLG equation:

$$\vec{m} = \frac{\vec{M}}{M_S}$$

$$\frac{d\vec{m}}{dt} = \gamma_0 (\vec{m} \times \vec{H}_{eff}) + \alpha [\vec{m} \times \frac{d\vec{m}}{dt}]$$

$$\vec{H}_{eff} = \frac{-1}{\mu_0 \vec{M}_S} \frac{\delta \epsilon}{\delta \vec{m}}$$

$$\vec{H}_{eff} = \frac{A}{\mu_0 \vec{M}_S} \frac{\delta (\nabla \vec{m})^2}{\delta \vec{m}} - \frac{1}{\mu_0 \vec{M}_S} \frac{\delta \epsilon_K}{\delta \vec{m}} + \vec{H}_{appl} + \vec{H}_d$$

$\vec{H}_{eff}$ = “exchange energy”+“anisotropy energy” +“external field”+“own field”

Magnetostatic interactions between cells have of **a long-range character**.

J. E. Milat, M. J. Donahue
Handbook of Magnetism and Advanced Magnetic Materials, John Wiley & Sons 2007

Magnetostatic coupling

Micromagnetic simulation*

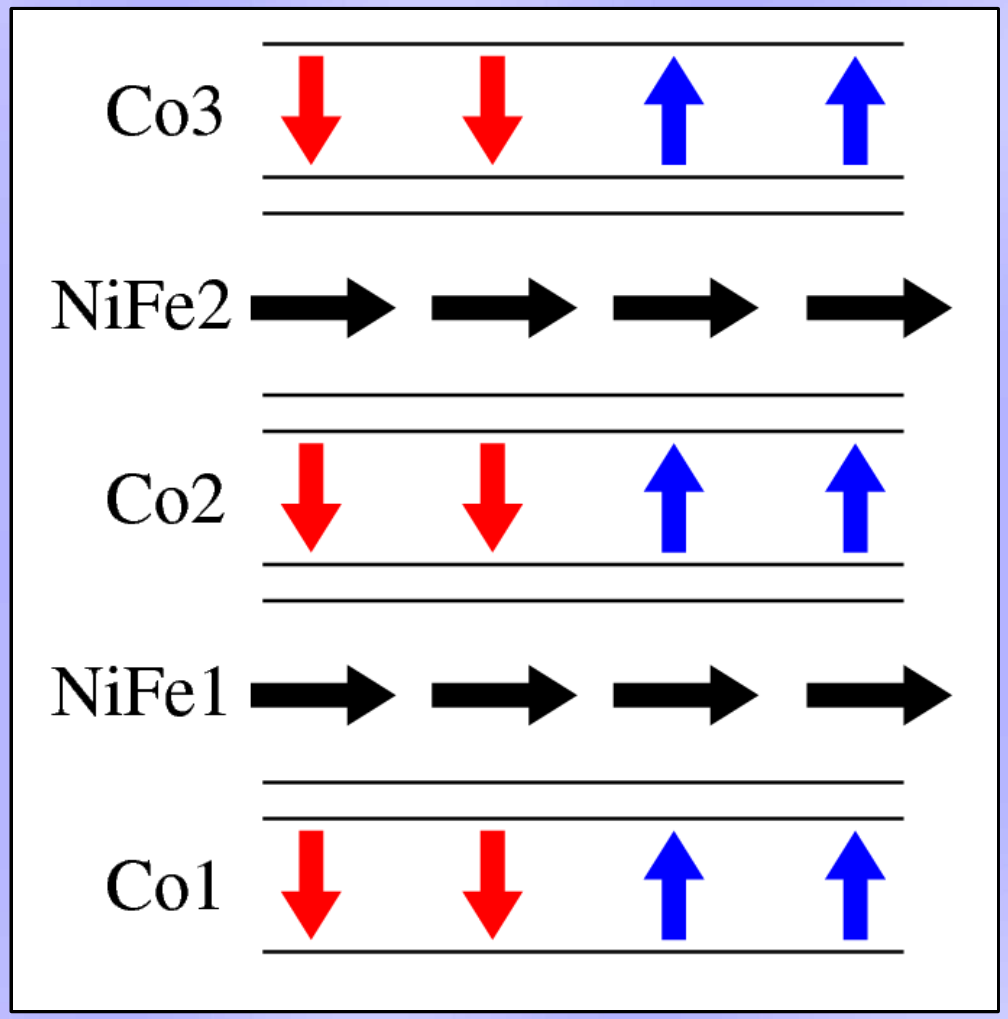

- symulation of remanent state
- starting configuration-stripe domains in Co sublayers
- starting configuration-monodomain state in NiFe sublayers

*Simulation with free oommf package from NIST; (1x1 μm^2)x55nm; Co domains 200 nm wide; α=0.5; regular mesh with cell size of (5x0.5x50nm^3); stiffness: Co: 30e-12 J/m, NiFe: 13e-12 J/m

Magnetostatic coupling

Micromagnetic simulation*

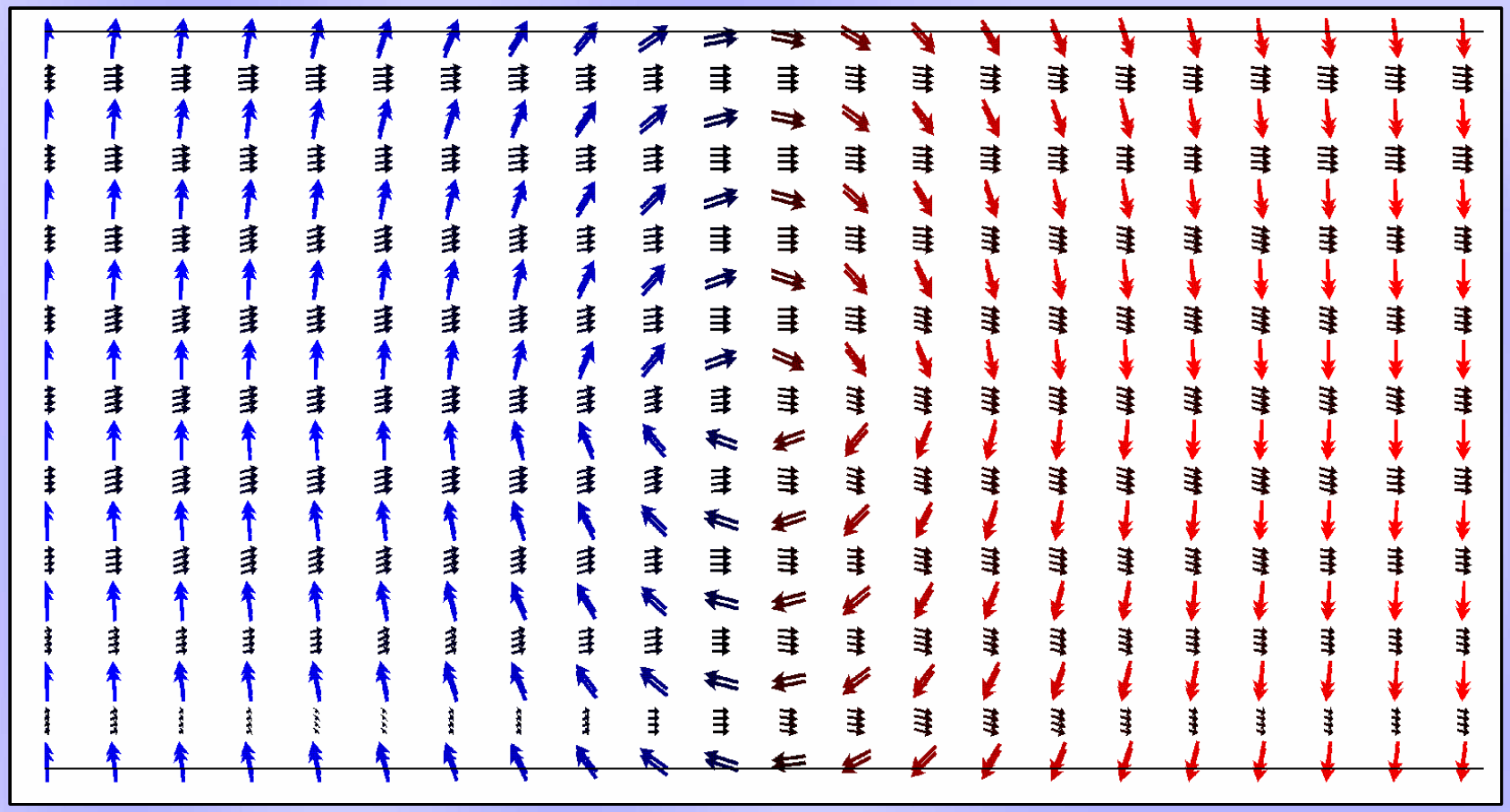

$[Co(1nm)/Au(1.5nm)/Ni_{80}Fe_{20}(2\ nm)/Au(1.5\ nm)]_9/Co(1nm)$

$H=0$

*Simulation with free oommf package from NIST; (1x1 μm^2)x55nm; Co domains 200 nm wide; α=0.5; regular mesh with cell size of (5x0.5x50nm^3); stiffness: Co: 30e-12 J/m, NiFe: 13e-12 J/m

Magnetostatic coupling

Micromagnetic simulation

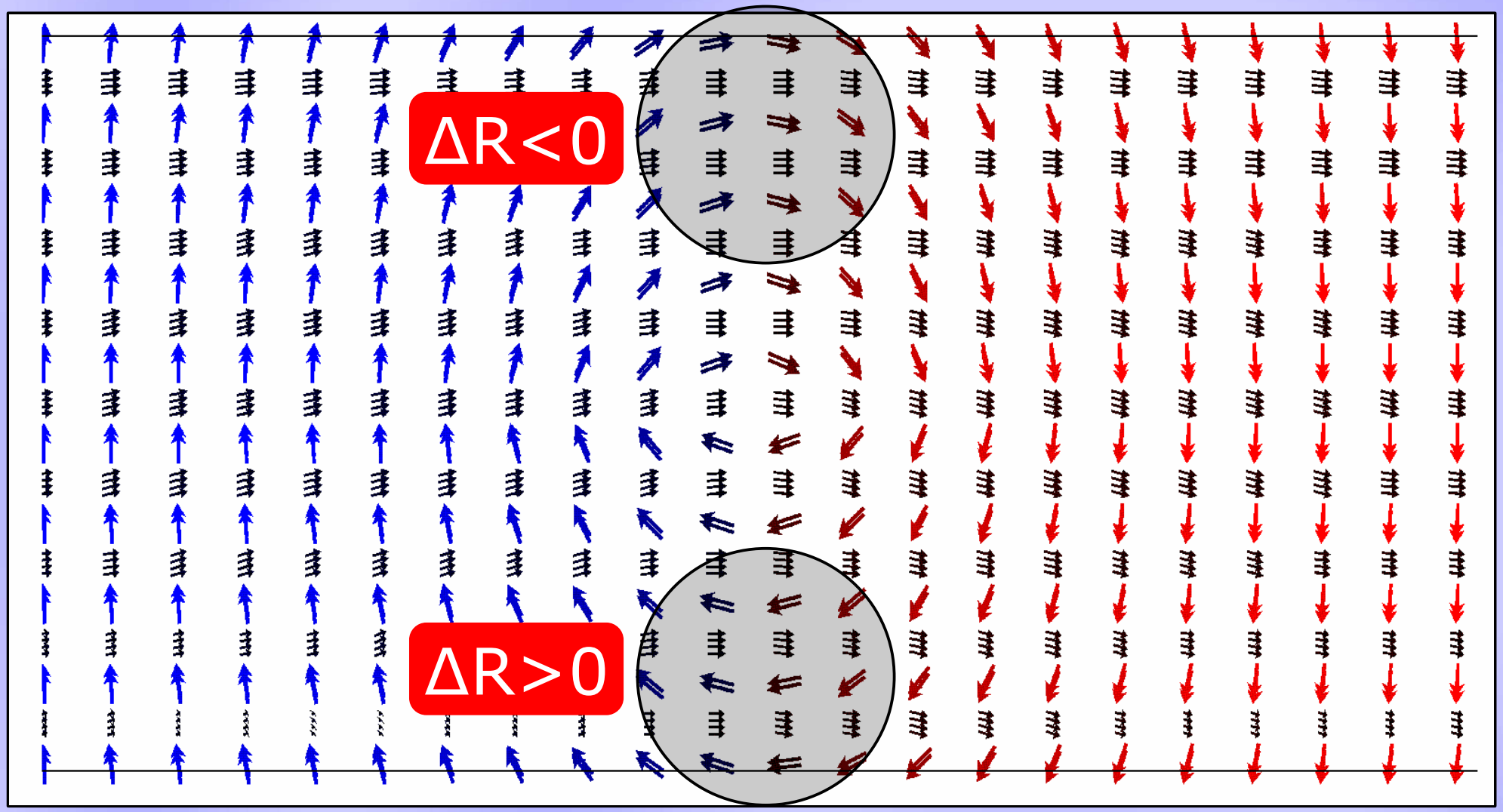

$$\Delta R \propto \cos(\varphi)$$

H=0

Magnetostatic coupling

Micromagnetic simulation

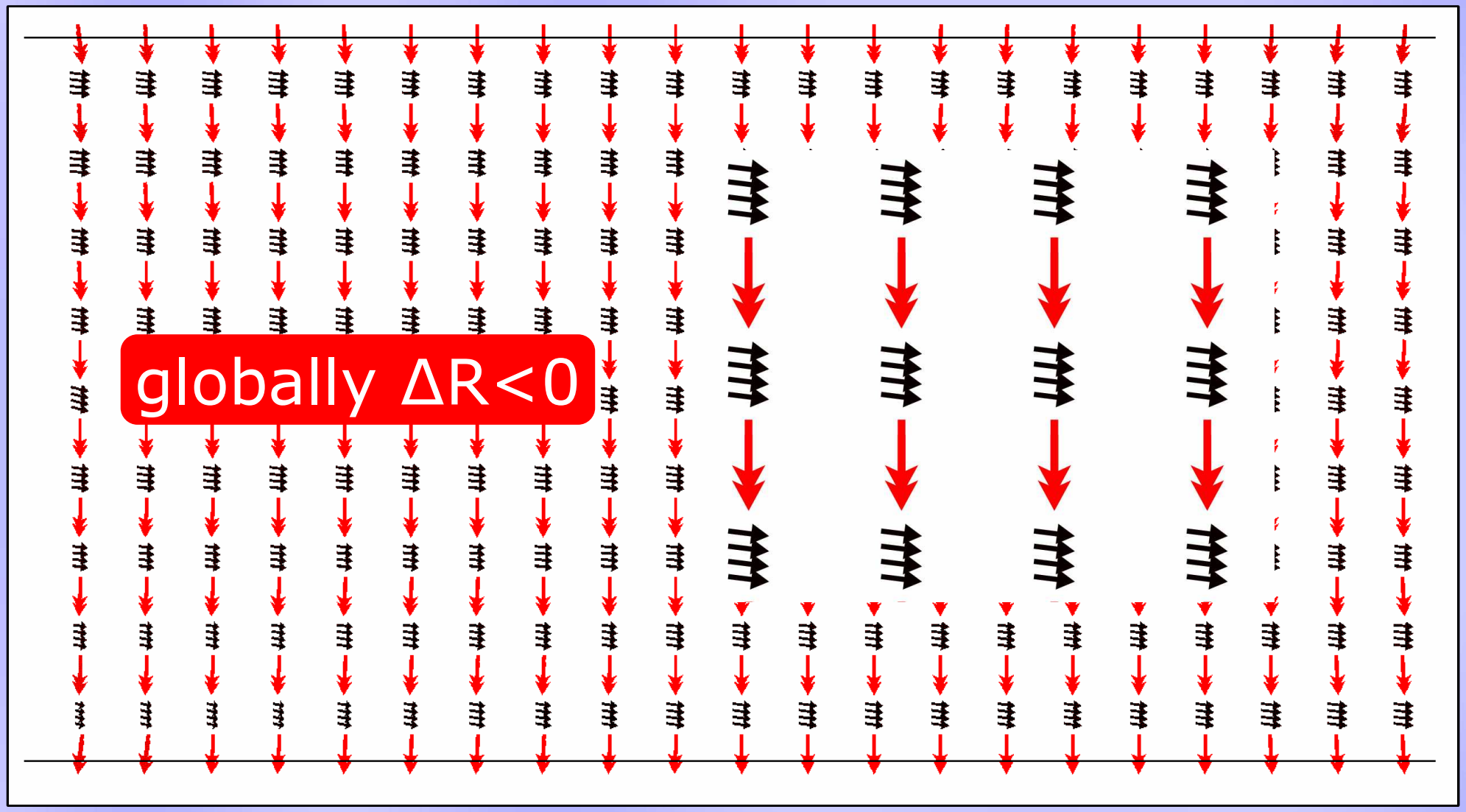

$$\Delta R \propto \cos(\varphi)$$

$H=0$

Magnetostatic coupling

Micromagnetic simulation

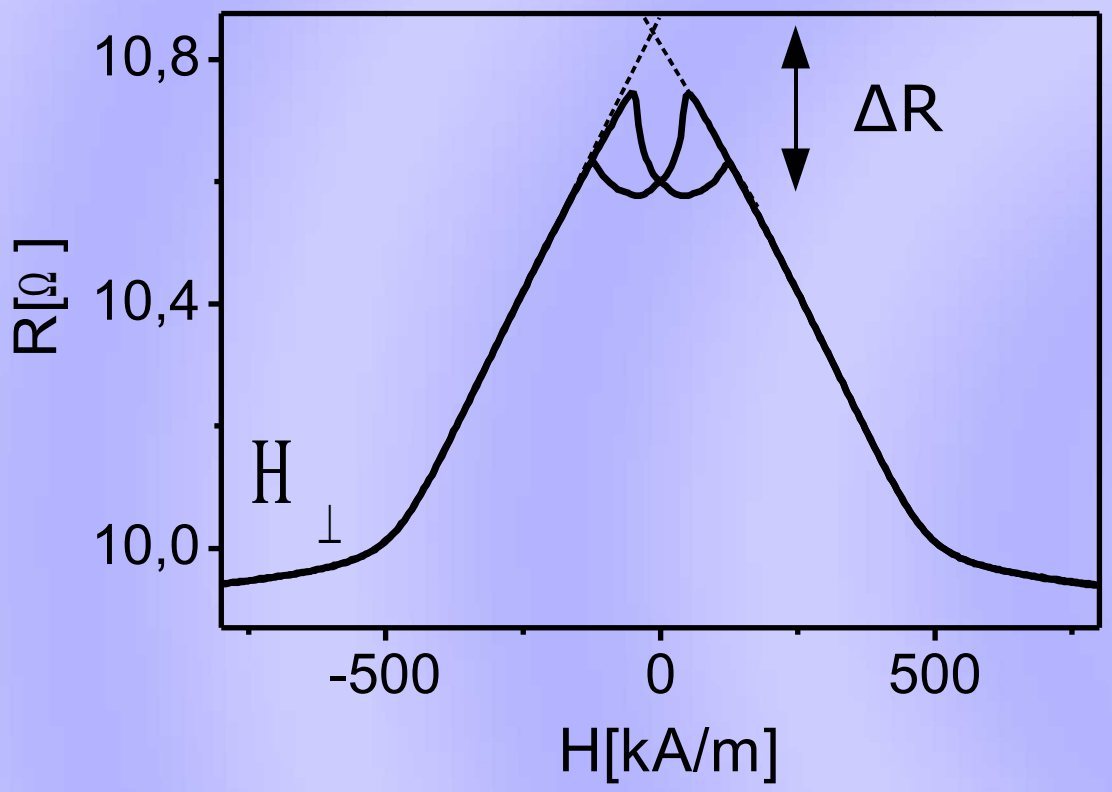

$\Delta\cos(\varphi)=0.265$

Magnetostatic interactions between Co and NiFe layers lead to the decrease of the average cosine of the angle between magnetic moments of neighboring sublayers ⇒ resistance decrease.

Magnetostatic coupling

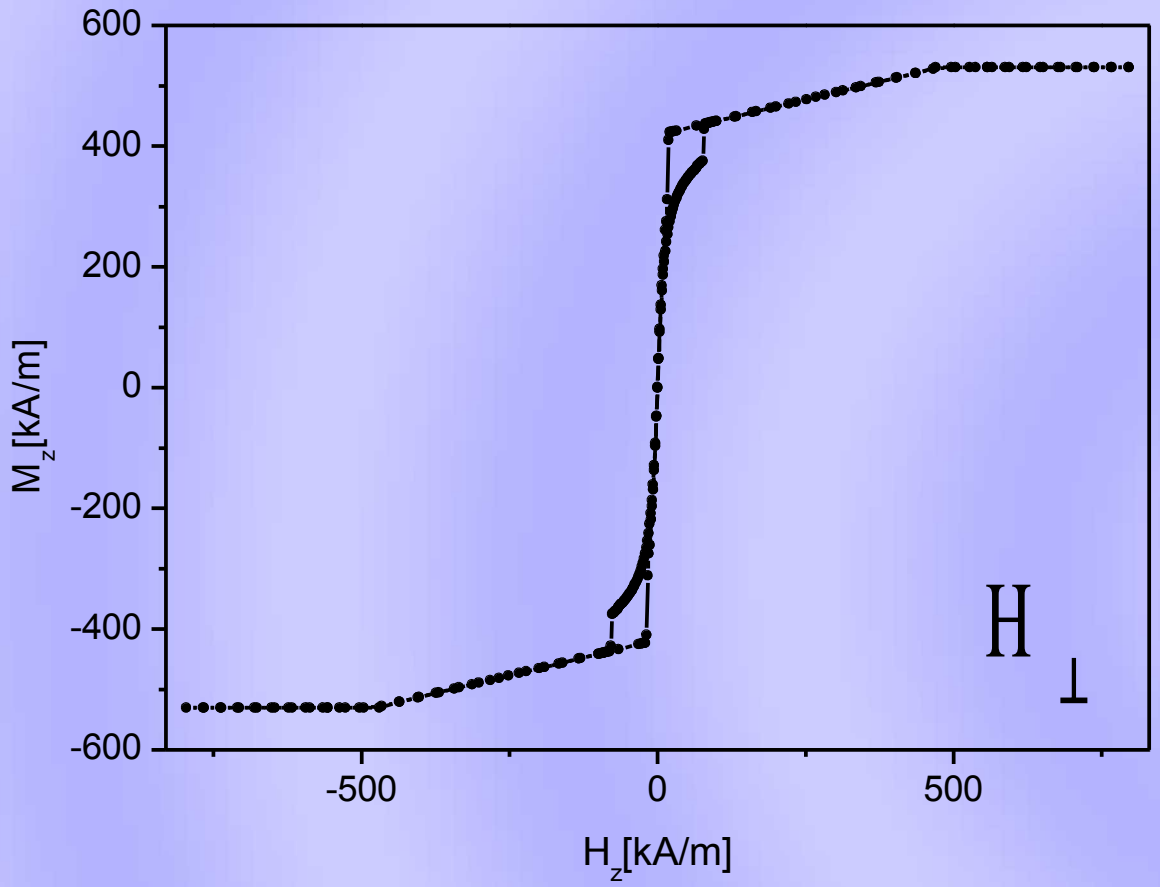

Micromagnetic simulation*

Co-perpendicular anisotropy

NiFe-shape anisotropy

measurement:

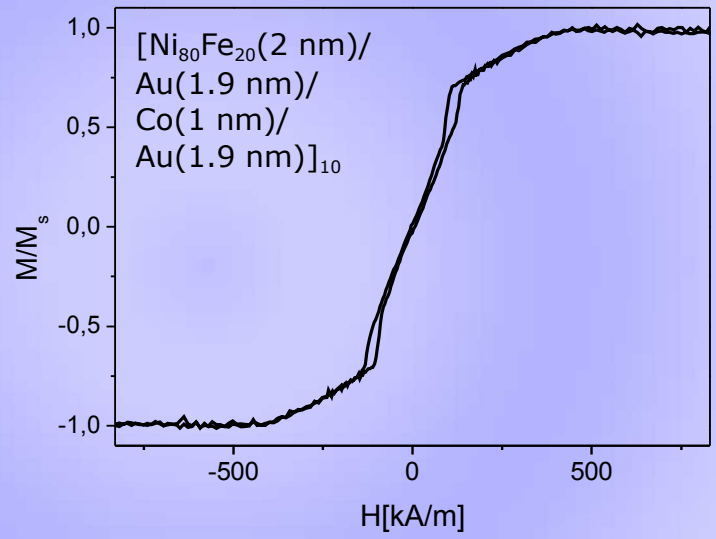

$[Co(1nm)/spacer(1nm)/NiFe(1nm)/spacer(1nm)]_4/Co(1nm)$

*Simulation with free oommf package from NIST (M.J. Donahue and D.G. Porter);
α=0.5;regular mesh with cell size of (5x**20000**x1nm^3);
stiffness: Co: 30e-12 J/m, NiFe: 13e-12 J/m

Magnetostatic coupling

Micromagnetic simulation

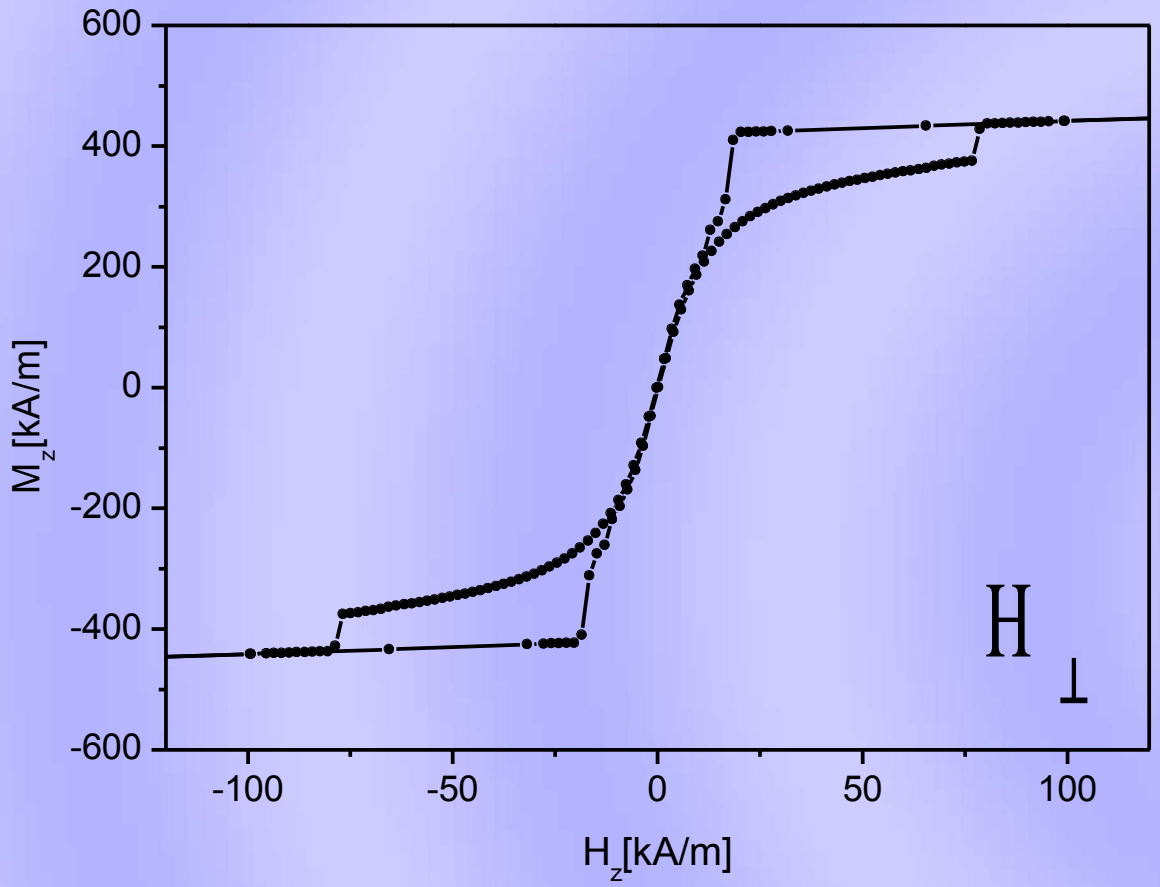

Co-perpendicular anisotropy

NiFe-shape anisotropy

measurement:

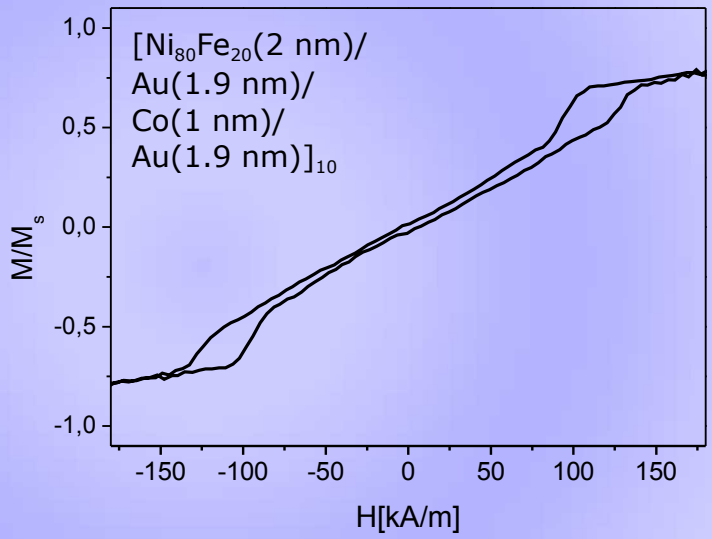

$[Co(1nm)/spacer(1nm)/NiFe(1nm)/spacer(1nm)]_4/Co(1nm)$

No attempts were made to exactly mirror the M(H) dependence ,i.e. , nucleation and annihilation fields.

Magnetostatic coupling

Micromagnetic simulation

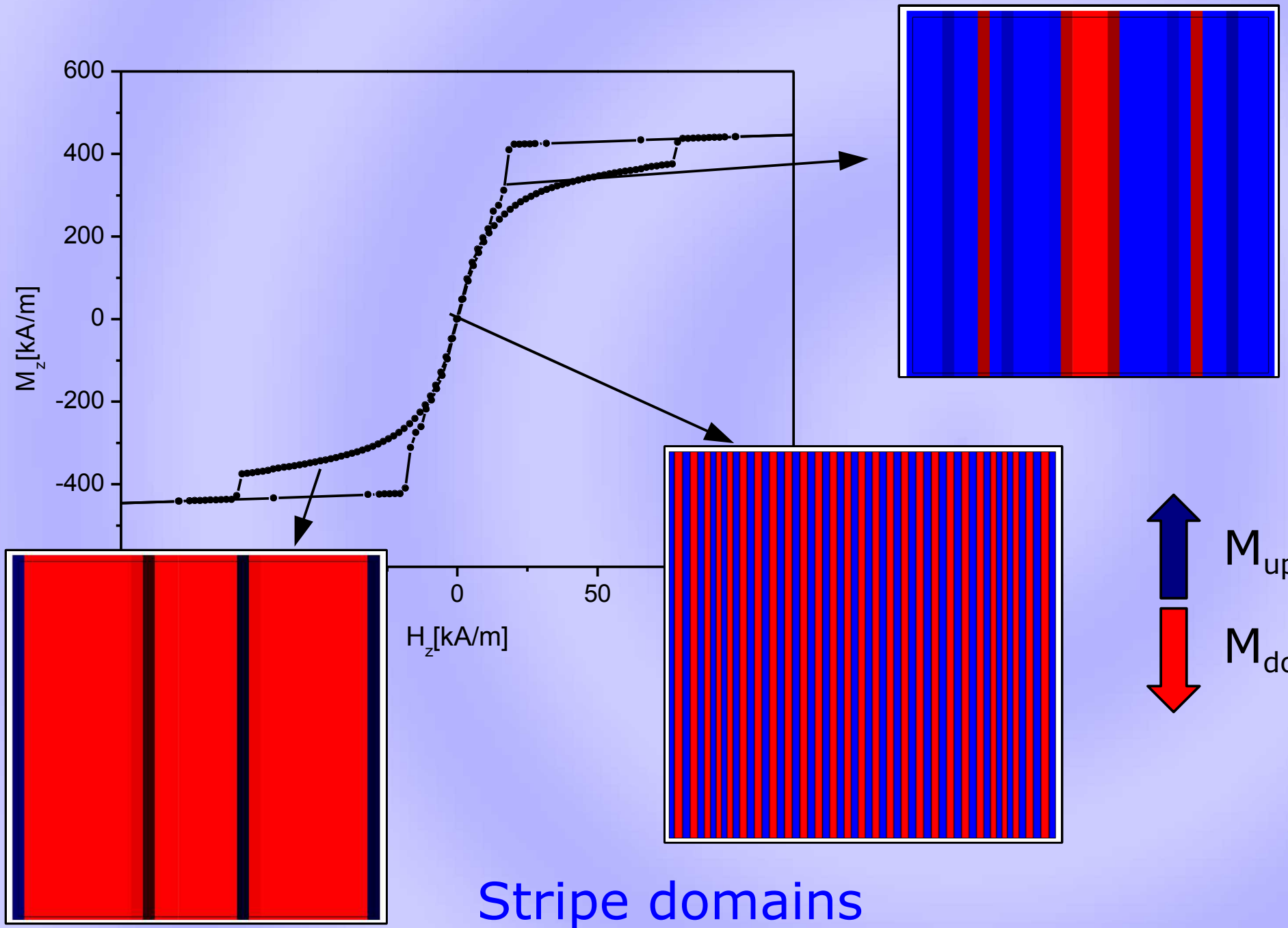

Stripe domains

Magnetostatic coupling

Micromagnetic simulation

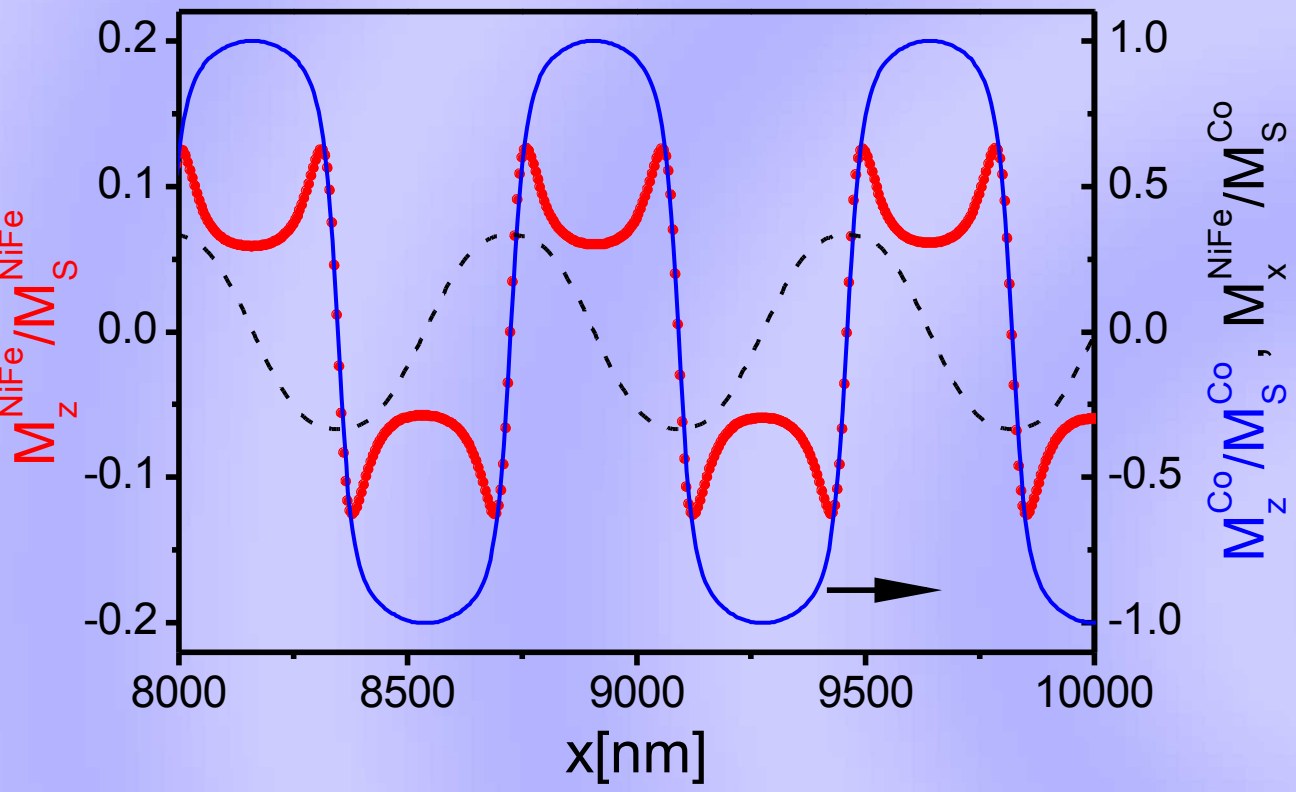

Field calculated from Biot-Savart law for zero DW width

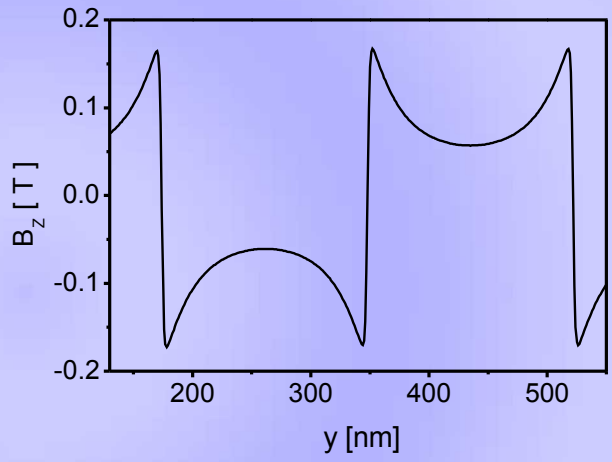

Magnetostatic interactions between Co and NiFe layers lead to the spatial replication of the z-component of magnetic moment of Co sublayers in NiFe sublayers ⇒ resistance decrease.

Magnetostatic coupling

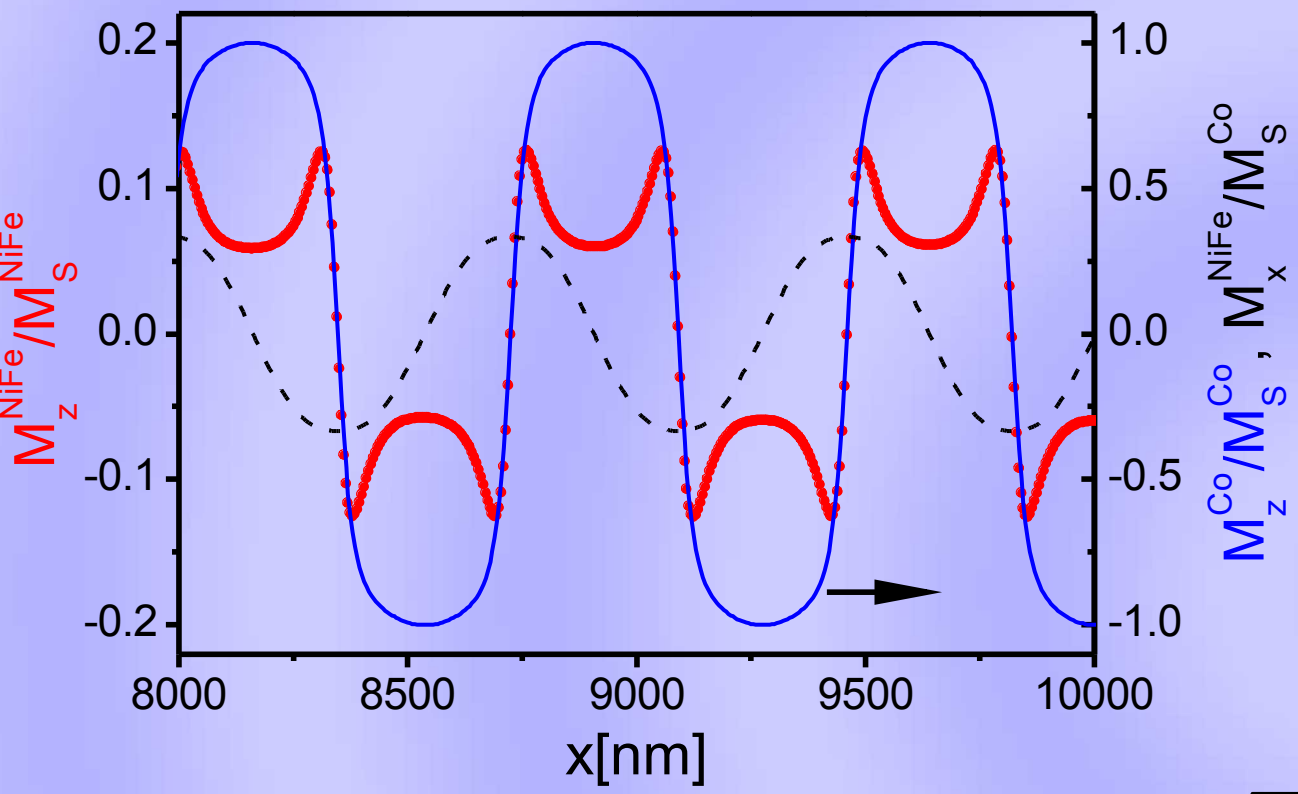

$$\Delta R_{GMR} = \frac{1}{n}\sum_{n}\cos\left(\phi_{NiFe-Co}\right)$$

Micromagnetic simulation

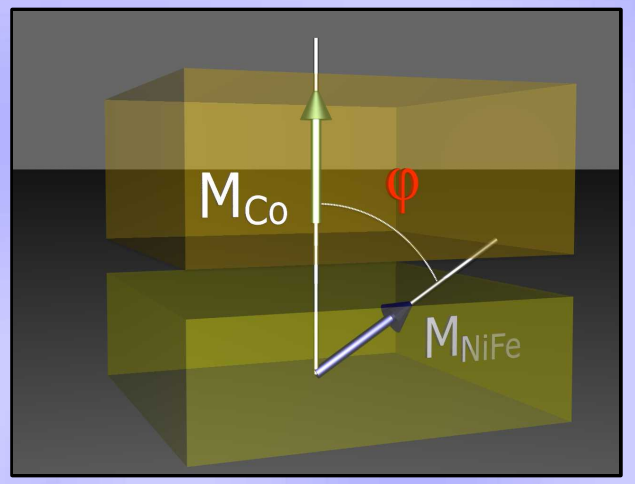

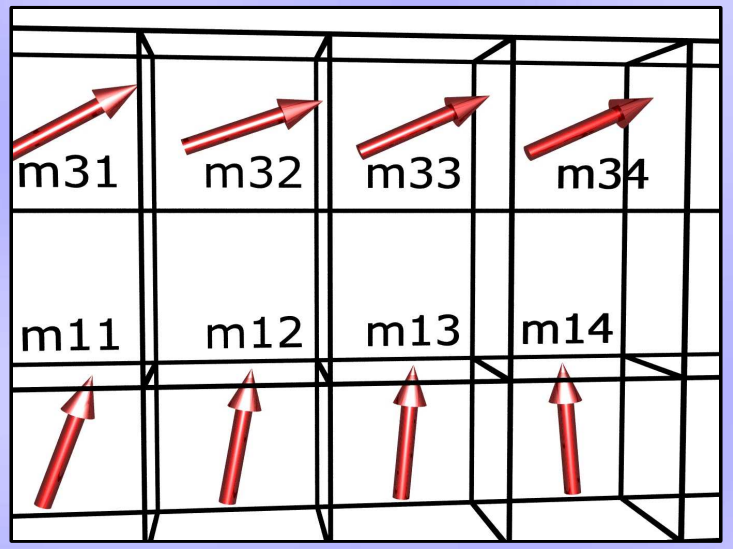

Magnetostatic coupling

Micromagnetic simulation

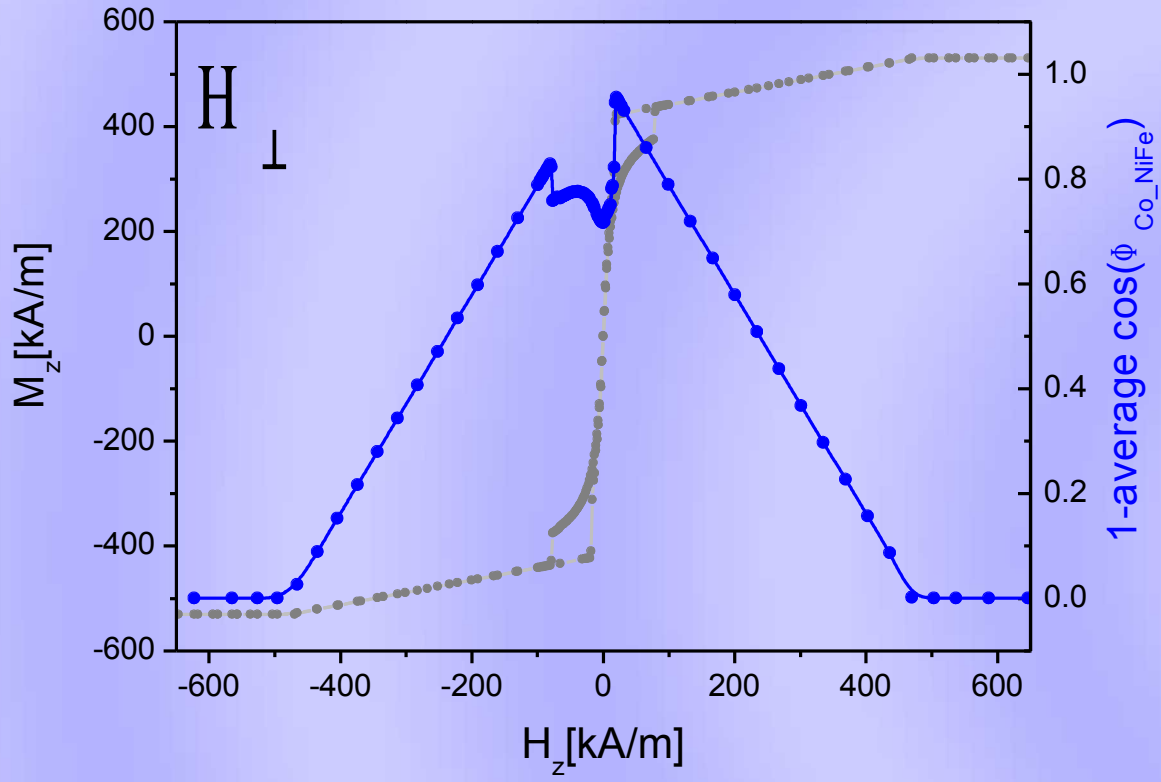

The GMR(H) dependence was calculated as proportional to an average cosine of the angle between magnetic moment direction of juxtaposed NiFe and Co cells.

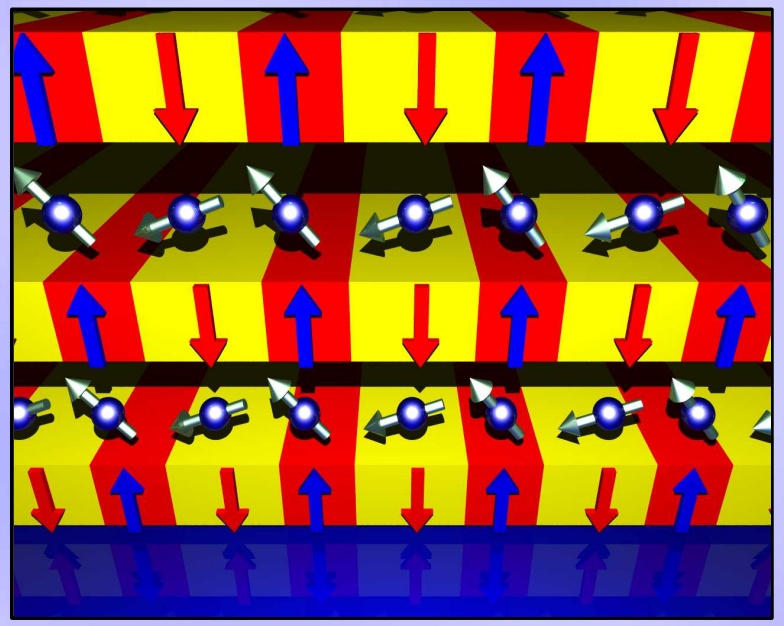

Giant magnetoresistance dependencies of NiFe/Au/Co/Au multilayers can be approximated from micromagnetic simulations.

Magnetostatic coupling

Micromagnetic simulation

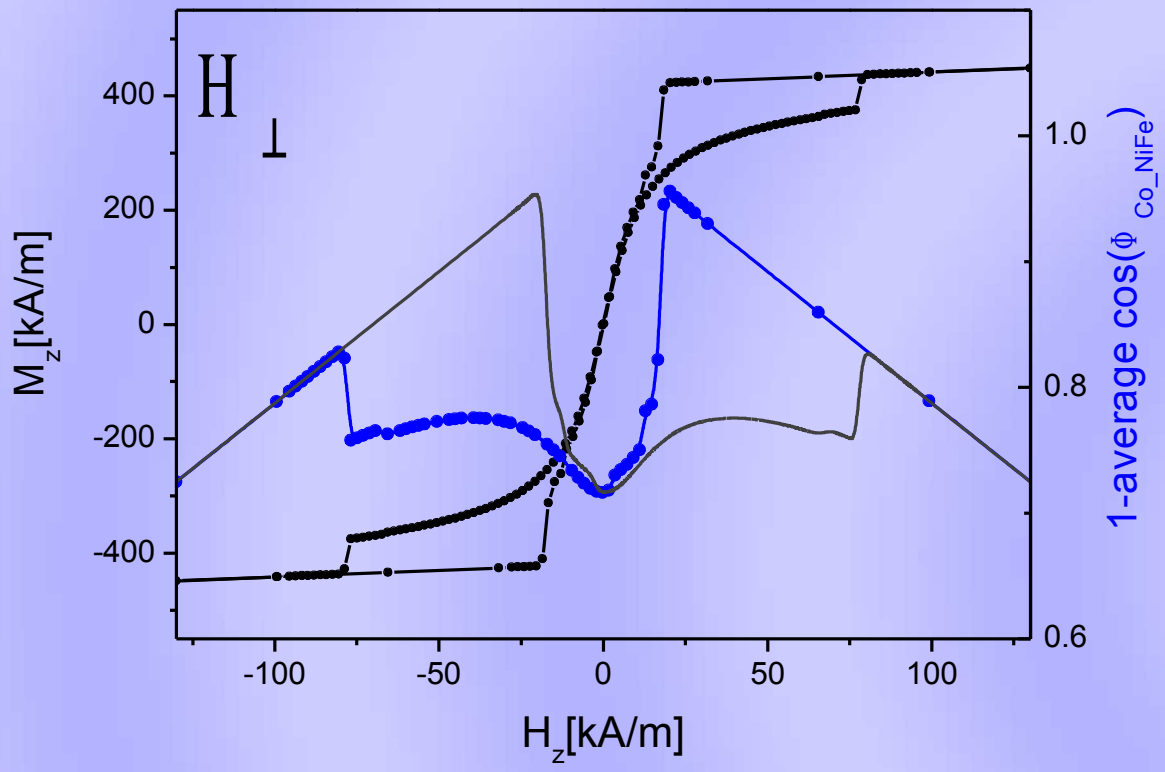

The GMR(H) dependence was calculated as proportional to an average cosine of the angle between magnetic moment direction of juxtaposed NiFe and Co cells.

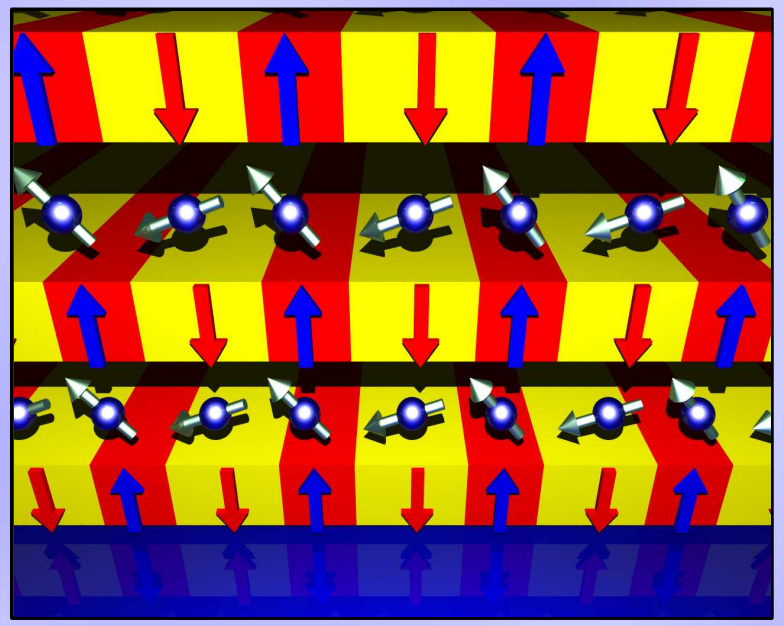

Giant magnetoresistance dependencies of NiFe/Au/Co/Au multilayers can be approximated from micromagnetic simulations.

Magnetostatic coupling

Micromagnetic simulation

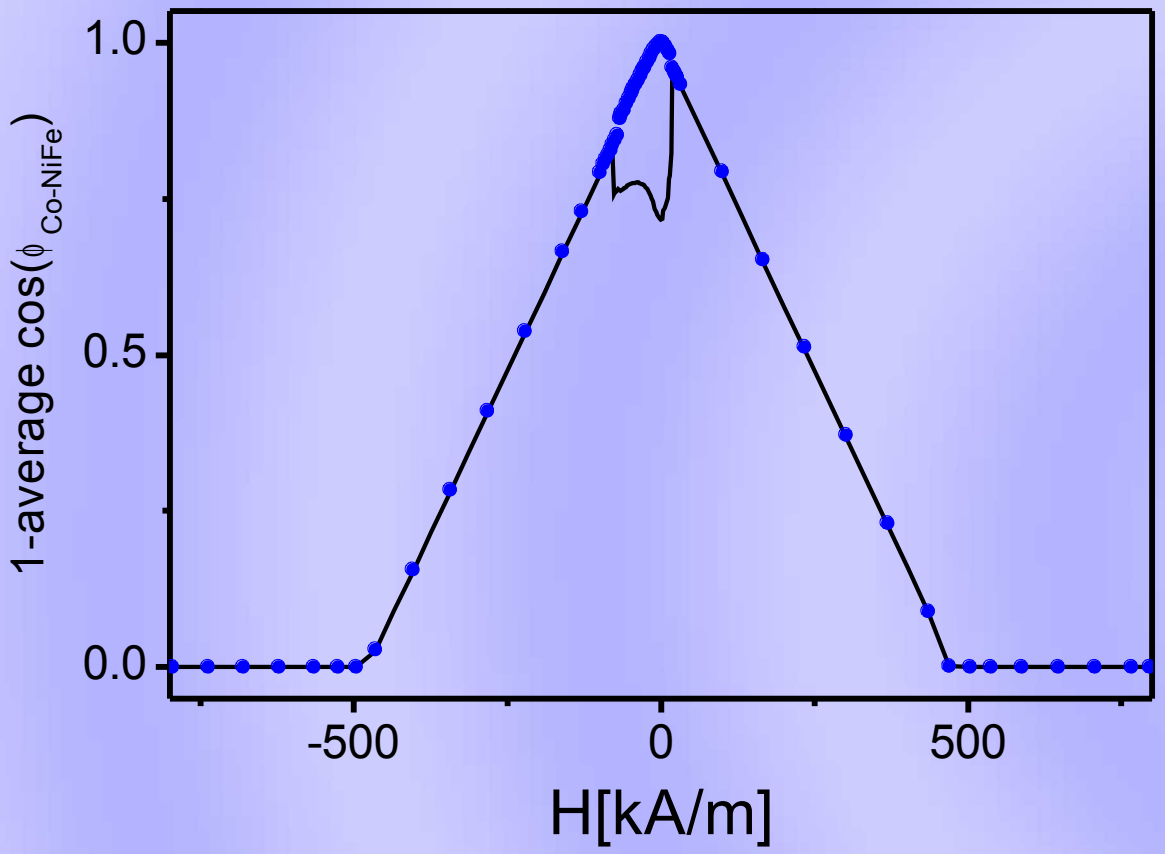

The GMR(H) dependence was calculated as proportional to an average cosine of the angle between magnetic moment direction of juxtaposed NiFe and Co cells.

••••• – no coupling

Without magnetostatic coupling between Co and NiFe layers there are no local minima of resistance.

Magnetostatic coupling

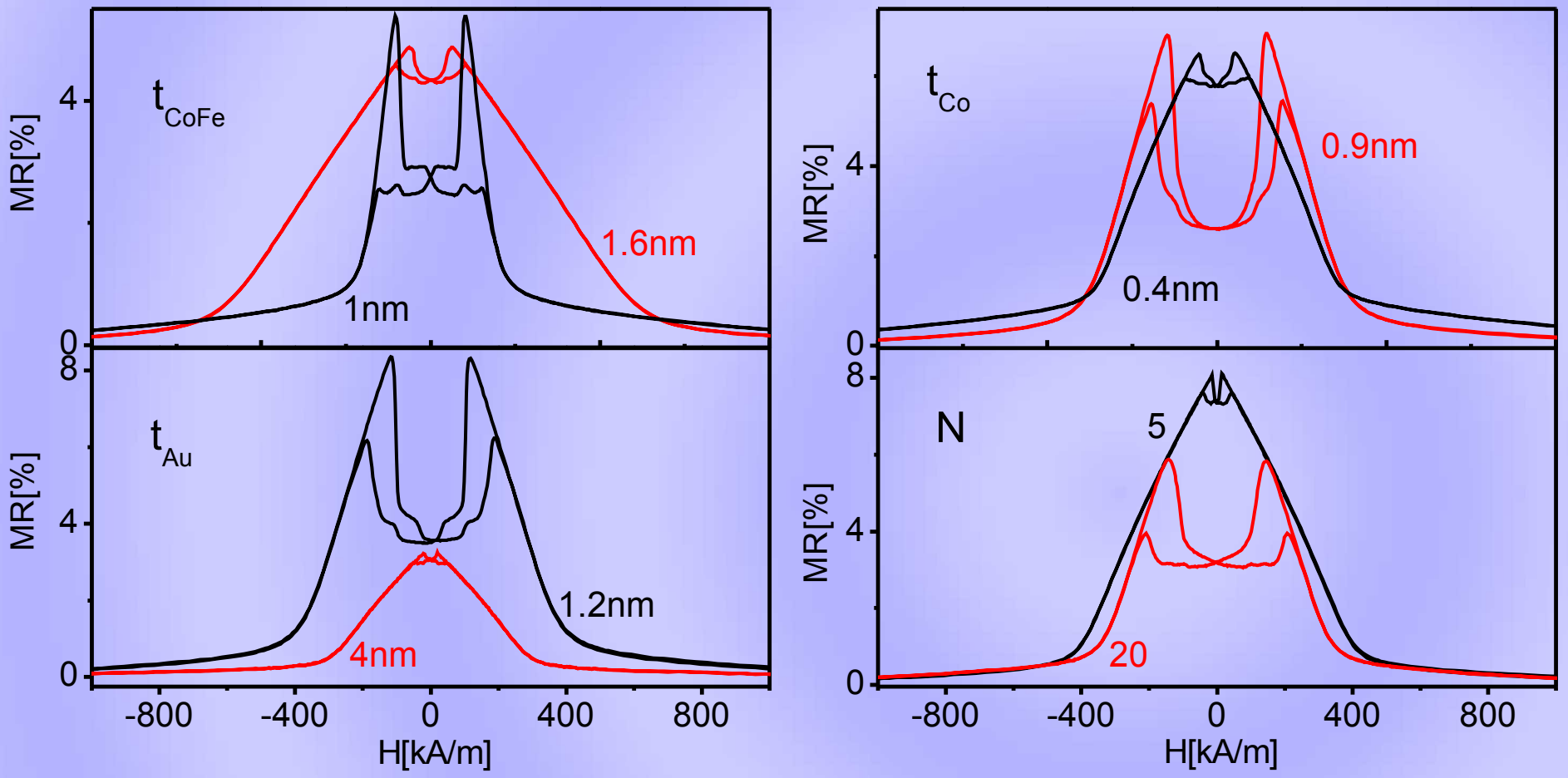

The strength of coupling between sublayers with perpendicular and in-plane anisotropy (depth of resistance minimum) depends on thicknesses of all types of sublayerslayers and on the number of repetitions.

Magnetostatic coupling

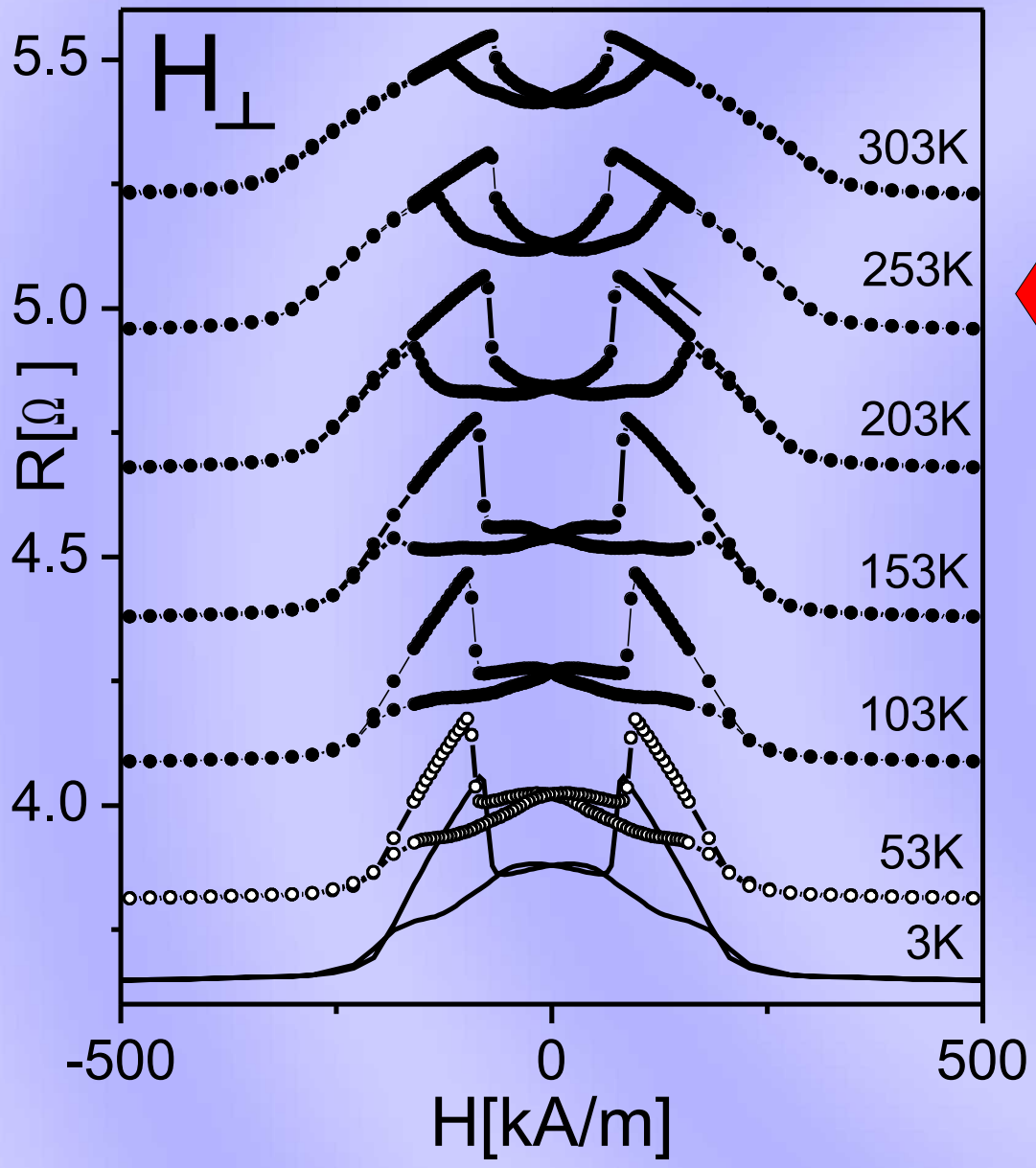

Micromagnetic simulation

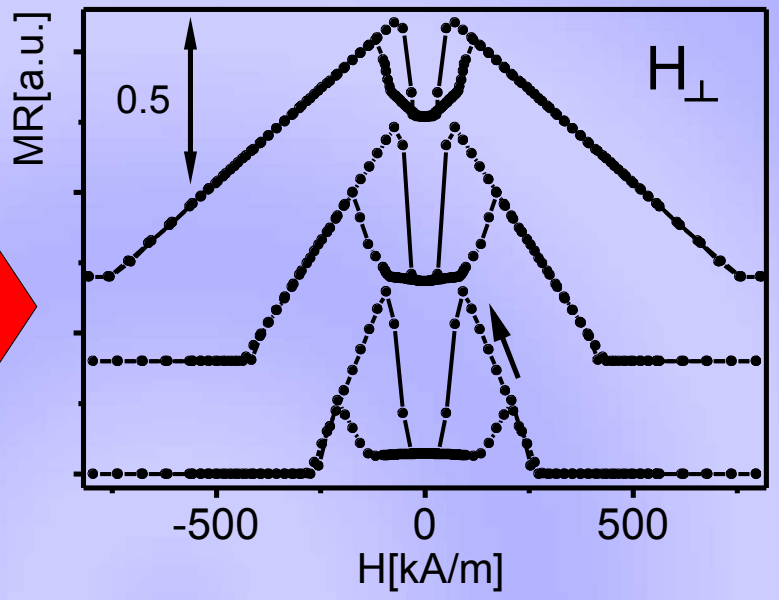

OOMMF simulation with changing perpendicular anisotropy of CoFe sublayers.
from top to bottom:
$K_U = 0.7 \times 10^6 J/m^3$, $K_U = 1 \times 10^6 J/m^3$ and $K_U = 1.15 \times 10^6 J/m^3$.

$[Co_{83}Fe_{17}(1.2\ nm)/Au(2.2\ nm)/Co(0.8\ nm)/Au(2.2\ nm)]_{10}$

Element selective measurements

Mössbauer spectroscopy

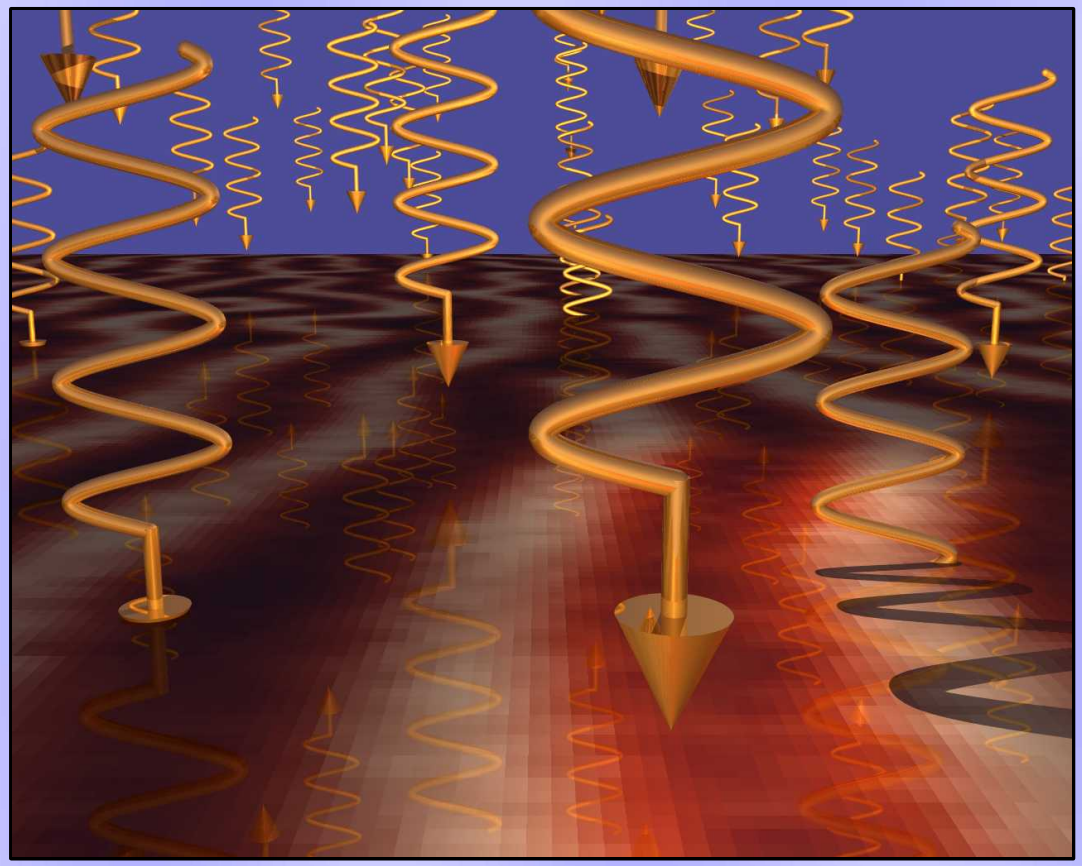

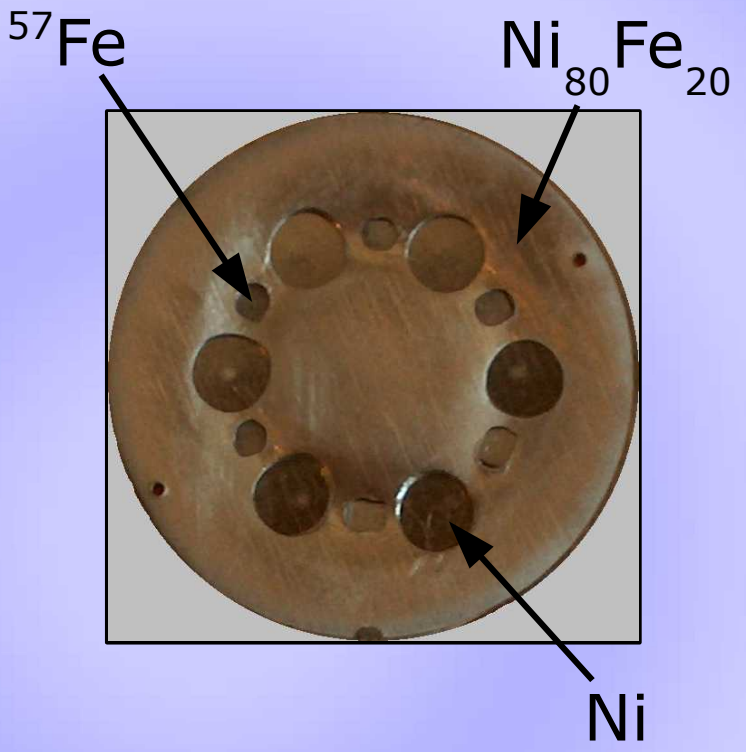

Conversion electron Mössbauer spectroscopy (CEMS)

^{57}Co source

^{57}Fe 95.3 at.%

^{57}Fe

$[Ni_{80}Fe_{20}/Au/Co/Au]_{10}$

Element selective measurements

Mössbauer spectroscopy

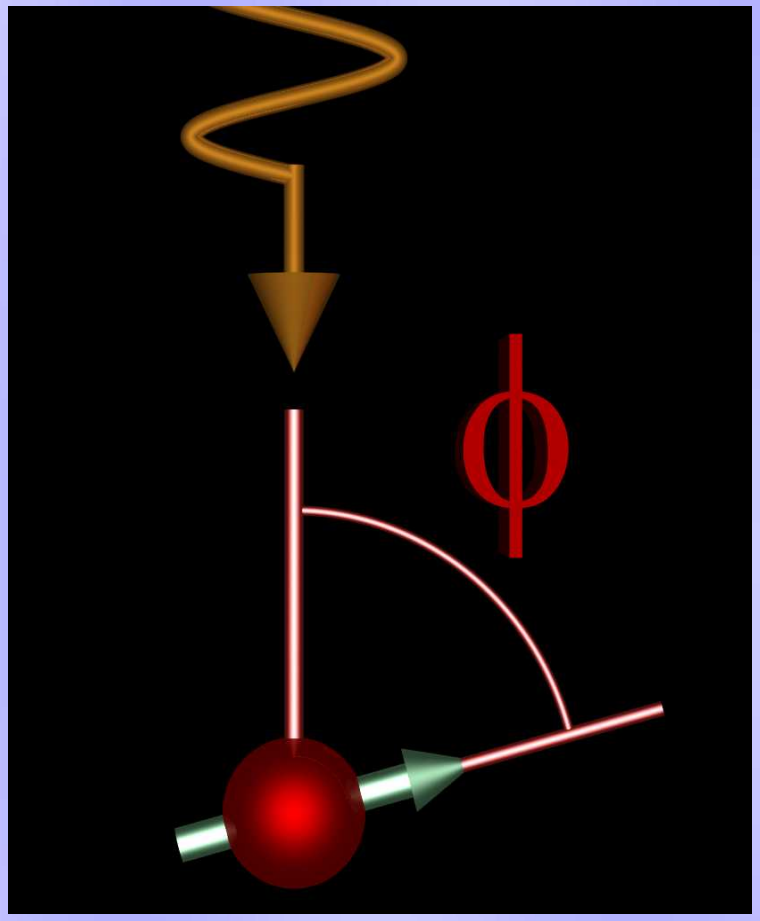

$$D_{23} = \frac{4\sin^2(\phi)}{(1+\cos^2(\phi))}$$

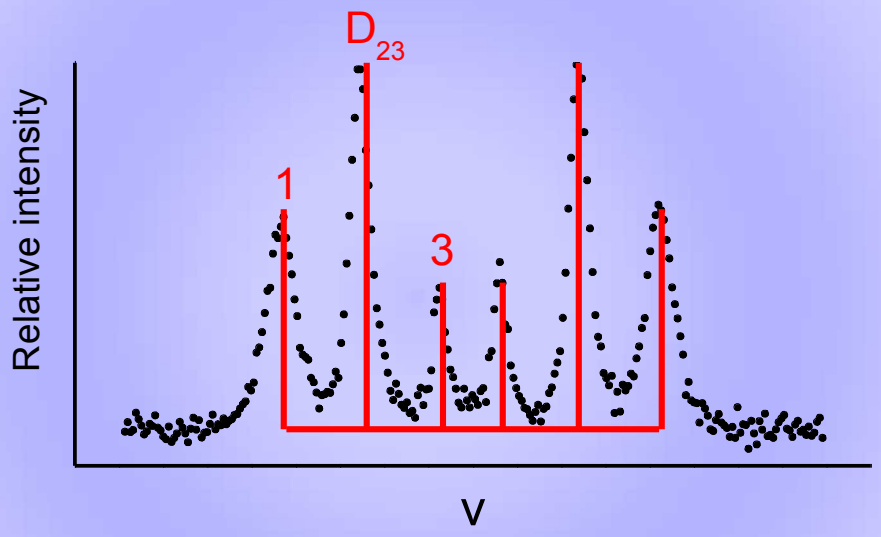

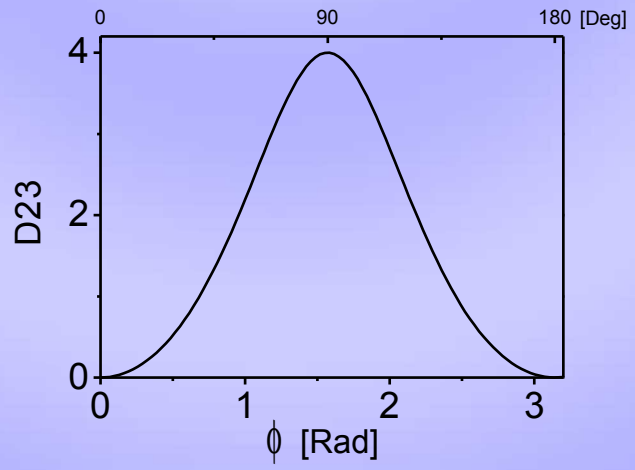

Relative intensities of the hyperfine lines vary with the angle φ between the incident γ-ray and the magnetic moment.

Element selective measurements

Mössbauer spectroscopy

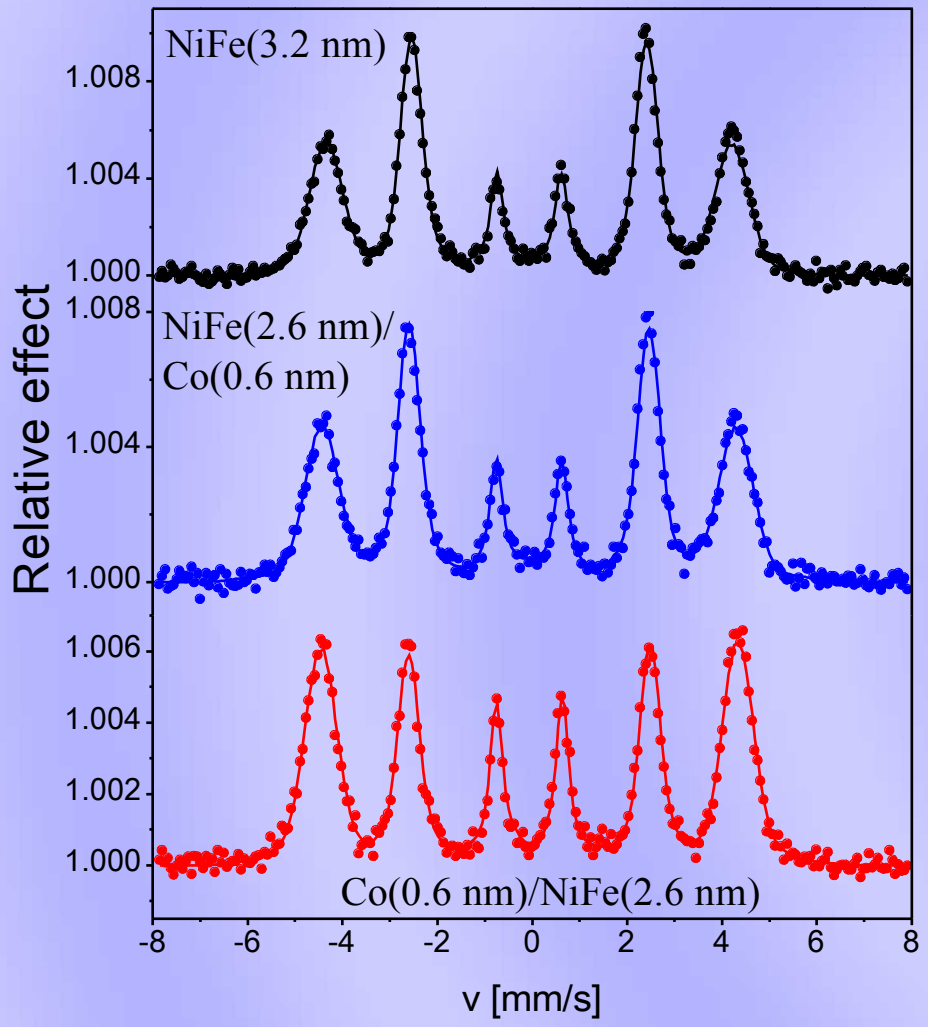

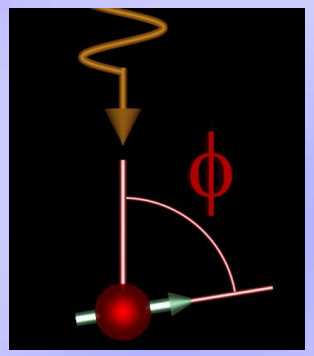

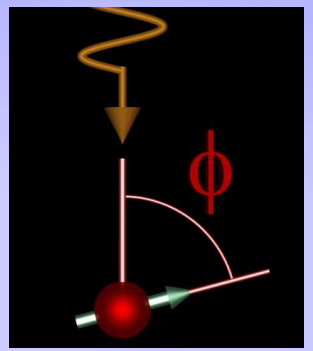

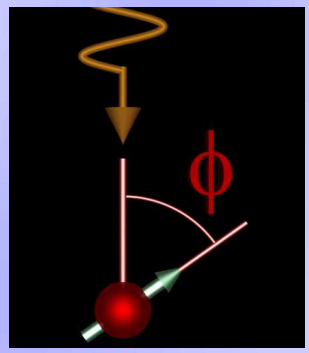

$[Ni_{80}Fe_{20}(3.2\ nm)/Au(2.4\ nm)/Co(0.8\ nm)/Au(2.4\ nm)]_{10}$

$[Ni_{80}Fe_{20}(2.6\ nm)/Co(0.6\ nm)/Au(2.4\ nm)/Co(0.8\ nm)/Au(2.4\ nm)]_{10}$

$[Co(0.6\ nm)/Ni_{80}Fe_{20}(2.6\ nm)/Au(2.4\ nm)/Co(0.8\ nm)/Au(2.4\ nm)]_{10}$

Element selective measurements

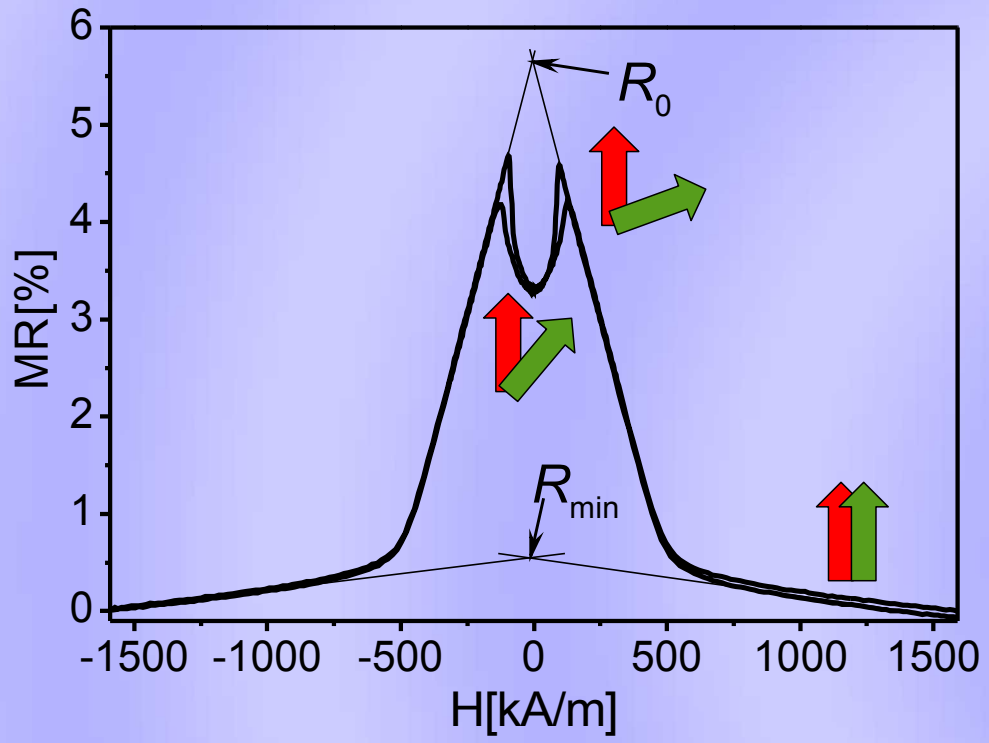

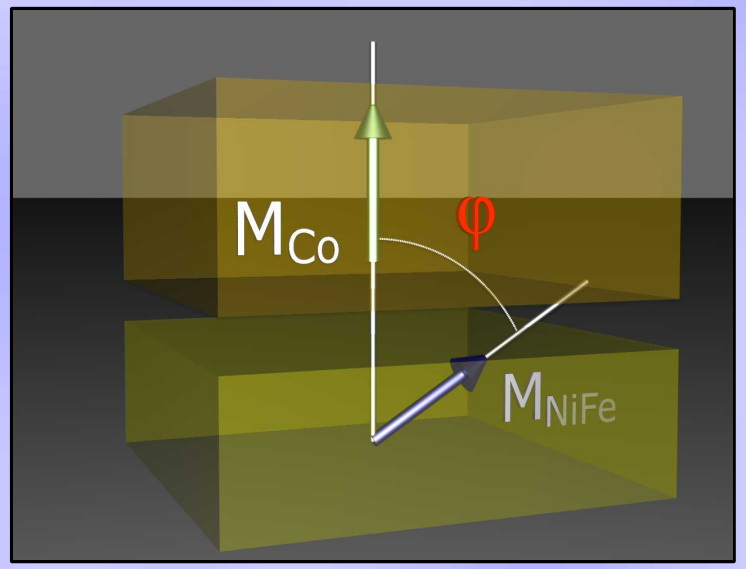

$$R = R_0 - (R_0 - R_{min})\cos(\varphi_{Co-NiFe})$$

Resistance measurements allow the determination of the average cosine of the angle between magnetic moments of **Co** and **NiFe** layers.

$[Ni_{80}Fe_{20}(2\ nm)/Au(2.4\ nm)/Co(1.2\ nm)/Au(2.4\ nm)]_{10}$

Element selective measurements

Mössbauer spectroscopy vs. GMR

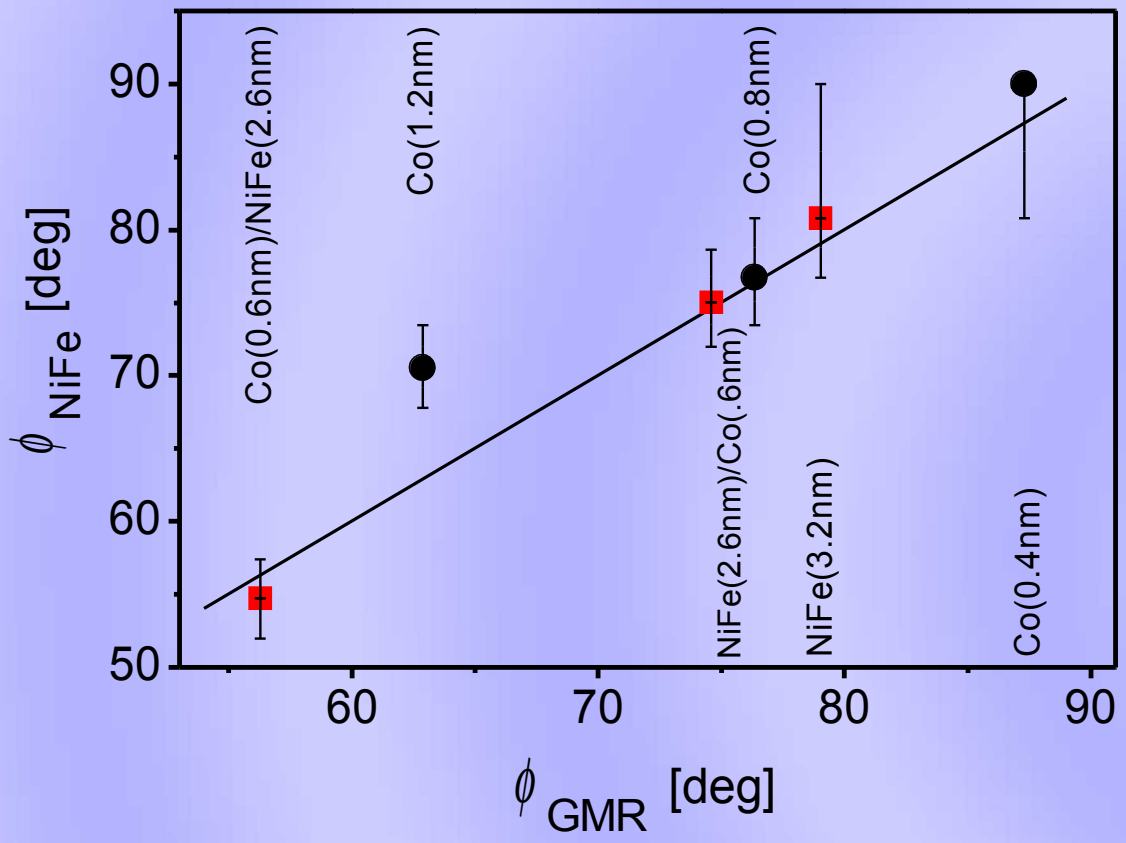

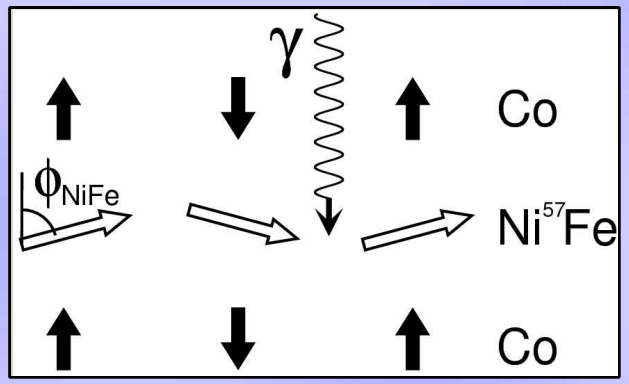

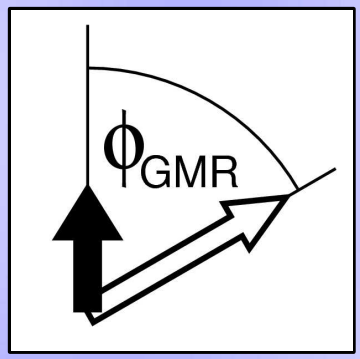

The magnetostatic fields of the Co domains cause the deflection of the magnetic moments of the NiFe layers. The deflection is stronger if the effective easy-plane anisotropy of NiFe layers is weaker.

$[\mathbf{X}/Au(2.4\ nm)/Co(0.8\ nm)/Au(2.4\ nm)]_{10}$

$[Ni_{80}Fe_{20}(2\ nm)/Au(2.4\ nm)/\mathbf{Co}/Au(2.4\ nm)]_{10}$

Soft x-ray resonant magnetic scattering (SXRMS)

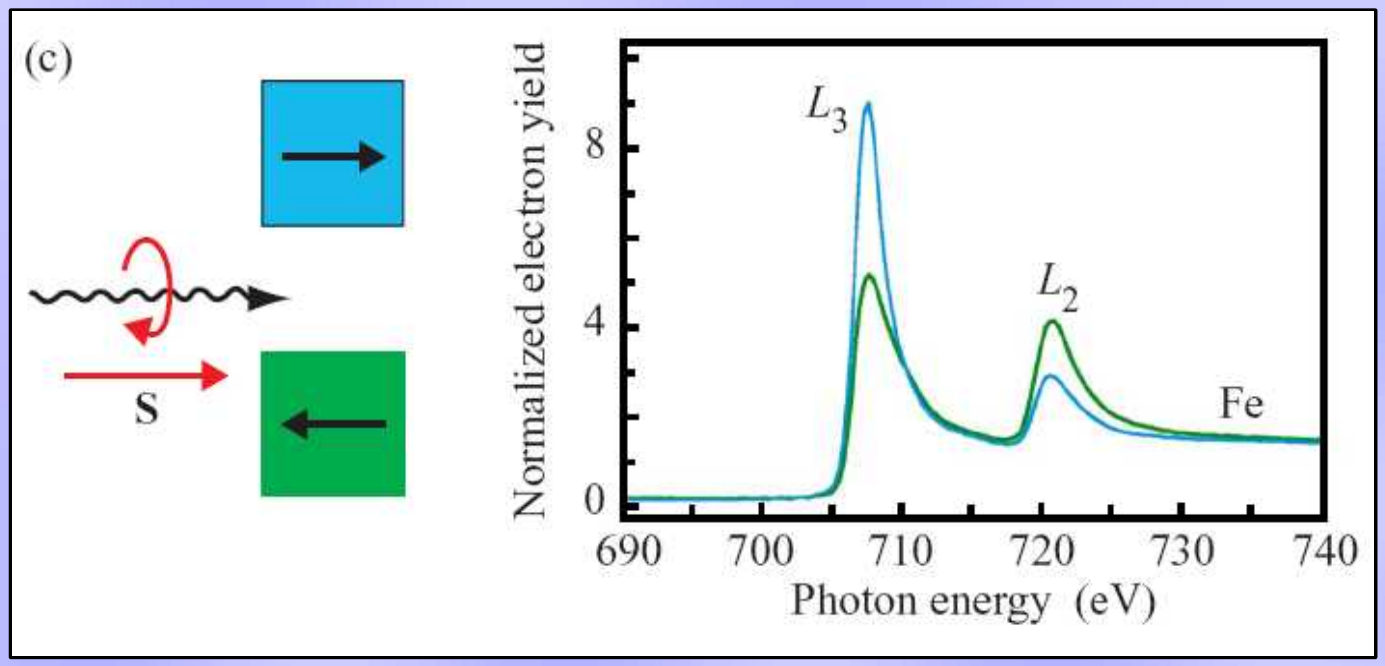

*

SXRMS at BESSY – measurement of the intensity of a reflected X-ray versus the external magnetic field (θ-2θ geometry).

Circularly polarized light

λ≈1.4 nm

interaction with core electrons

photon energy tuned to absorption edge

⇩

elemental selectivity

Sampling depth ~ 10 nm

ALICE diffractometer at the undulator beamline UE56/2-PGM2 at BESSY II (Berlin)

*graphics source:ssrl.slac.stanford.edu/stohr/xmcd.htm
see ssrl.slac.stanford.edu/stohr/X-Rays_and_Magnetism.ppt

Soft x-ray resonant magnetic scattering (SXRMS)

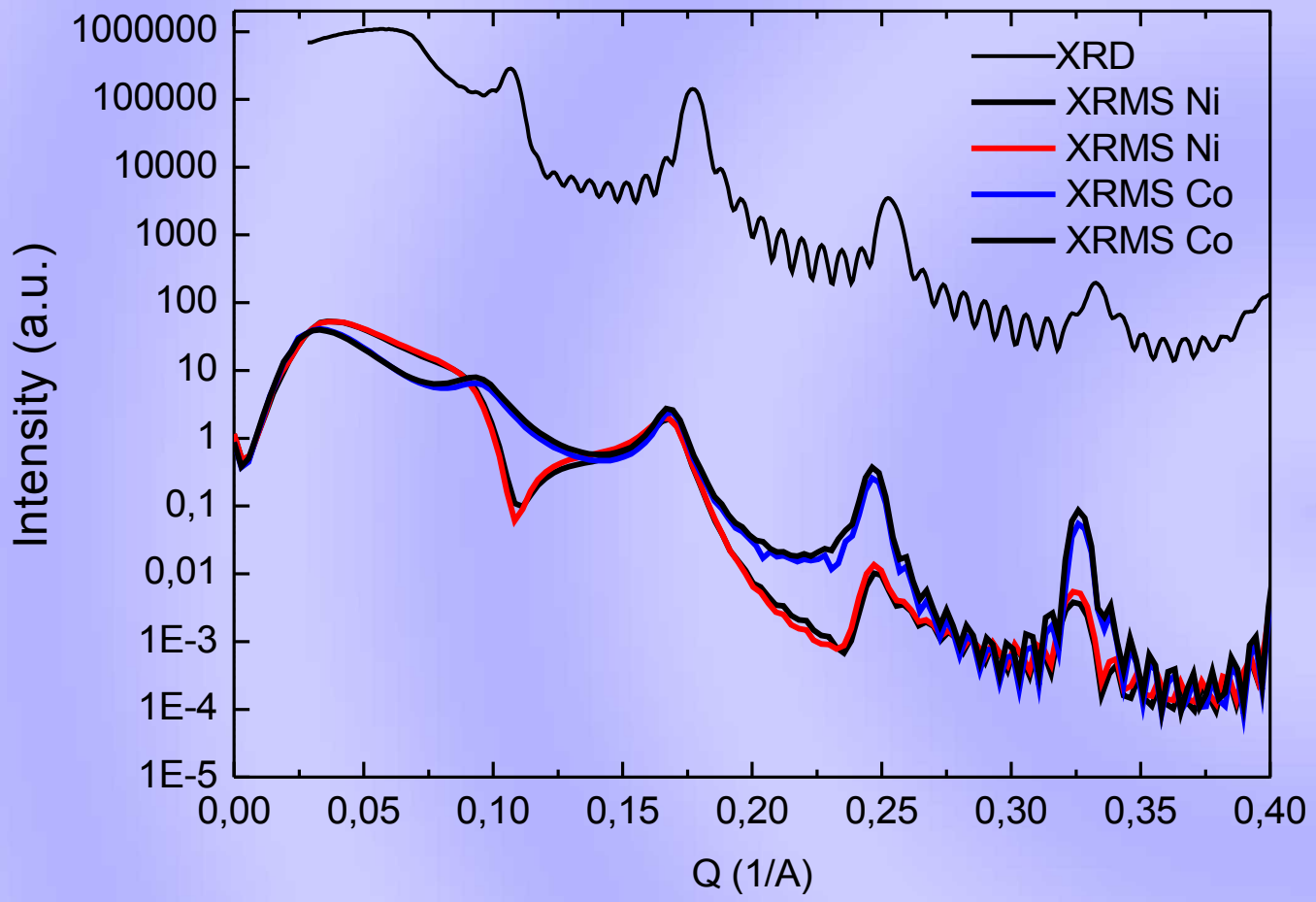

Cu K_α **8048** eV

Ni 853 eV

Co 778 ev

$[Ni_{80}Fe_{20}(2\ nm)/Au(2\ nm)/Co(0.8\ nm)/Au(2\ nm)]_{10}$

Soft x-ray resonant magnetic scattering (SXRMS)

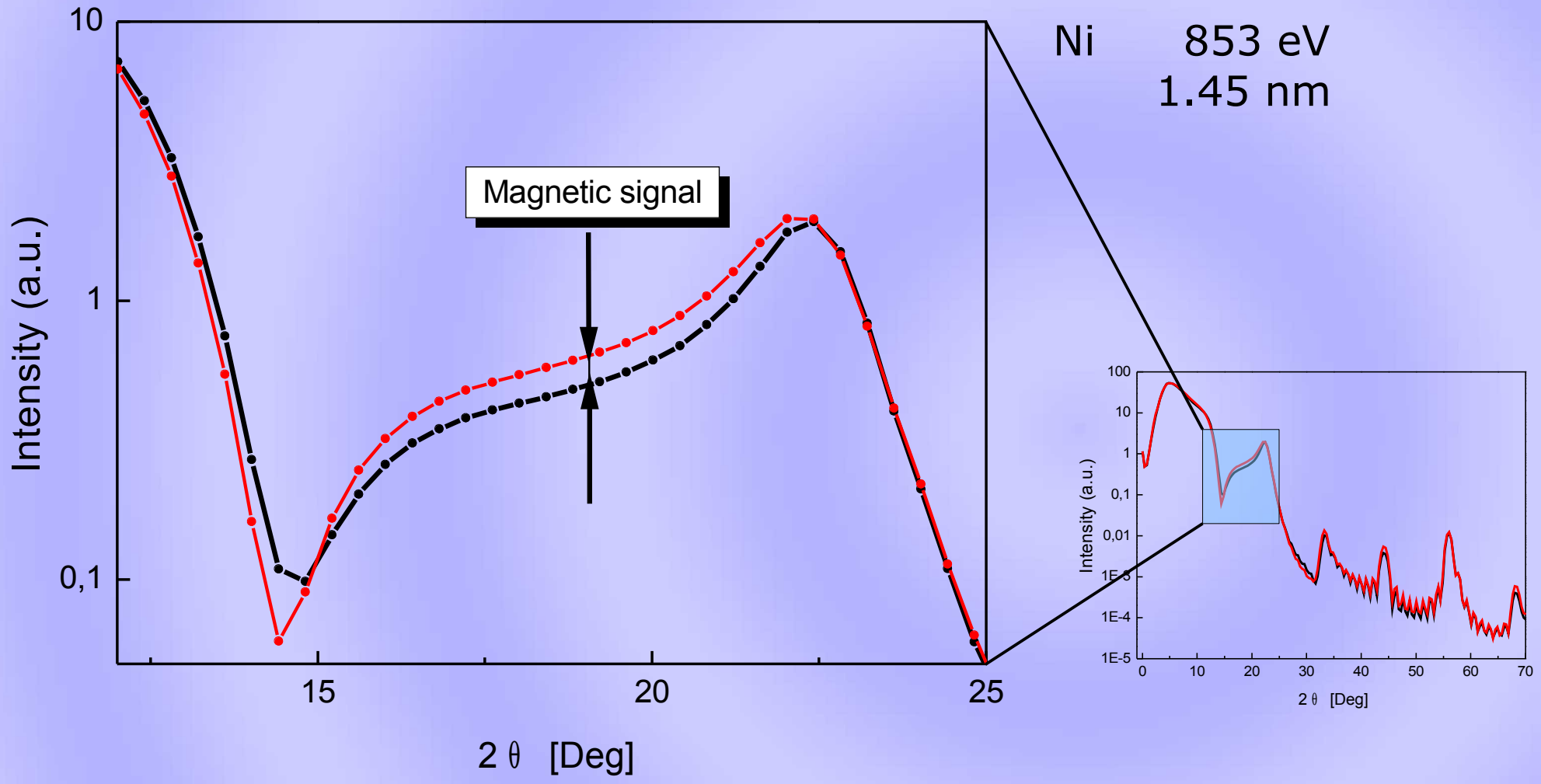

$[Ni_{80}Fe_{20}(2\ nm)/Au(2\ nm)/Co(0.8\ nm)/Au(2\ nm)]_{10}$

ALICE diffractometer at the undulator beamline UE56/2-PGM2 at BESSY II (Berlin)

Soft x-ray resonant magnetic scattering (SXRMS)

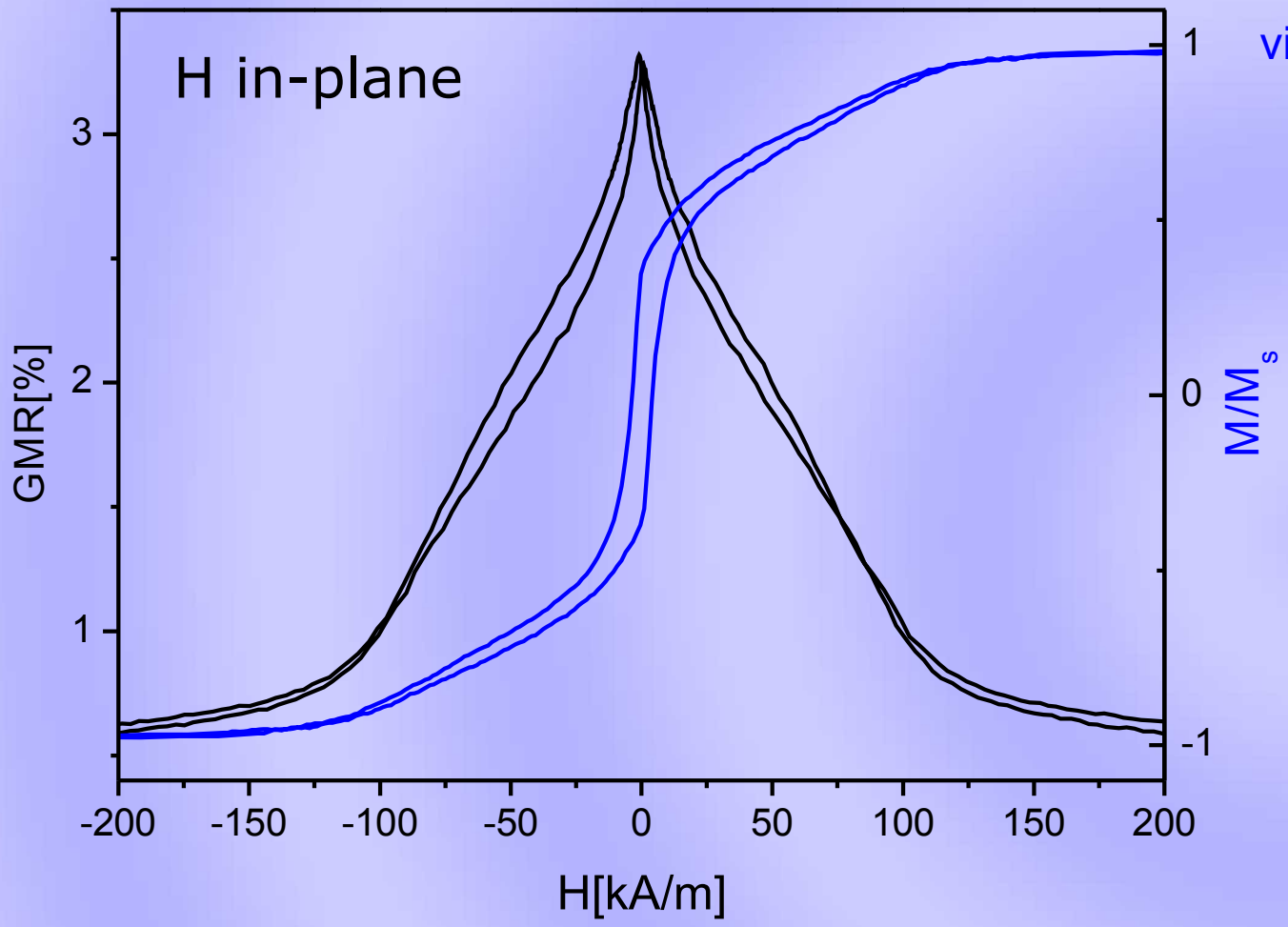

vibrating sample magnetometry

R(H)⟷M(H)

$[Ni_{80}Fe_{20}(2\ nm)/Au(2\ nm)/Co(1.1\ nm)/Au(2\ nm)]_{10}$

Soft x-ray resonant magnetic scattering (SXRMS)

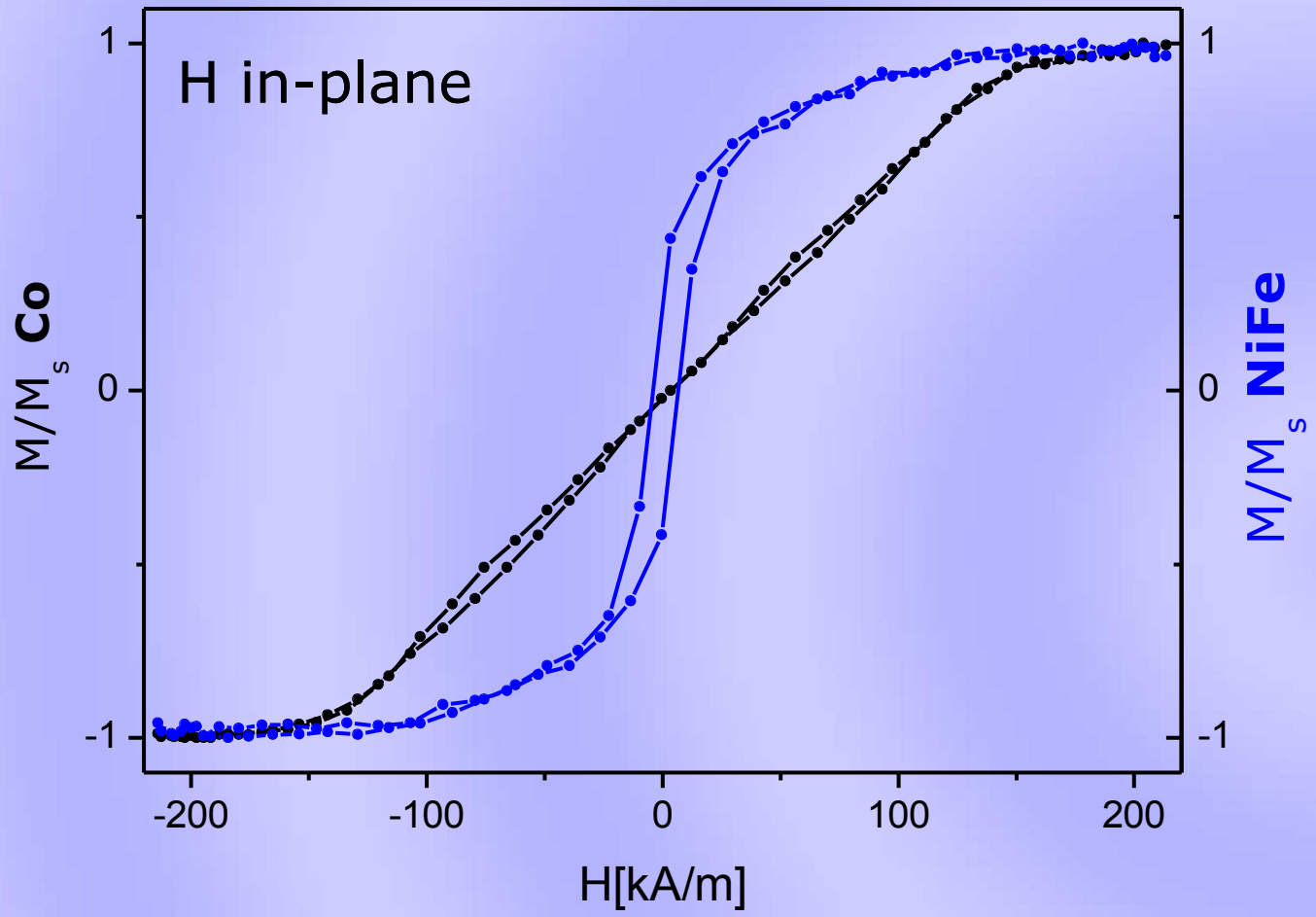

XRMS allows independent measurement of M(H) dependence of **Co** and **NiFe** layers.

Θ=8.5Deg
E=853eV (Ni L_3)
E=778eV (Co L_3)

$$M/M_s \propto [2\mathrm{I}(H) - I^+ - I^-]/(I^+ - I^-)$$

[**$Ni_{80}Fe_{20}$**(2 nm)/Au(2 nm)/**Co**(1.1 nm)/Au(2 nm)]$_{10}$

Soft x-ray resonant magnetic scattering (SXRMS)

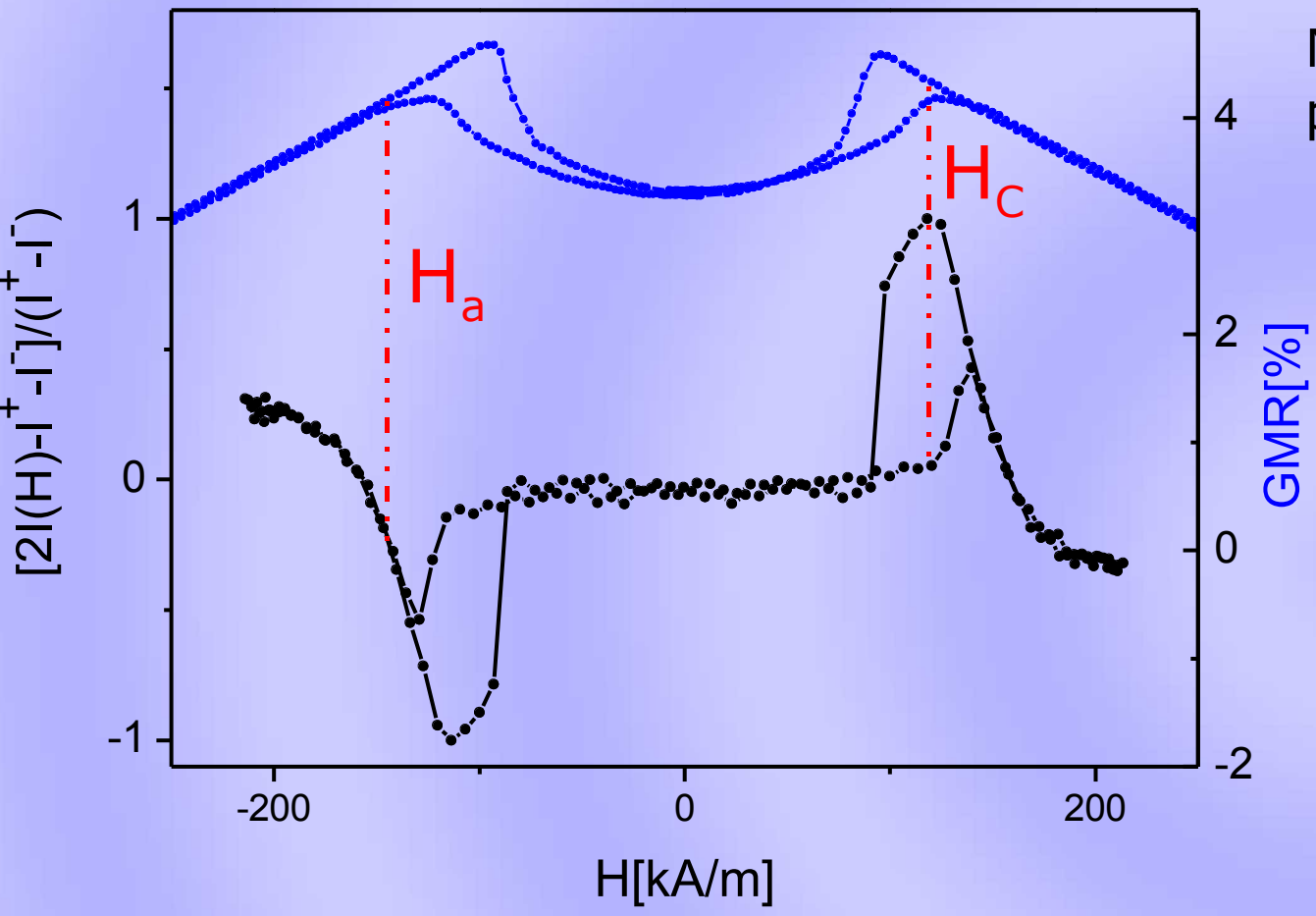

Magnetic field applied perpendicularly

SXRMS signal from **NiFe layers** shows fields characteristic for Co layers reversal:
-creation of the stripe domain structure (H_c)
-annihilation field of domain structure (H_a)

$[\mathbf{Ni_{80}Fe_{20}(2\ nm)}/Au(2\ nm)/Co(1.1\ nm)/Au(2\ nm)]_{10}$

XMCD-PEEM

Sincrotrone Trieste **ELETTRA**
S.C.p.A. di interesse nazionale

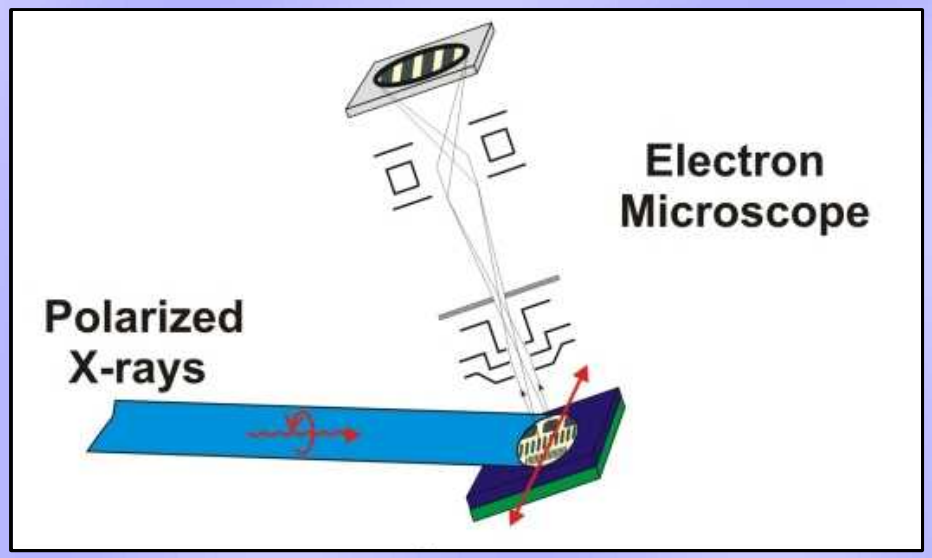

*graphics from: ssrl.slac.stanford.edu/stohr/xmcd.htm

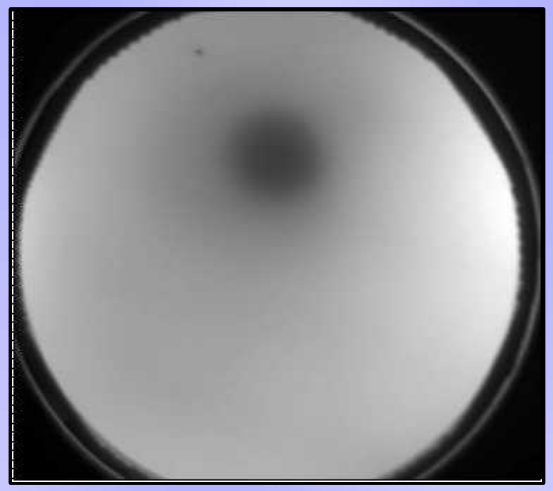

σ^L

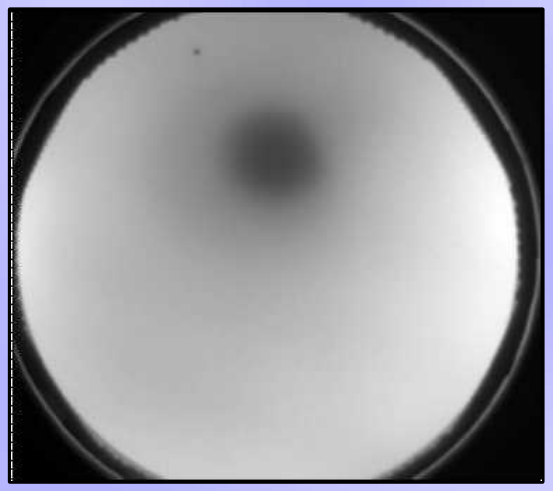

σ^R

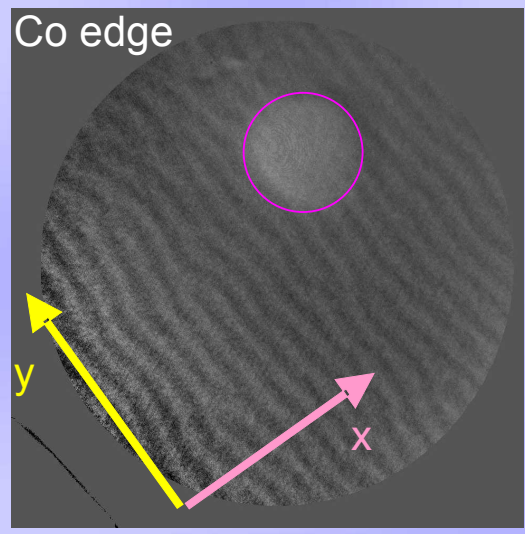

XMCD-PEEM

Sincrotrone Trieste **ELETTRA**
S.C.p.A. di interesse nazionale

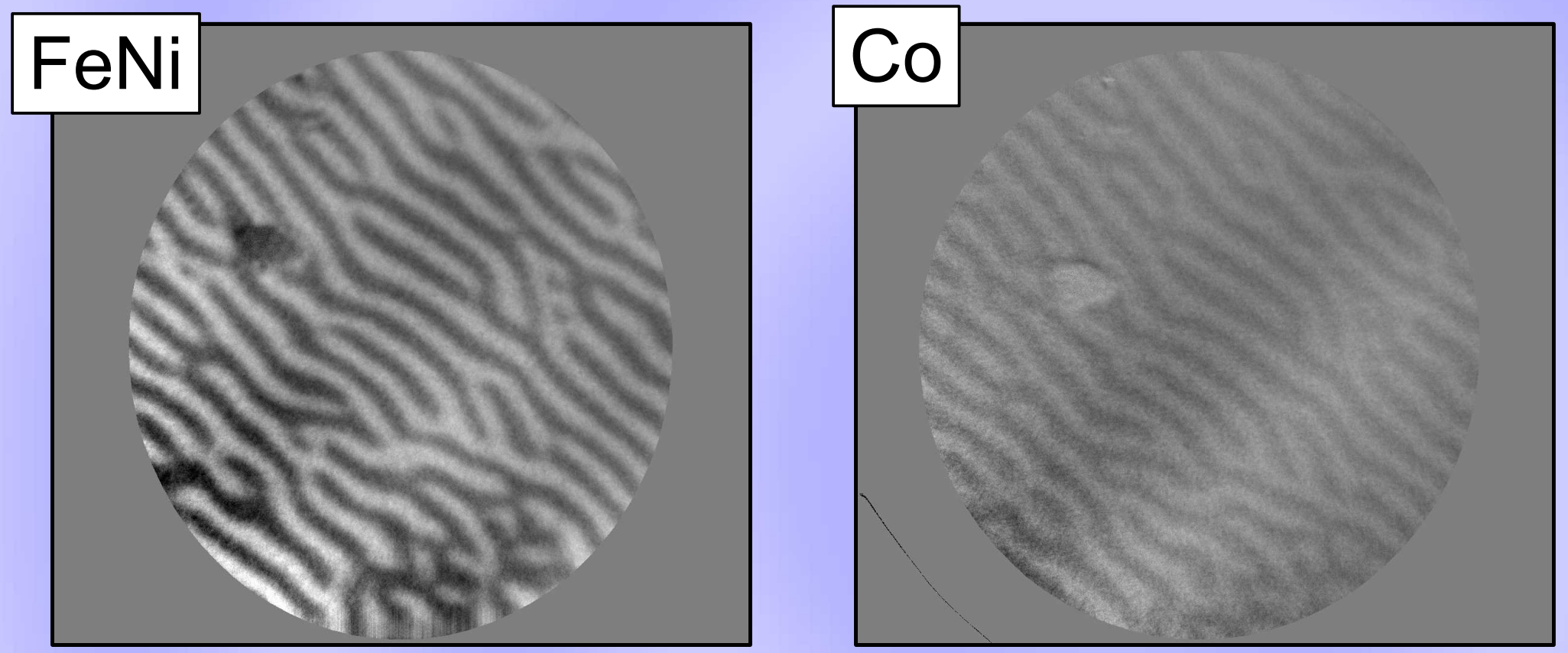

Experimental confirmation of the replication of the Co stripe domains in the perpendicular component of NiFe sublayers magnetization.

$[Ni_{80}Fe_{20}(2\ nm)/Au(2\ nm)/\mathbf{Co}(\mathbf{0.8}\ nm)/Au(2\ nm)]_{10}/Ni_{80}Fe_{20}(2\ nm)$

after in-plane ex-situ magnetazing in 0.7T

XMCD-PEEM

Sincrotrone Trieste **ELETTRA**
S.C.p.A. di interesse nazionale

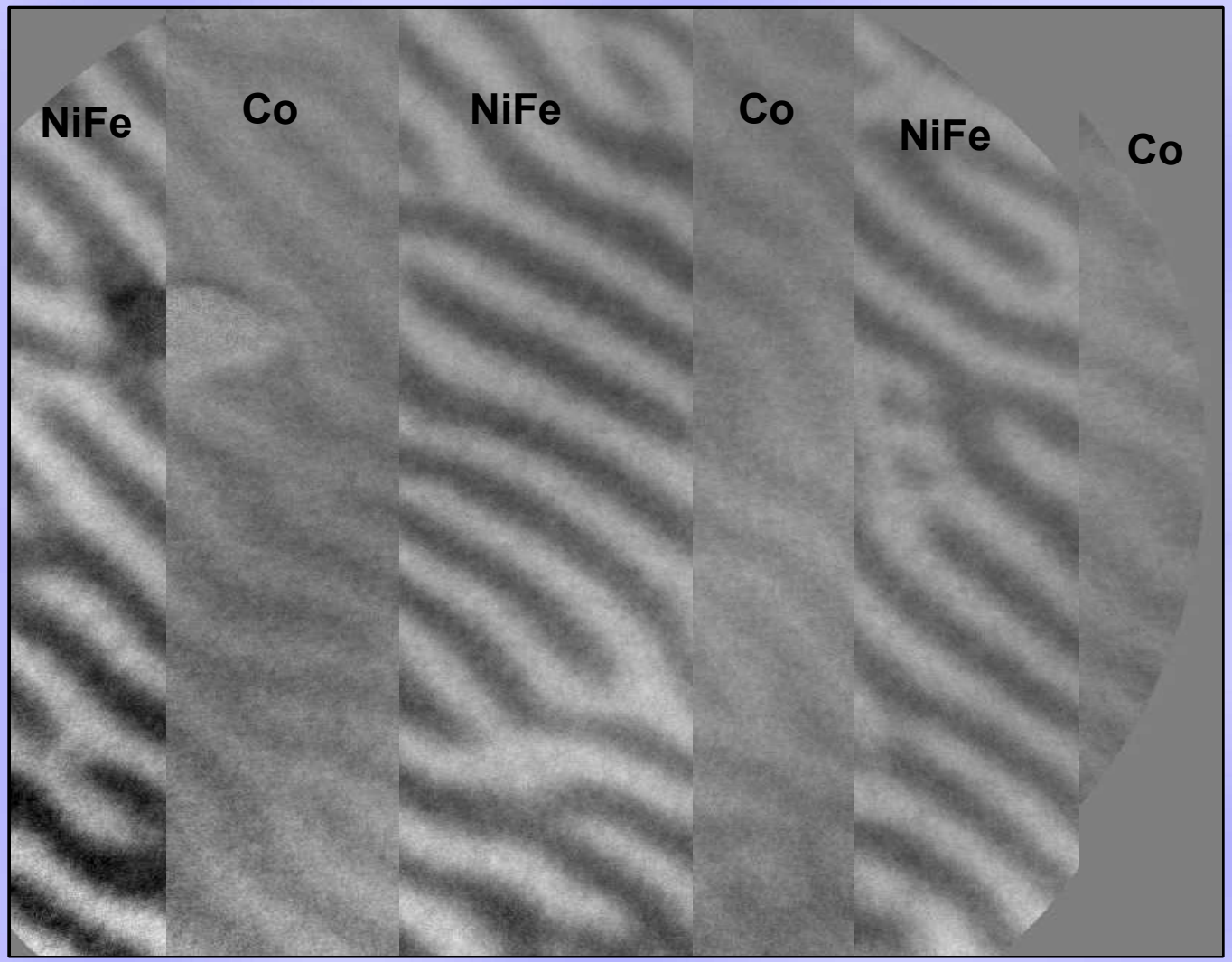

Experimental confirmation of the replication of the Co stripe domains in the perpendicular component of NiFe sublayers magnetization.

He Ion bombardment*

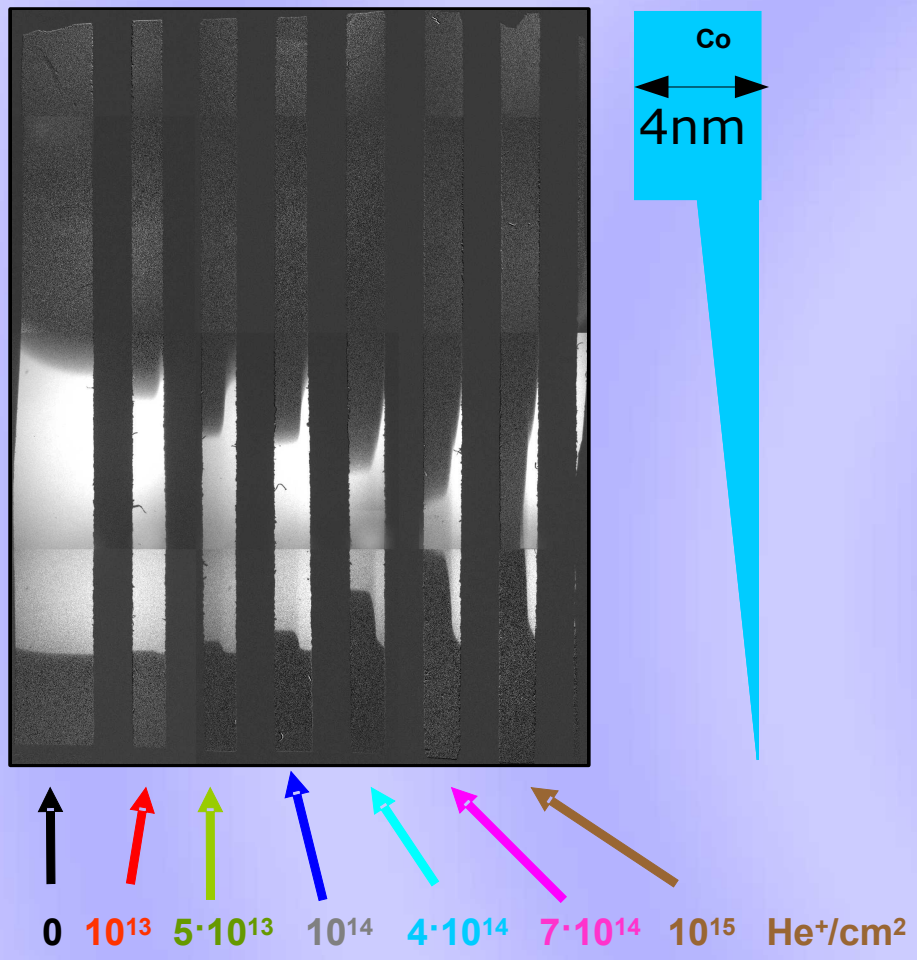

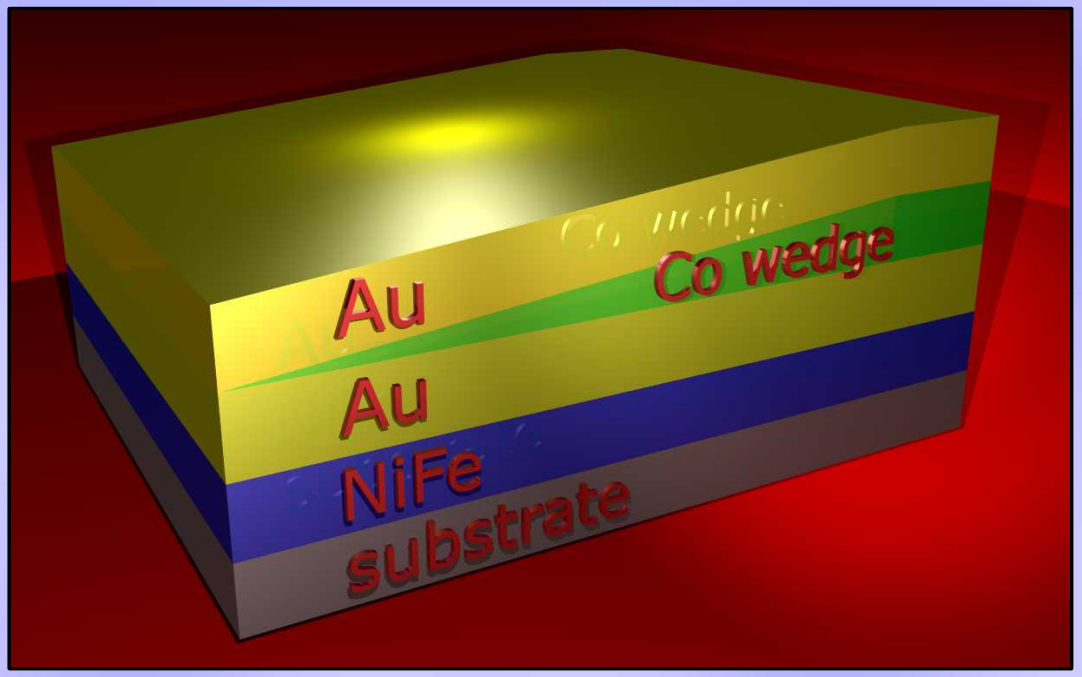

Magnetooptical Kerr effect observation of magnetic structurization caused by ion bombardment:

10keV He^+

non-topological patterning

Si(100)/buffer/$Ni_{80}Fe_{20}$-2nm/Au-3nm/Co wedge/Au-3nm

*P. Kuświk *et al.*, *ACTA PHYSICA POLONICA A* ***113***, *651 (2008)*

He Ion bombardment*

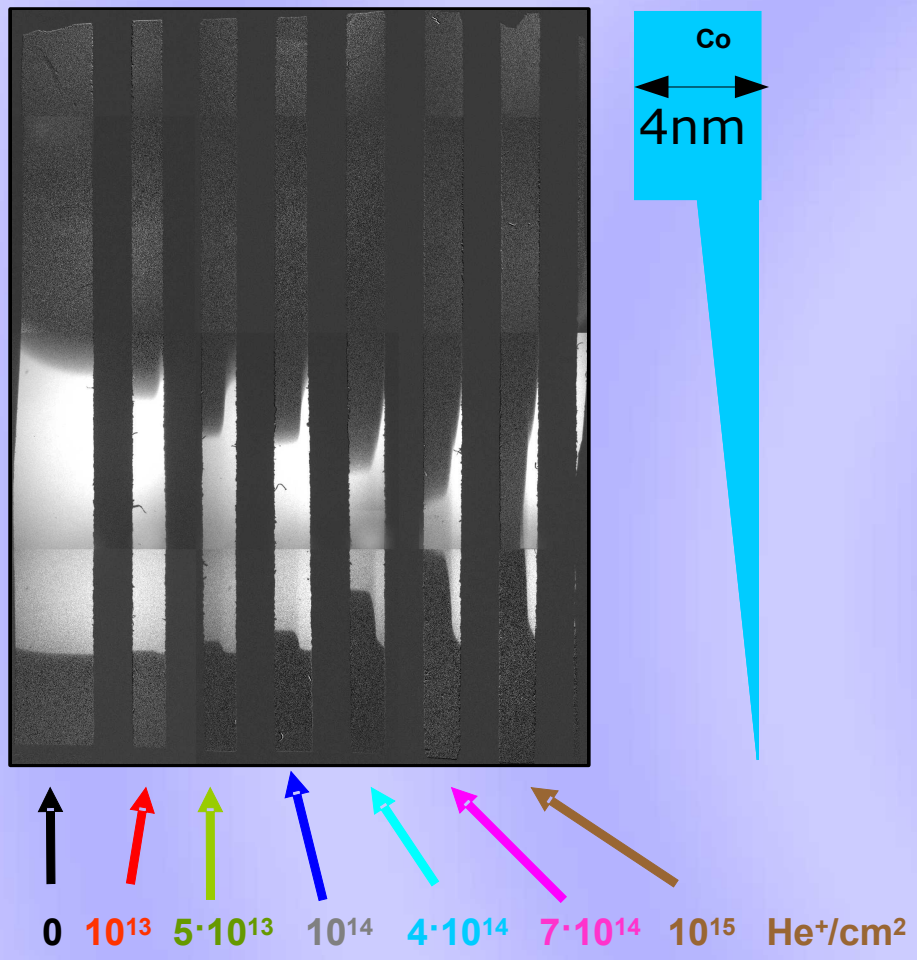

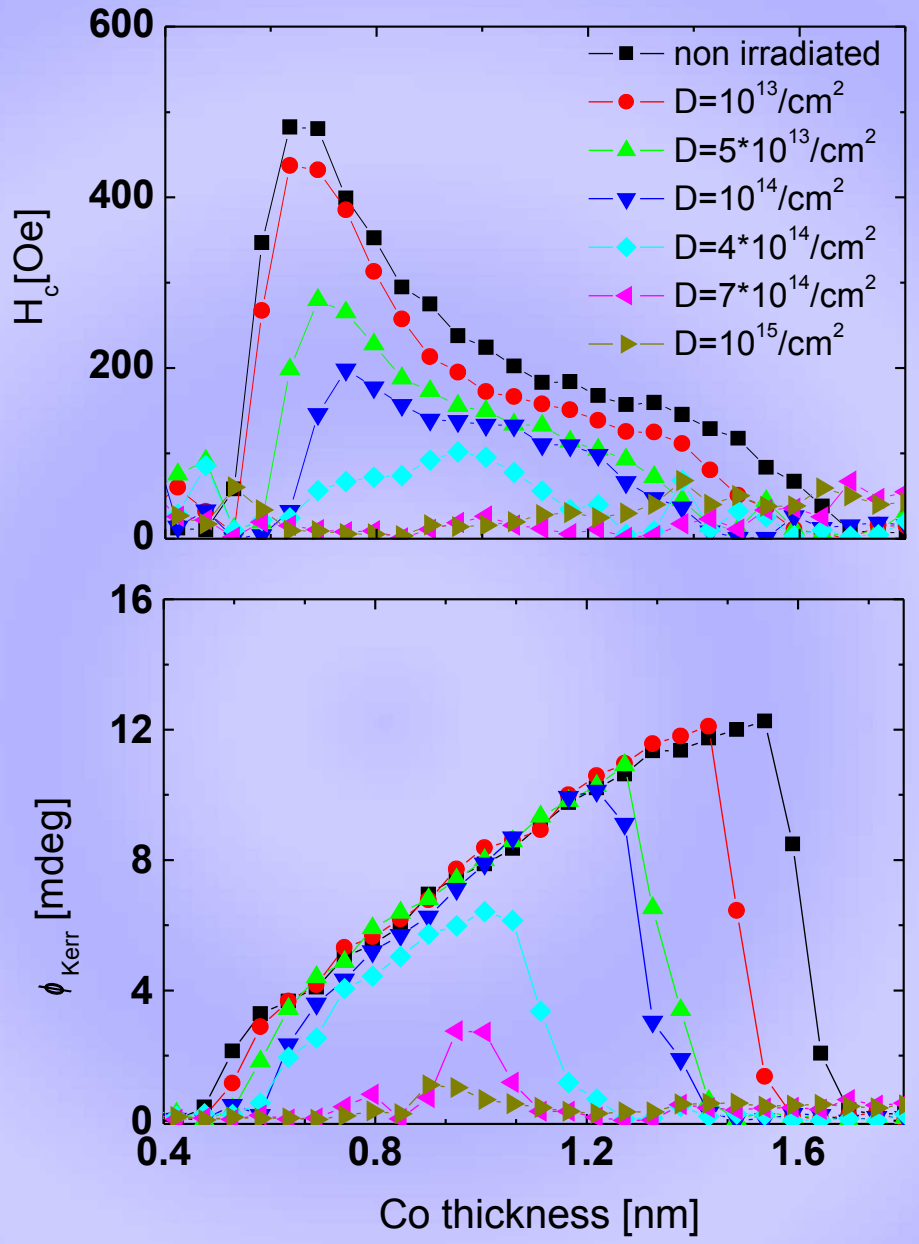

Si(100)/buffer/$Ni_{80}Fe_{20}$-2nm/Au-3nm/Co wedge/Au-3nm

*P. Kuświk *et al.*, *ACTA PHYSICA POLONICA A* ***113***, *651 (2008)*

He Ion bombardment*

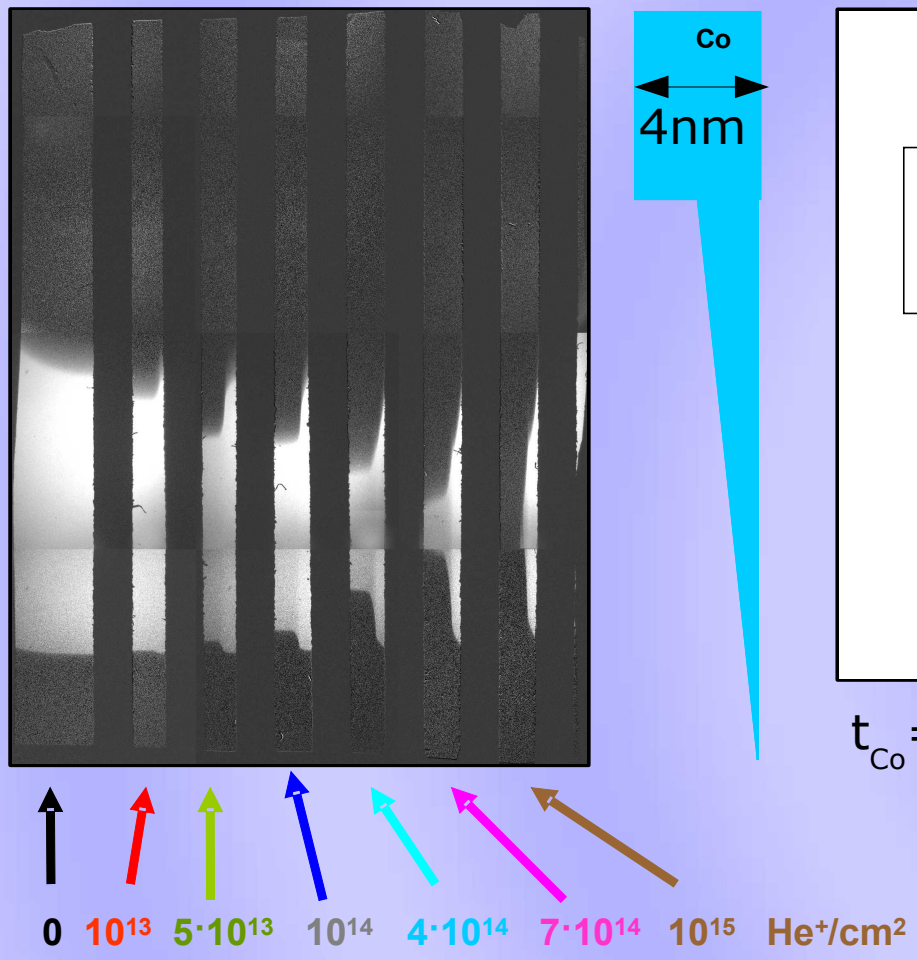

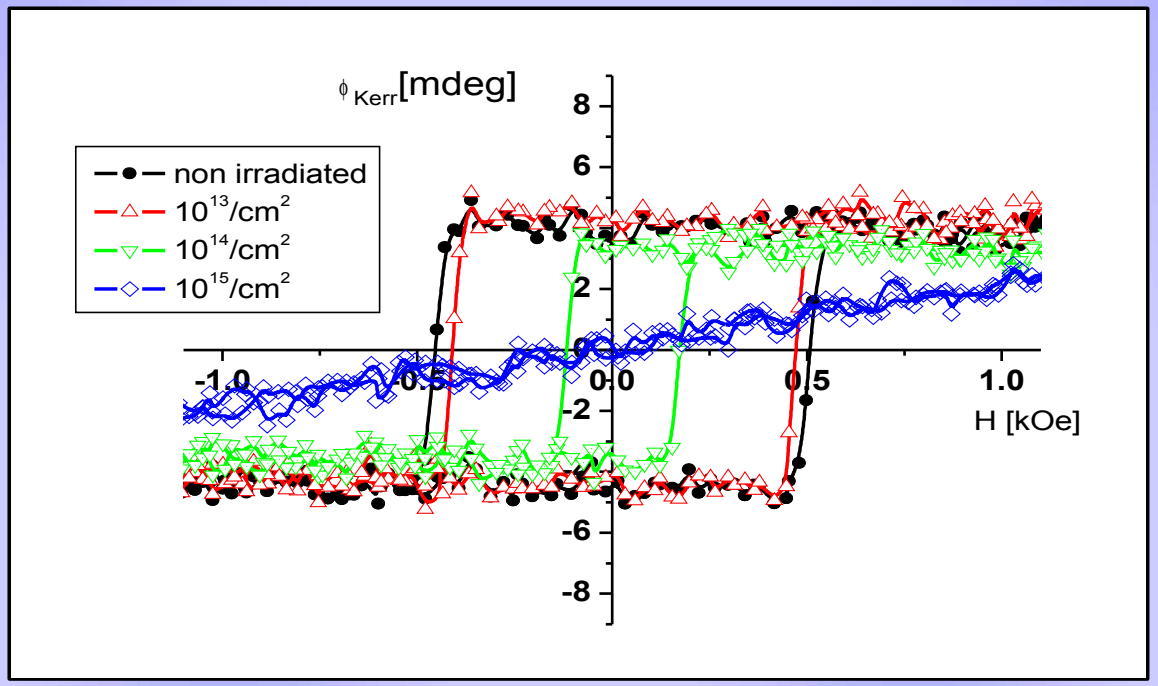

t_{Co}=0.6nm, M(H) for Co sublayers only

Negligible changes of magnetic properties for doses ≤ 10^{13} ion/cm^2

Si(100)/buffer/$Ni_{80}Fe_{20}$-2nm/Au-3nm/Co wedge/Au-3nm

*P. Kuświk *et al.*, *ACTA PHYSICA POLONICA A* ***113***, *651 (2008)*

He Ion bombardment*

He^{+}(10 keV, 6×10^{14} ions cm^{-2})

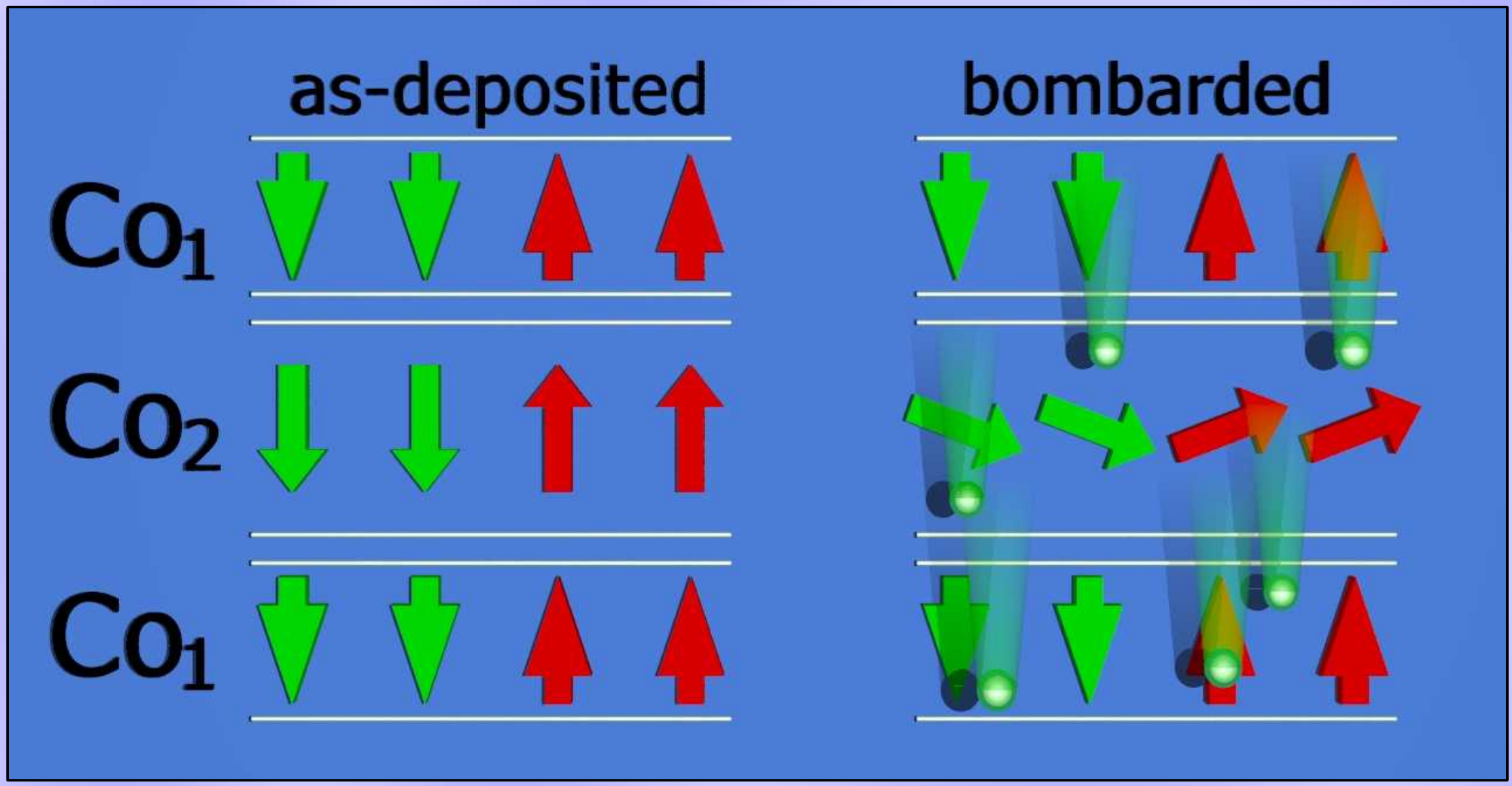

$[Co1(0.6\ nm)/Au(4\ nm)/Co2(1\ nm)/Au(4\ nm)]_4$

*together with Ehresmann AG, Kassel (www.physik.uni-kassel.de/ehresmann)

He Ion bombardment*

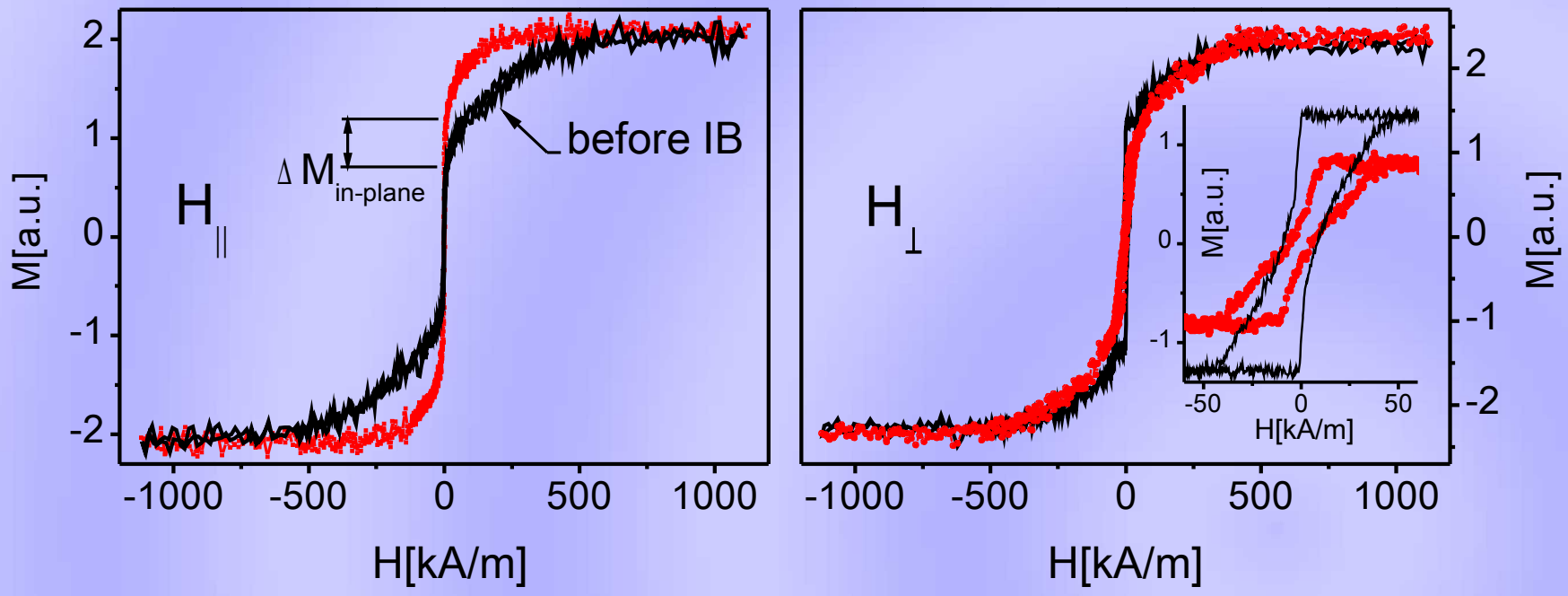

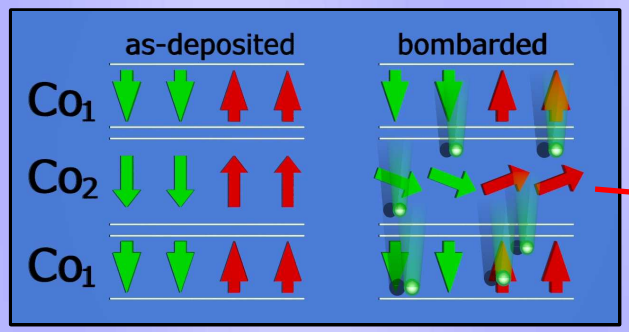

$$K_{eff} = \frac{2K_{1s}}{t_{Co}} + K_{1v} - \frac{1}{2}\mu_0 (M_S^{Co})^2$$

$[Co1(0.6\ nm)/Au(4\ nm)/Co2(1\ nm)/Au(4\ nm)]_4$

*together with Ehresmann AG, Kassel (www.physik.uni-kassel.de/ehresmann)

He Ion bombardment

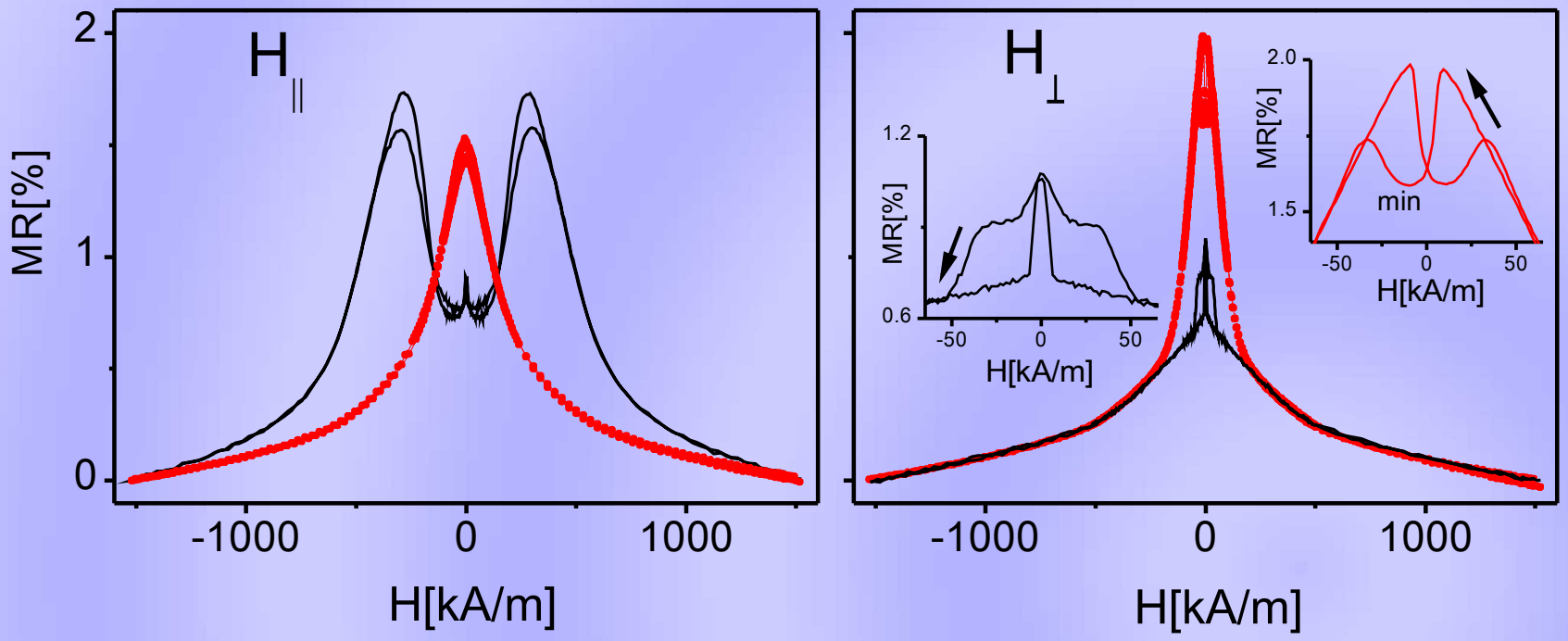

The resistance measurements confirm the observation inferred from the M(H) measurements:
the IB led to the switching of the EA direction in the 1 nm thick Co layers while the 0.6 nm thick layers preserved the perpendicular effective anisotropy.

$[Co1(0.6\ nm)/Au(4\ nm)/Co2(1\ nm)/Au(4\ nm)]_4$

He Ion bombardment

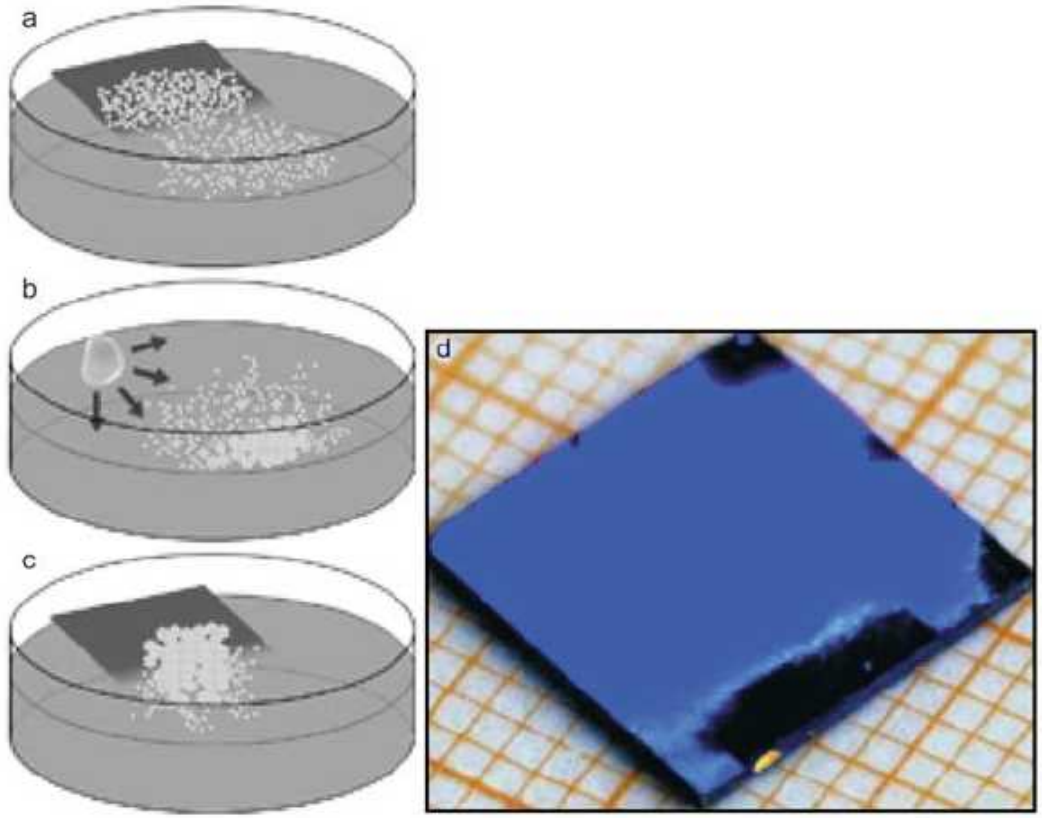

Fig. 1. The preparation process of monolayerd masks: application of latex beads onto water surface (a); consolidation of particles (b); and liftoff of ordered monolayer (c). The 1×1 cm^2 silicon wafer covered with monolayer built from 496 nm PS-latex beads: most of the surface does not contain any grain boundaries, which is represented as a monochrome light interference color (d).

Magnetic patterning

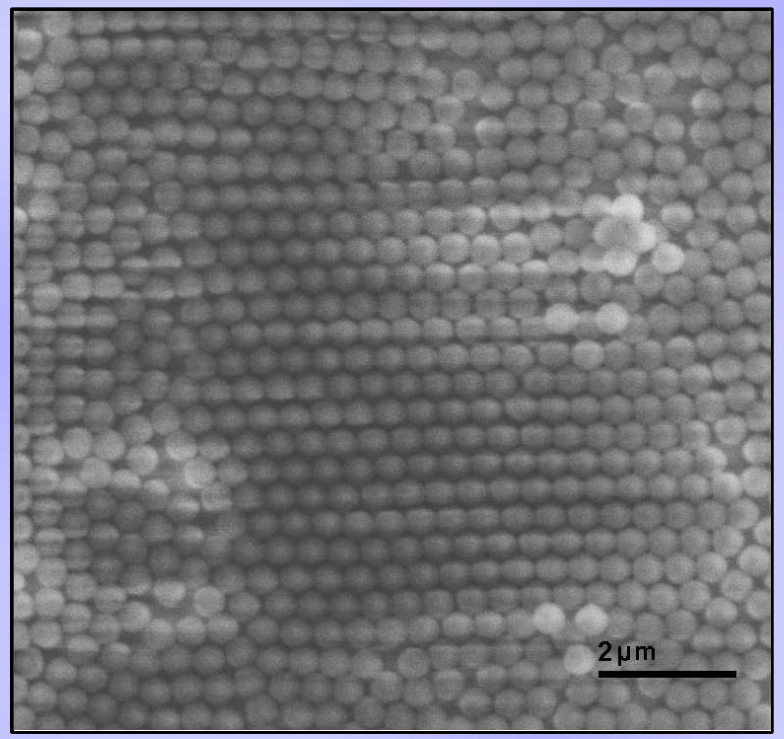

***W. Glapka, P. Kuświk** *et al.*,
ACTA PHYSICA POLONICA A ***115****, 348 (2009)*

polystyrene nanospheres (**diameter 470 nm**) were deposited on the multilayer surfaces via a self-assembly process realized by **a dip coating**.

J. Rybczyński *et al*. Colloids and Surfaces A: Physicochem. Eng. Aspects 219, 1 (2003)

He Ion bombardment

Magnetic patterning

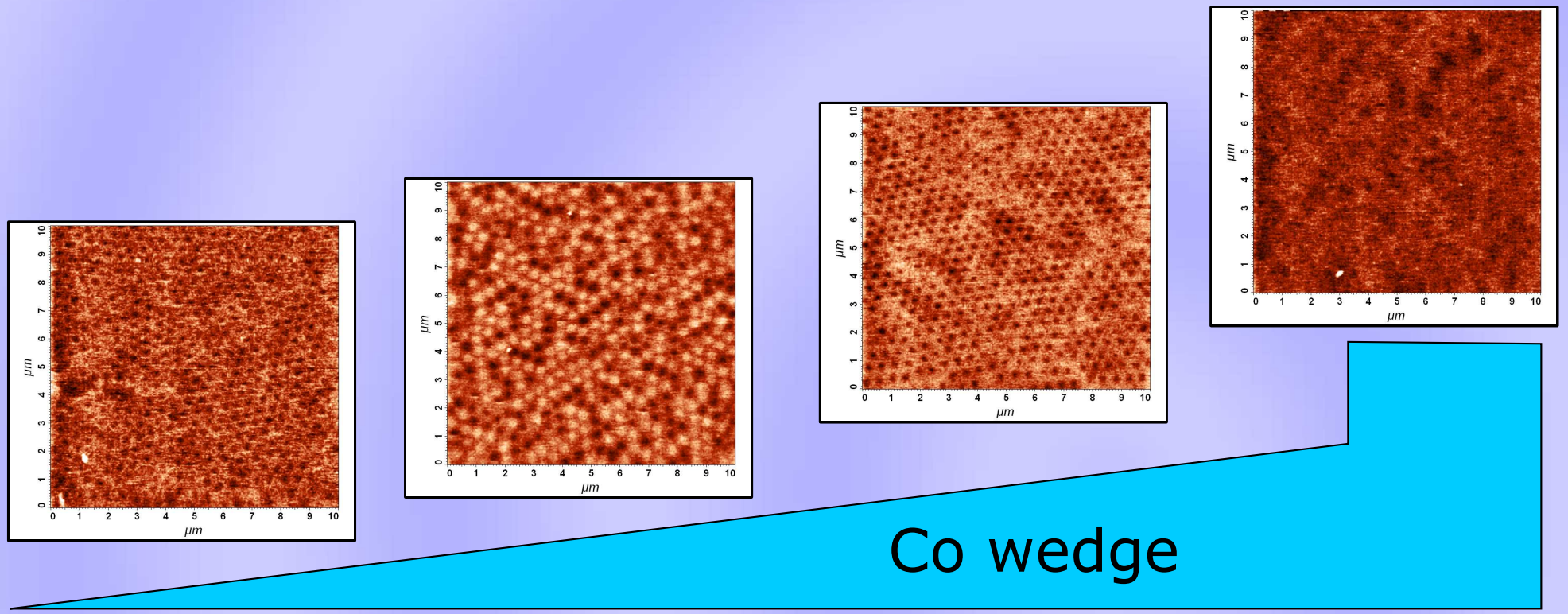

$[Ni_{80}Fe_{20}(2\ nm)/Au(3\ nm)/\mathbf{Co}(\mathbf{wedge})/Au(3\ nm)]_{10}$

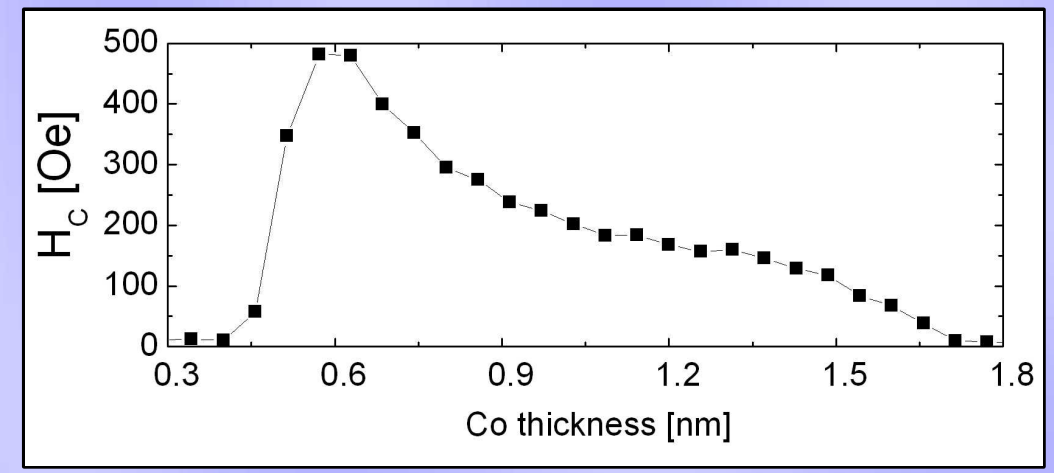

*W. Glapka, P. Kuświk *et al.*,
ACTA PHYSICA POLONICA A ***115****, 348 (2009)*

He Ion bombardment

Magnetic patterning

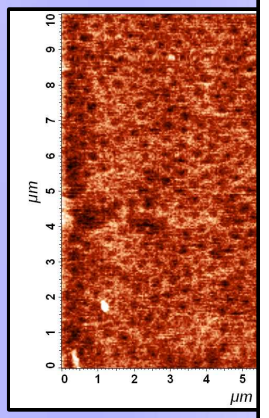

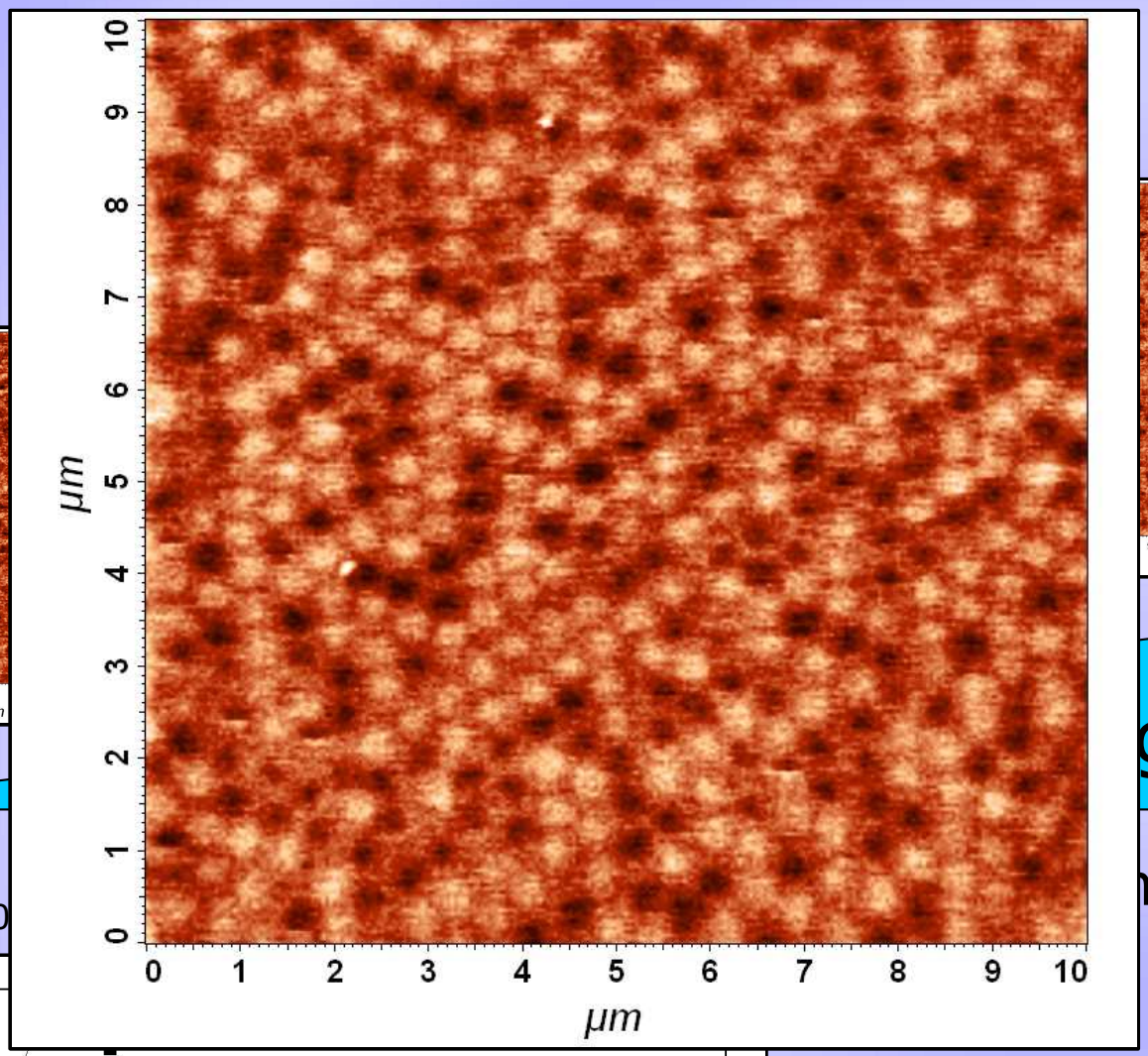

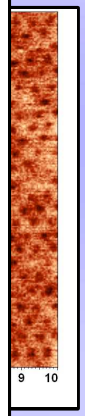

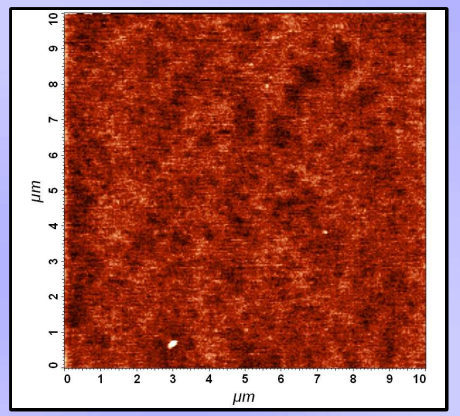

ge

$[Ni_{80}Fe_{20}$ m)]$_{10}$

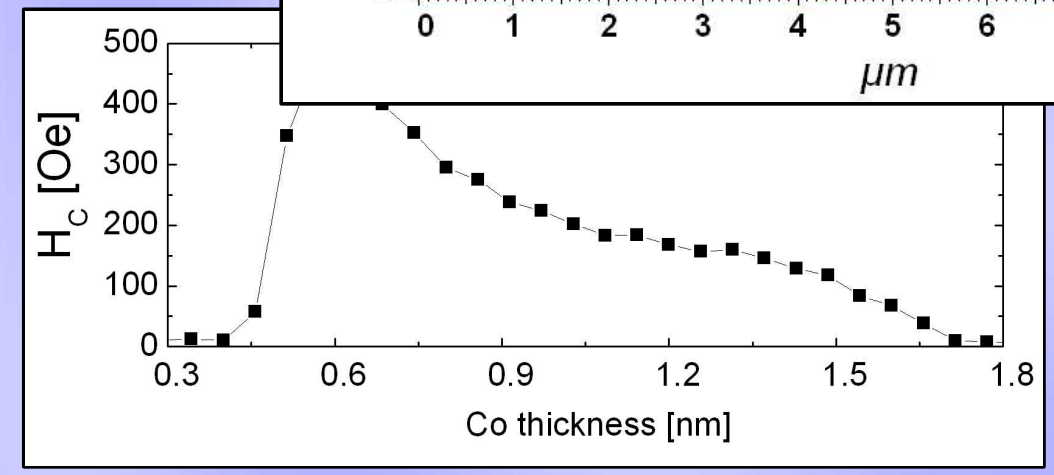

*W. Glapka, P. Kuświk *et al.*,
ACTA PHYSICA POLONICA A ***115****, 348 (2009)*

Conclusions

- $F_{||}/Au/F_{\perp}/Au$ MIs represent new type of spin-valves
- Magnetostatic coupling influences magnetic reversal of $F_{||}/Au/F_{\perp}$ MIs
- $F_{||}/Au/F_{\perp}$ MIs are suitable for a non-topological magnetic patterning

Zakopane 2009

Thank you for your attention